The role of pathogen effector proteins in altering host plant transcription

Mary Louise Tetlow

A thesis submitted for the degree of
Doctor of Philosophy

School of Life Sciences
University of Warwick

September 2015

Table of Contents

List of Figures

List of Tables

Acknowledgements

I would like to express many thanks to my supervisors Prof. Jim Beynon and Dr. Katherine Denby for their support. I have greatly appreciated Jim's fantastic help and guidance throughout the course of my project. Also thank you to Katherine for many helpful suggestions and comments on my work both as an advisor and more recently as a supervisor. Similarly, many thanks to Dr. Sarah Harvey for her kind help in many ways including demonstrating techniques, making suggestions for experiments and providing helpful comments on my work. I would also like to thank Dr. Jens Steinbrenner for his greatly appreciated support particularly during my first year but also for his continued guidance. In a similar way, thank you to Alison Eyres and Dr. Polly Downtown for helping me to get established with the 3C techniques. Furthermore, I would like to express a great deal of gratitude to my advisory panel members Prof. Eric Holub and Dr. Alex Jones. Thank you to Eric for his interest and insights and also to Alex for her great advice and help with the Co-IP experiments. Also thanks to Dr. Daniel Tomé for his Co-IP protocol and support in the lab.

I am also very grateful to those who have shared their work and materials, making this project possible. Firstly, I would like to express thanks to Prof. Peter Fraser and Dr. Stefan Schoenfelder at the Babraham Institute (University of Cambridge) for sharing their protocols and allowing time to meet up. A big thank you also to Dr. Alessandra Devoto at Royal Holloway (University of London) for kindly providing an *Arabidopsis* cell suspension culture.

I would also like to thank all of my friends, colleagues and previous members of the Beynon group including Rachel Clewes and Gemma Barnes for being friendly and supportive. Thanks to Tina Payne, for her fantastic help with growing and maintaining plants, also to Tim Coker for his help with microarray data analysis.

Thanks to my Mum and Dad, Emily and Luke for being really thoughtful and helping in so many ways. Finally to Daniel for always being interested and kind.

Declaration

This thesis is submitted to the University of Warwick in support of my application for the degree of Doctor of Philosophy. It has been composed by myself and has not been submitted in any previous application for any degree. It has been prepared in accordance with the university guidelines. The work presented was carried out by myself, unless otherwise stated.

Abstract

Plant pathogens secrete effector proteins in order to overcome immunity in plants stimulated by common microbial patterns. The genomes of oomycete pathogens including *Hyaloperonospora arabidopsidis* (*Hpa*) are predicted to contain a large number of effectors. These experiments focussed on characterising an interaction between predicted *Hpa* effector HaRxL14 and *Arabidopsis* protein phosphatase type-2CA (PP2CA), which functions as a co-receptor in response to the phytohormone abscisic acid (ABA). This interaction was previously identified in a yeast two-hybrid screen. Bimolecular fluorescence complementation experiments verified an interaction in the nucleus. Over-expression of the effector *in planta* enhances susceptibility of *Arabidopsis* to *Hpa*, although knocking-out *PP2CA* in the host did not have a clear effect on infection. Furthermore, a potential role for the interaction in enhancing host signalling associated with ABA was highlighted from microarray analysis of *Arabidopsis* lines over-expressing the effector. The up-regulation of various ABA-related genes supports previous findings that ABA may disrupt host response to biotrophic pathogens.

Furthermore, it was hypothesised that phytohormones including jasmonic acid (JA), ABA, and salicylic acid (SA) could have a role in coordinating host transcription at the level of chromosome conformation. Progress was made towards optimising a method for use with *Arabidopsis* related to chromosome conformation capture (3C). These experiments began to examine the spatial interactions of JA-induced genes in *Arabidopsis*. This method could be used to determine if related genes co-localise at specialised transcription factories. These transcription factories have previously been studied in other models including mammals, although their potential role in plants is currently not well understood. Overall, a *Hpa* effector was shown to interact with host protein PP2CA potentially to up-regulate ABA-related genes. It remains to be established if phytohormones have a role in coordinating transcription through manipulating spatial interactions of genes.

Abbreviations

3C chromosome conformation capture

4C circularized chromosome conformation capture

ABA abscisic acid

AVR avirulence protein

BAC bacterial artificial chromosome

Co-IP co-immunoprecipitation

Col-0 Columbia-0

DAMP damage-associated molecular pattern

EDTA ethylenediaminetetraacetic acid

ETI effector-triggered immunity

ETS effector-triggered susceptibility

FISH fluorescent *in situ* hybridisation

GA gibberellic acid

Hi-C genome-wide chromosome conformation capture

Hpa *Hyaloperonospora arabidopsidis*

HRP horseradish peroxidase

JA jasmonic acid

Ler Landsberg erecta

MAMP microbe-associated molecular pattern

NB-LRR nucleotide binding leucine rich repeat

NGS next-generation sequencing

PP2CA protein phosphatase type-2CA

PTI pattern-triggered immunity

PYR/PYL/RCAR pyrabactin resistance (PYR1)/PYR1-like (PYL)/regulatory components of ABA receptors (RCAR)

RXLR arginine, any, leucine, arginine

SA salicylic acid

SCRIBL sequence capture of multiple regions interacting with bait loci

SnRK sucrose non-fermenting related kinase

ROS reactive oxygen species

TAD topologically associating domains

1 Introduction

1.1 The diversity of plant pathogens

Plants are infected by a variety of pathogenic microorganisms including viruses, bacteria, fungi, oomycetes and nematodes (Bebber *et al*., 2014). In addition, it has recently been found that plants are capable of taking up prions from infected soil and that grasses may act as vectors for prion transmission without symptoms of disease (Pritzkow *et al*., 2015). Plant pathogens can cause a range of symptoms in their hosts including late blight in potatoes (*Phytophothara infestans*, oomycete), cankers on citrus trees (*Xanthamonas axonopodis*, bacteria) and stem rusts on wheat (*Puccinia graminis*, fungus; Akino *et al*., 2013; Anderson *et al*., 2004; Leonard and Szabo, 2005). These pathogens have a range of lifestyles and therefore the progress of infection can be highly variable, even with similar organisms. For instance, a minimum of six out of twelve orders of the *Dothidiomycete* class of fungi are plant pathogens (Ohm *et al*., 2012). These include necrotrophic pathogens, which kill and feed on dead plant tissue as part of their colonisation, including *Stagonospora nodorum* which infects wheat (Dangl and Jones, 2001; Ohm *et al*., 2012). Biotrophic pathogens depend on living host tissue during their growth and infection, such as *Cladosporium fulvum* which infects tomato (Dangl and Jones, 2001; Ohm *et al*., 2012). Pathogens may also switch lifestyle, as with hemibiotrophs such as *Phytophthora infestans*, which are initially biotrophic but become necrotrophic during the final stages of infection (Bos *et al*., 2010). Overall, plant-pathogen interactions are varied and this is reflected in the substantial complexity of the molecular pathways in the pathogen and host associated with infection and immunity respectively.

1.1.1 Plant disease and food security

Globally plant pathogens account for a significant proportion of crop losses, which has been estimated as 10 to 16% on average annually between 2001 and 2003, based on various crops and regions (Oerke, 2005). Some of the most devastating pathogens

include *Puccinia graminis*, which infects cereal crops and forms a destructive stem rust in wheat (Anderson *et al*., 2004). Another pathogen with historic and current implications for global food security is *Phytophothora infestans*, the causative agent of late blight in potatoes and other members of the *Solanaceae* including tomatoes (Akino *et al*., 2013). Recent evidence suggests that plant pathogens are advancing towards the poles of the Earth (Bebber *et al*., 2013). This is caused in part by a rise in average surface temperatures, leading to climates becoming more hospitable and conducive to the growth of pathogens. Therefore, regions that had not previously identified specific plant pathogens are beginning to see crop losses to these new invaders (Bebber *et al*., 2013). This suggests that future challenges to global food security are not only likely to include current issues, such as pathogen resistance to pesticides and loss of resilience in crop varieties, but also expanded environmental range of pathogens.

1.1.2 *Arabidopsis thaliana* and *Hyaloperonospora arabidopsidis* as a model pathosystem for investigating plant immunity

The small temperate plant *Arabidopsis thaliana* (subsequently referred to as *Arabidopsis*) has in recent decades become a widely studied plant model in genetics and cell biology (Martienssen, 2000; Meinke, 1998). Extensive sequencing and gene annotation projects have meant that *Arabidopsis* is at the heart of extensive resources for biological research (*Arabidopsis* Genome Initiative, 2000; Berardini *et al*., 2015; Bevan and Walsh, 2005). The short lifecycle and small genome size of *Arabidopsis* have meant that the plant has a lot of benefits as an experimental system when compared to the long growth cycles and field conditions required for crop plants including wheat (Bressan *et al*., 2001; Bruce *et al*., 2015). *Arabidopsis* (a member of the *Brassicaceae* family) is a relative of Brassica crops (including *Brassica napus*), which account for 12% of global vegetable oil for human consumption (Martienssen, 2000; Paterson *et al*., 2001).

Arabidopisis has a range of approximately 750 genetically similar but non-identical ecotypes that occur across regions including Europe and North America (TAIR website). This provides a resource for the identification of genes associated with

enhanced resistance to pathogen invasion. *Arabidopsis* is a host for a range of pathogens, some with economic significance such as *Pseudomonas syringae*, *Botrytis cinerea* and *Hyaloperonospora* species (Coelho *et al*., 2012; Denby *et al*., 2004; Whalen *et al*., 1991). The infection of *Arabidopsis* with oomycete *Hyaloperonospora arabidopsidis* (*Hpa*; formerly *Peronospora parasitica*) has become a model pathosystem for pathology research since the 1990s, although this interaction was initially identified in the 1900s (Coates and Beynon, 2010; Koch and Slusarenko, 1990; McDowell, 2014).

Hpa is a biotrophic pathogen, which has both sexual and asexual stages in its lifecycle. The pathogen initiates infection of *Arabidopsis* with asexual sporangiospores (on leaves) or sexual oospores (on the roots; Caillaud *et al*., 2012b). This is followed by formation of an appressorium allowing the penetration of hyphae into the space between epidermal cells (Coates and Beynon, 2010). This is followed by the development of haustorial structures with the epidermal cells and eventually the mesophyll cells as the hyphae grow further through the apoplastic space (Koch and Slusarenko, 1990). These haustoria are the surface through which the pathogen absorbs nutrients and water and transfers effector proteins to the host, which interfere with the host immune response (Coates and Beynon, 2010). Eventually the pathogen will produce asexual spores (sporangia) held on branched structures (sporangiophores) or sexual oospores when hyphae come into contact (Coates and Beynon, 2010). These oospores may undergo a period of winter dormancy in leaf debris in the soil before infection of a new host (Slusarenko and Schlaich, 2003).

This model benefits from the various pathogen isolates with differential ability to infect *Arabidopsis* accessions, named according to their location of discovery and an accession appropriate for propagation (e.g. Emoy2, Location: East Malling, Accession: Oyctese; Holub, 2008). As a result of coevolution of pathogen isolates alongside their hosts, these have compatible interactions (i.e. the pathogen is able to infect the host) with specific *Arabidopsis* accessions and non-compatible with others (Coates and Beynon, 2010; Nemri *et al*., 2010). Therefore, this pathosystem provided opportunities to map and clone genes associated with resistance, referred to as Recognition of *Peronospora parasitica* (RPP) genes, and study the pathways associated with the proteins more closely (Holub, 2008; Nemri *et al*., 2010).

1.2 The plant immune response

The plant immune system has often been described as a tiered response, meaning that there are various barriers to infection utilised by the host (Jones and Dangl, 2006). These modes of host protection are initially non-specific physical barriers but can also be highly specific molecular interactions if these initial defences are breached. The layers of the plant immune response can generally be divided into the categories described in the following sections.

1.2.1 Physical and antimicrobial barriers to infection

Plants have many physical defences to prevent colonisation by pathogens. These include the waxy cuticle, which covers the surfaces of the leaves. For instance, *Berberis vulgaris,* which is an alternative host of *Puccinia graminis*, is more resistant to the pathogen in maturity (Leonard and Szabo, 2005). This resistance is likely to be due the thickening of the waxy cuticle, which inhibits penetration of the basidiospore germ tube (Leonard and Szabo, 2005). Plants also synthesise defence factors, which inhibit the growth of pathogens including terpenoids, alkaloids, phytoalexins, phenolics and defensins (Lacerda *et al*., 2014). These defensins are short cationic peptides with antimicrobial properties, which have a crucial role in protecting developing seeds and seedlings through to various mature cell types and structures including leaves and flowers (Lacerda *et al*., 2014). These types of biochemical defenses are often sufficient to deter potential invaders although some have necessary adaptations to overcome these general front line defences.

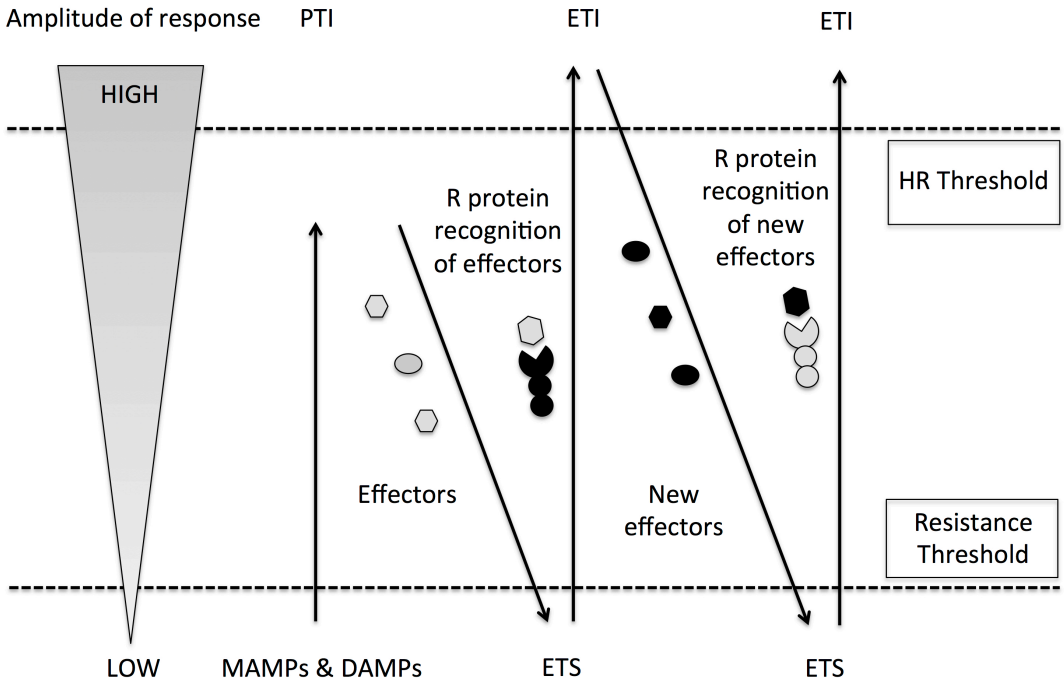

Figure 1. Host-pathogen interactions may lead to host susceptibility or resistance. This illustration is based on the Zig-Zag model (Jones and Dangl, 2006). Upon recognition of MAMPs or DAMPs through pattern recognition receptors, an immune response is triggered leading to pattern-triggered immunity (PTI). This host response may be overcome by pathogen effectors, resulting in effector-triggered susceptibility (ETS), which is a higher magnitude of response. Recognition of these effectors by host resistance proteins in turn induces effector-triggered immunity (ETI). A host-pathogen evolutionary arms race may then ensue in which new effectors and resistance proteins lead to either susceptibility or resistance of the host. Adapted by permission from Macmillan Publishers Ltd: Nature (Jones and Dangl, 2006), copyright (2006).

1.2.2 Pattern–triggered immunity (PTI)

Plants are able to recognise common features of invading pathogens known as microbe associated molecular patterns (MAMPs). These MAMPs are highly conserved structures such as the flagellum of motile bacteria and chitin in fungi, which initiate a response known as pattern-triggered immunity (PTI, Figure 1). The detection of these patterns is often dependent on leucine rich repeat receptor-like kinases (LRR-RLKs) including FLAGELLIN SENSING 2 (FLS2), which interacts with another LRR-RLK BRASSINOSTEROID INSENSITIVE 1-associated receptor kinase 1 (BAK1) and initiates a mitogen-activated protein kinase (MAPK) signalling cascade (Sun *et al*., 2013; Zipfel *et al*., 2004). Following stimulation of FLS2 and BAK1 with flg22 (a peptide representing a conserved active epitope in the amino terminus) the differential regulation of over 1150 genes (966 of which are up-regulated) occurs in the host (Zipfel *et al*., 2004). Host responses that occur as a result of MAMP stimulation include the production of reactive oxygen species (ROS), ion fluxes across the plasma membrane and the production of antimicrobial peptides. In addition, a large number of up-regulated genes were LRR-RLKs suggesting that perception of one MAMP leads to higher sensitivity to others (Zipfel *et al*., 2004).

Other molecules that initiate a similar response to MAMPs occur as a result of the damage caused to cells during the process of infection. These damage-associated molecular patterns (DAMPs) are an alternative mode for plants to detect potential invaders. For instance, oligogalacturonides (OGs) are released and perceived by wall-associated kinases during the break down of the cell wall and the stimulated pathways are interlinked with those associated with MAMPs LRR-RLKs (Ferrari *et al*., 2013). These OGs signal potential danger as fungal enzymes degrade the cell wall in preparation for hyphal penetration (Bartels and Boller, 2015). The outcome is highly similar to that associated with MAMP stimulation including production of callose, chitinase and ROS but also includes the modulation of development pathways (Ferrari *et al*., 2013).

1.2.3 Effector-triggered susceptibility (ETS)

1.2.3.1 Pathogen effectors

Pathogens may secrete effector proteins to sabotage this pattern recognition response and to generally favour survival and reproduction (Figure 1; Jones and Dangl, 2006). The first effector was identified in *P. syringae* pv. *glycinea* when a cosmid library was transferred between specific race of the pathogen. This led to a change in the host specificity from virulent to avirulent on the relevant soybean cultivar with the recipient (Staskawicz *et al*., 1984). It has since been shown that effector proteins are common to a range of diverse microorganisms. These include bacteria (*Xanthamonas* species), fungi (*Cladosporium fulvum*), nematodes (*Globodera pallida*) and oomycetes (*Phytophthora infestans* and *Hpa*; Birch *et al*., 2009; Boch *et al*., 2014; Fabro *et al*., 2011; Mitchum *et al*., 2013; Stergiopoulos and de Wit, 2009). Pathogens may transfer these effectors to the host plant cells through type III secretion systems in bacteria, via haustoria in oomycetes or the stylet of nematodes (Chisholm *et al*., 2006; Feng and Zhou, 2012).

Effectors have evolved to disrupt signalling pathways and immune responses in a manner conducive to pathogen survival. Examples of effector action include mimicking transcription factors and the sequestration of chitin to subvert stimulation of PTI (Canonne and Rivas, 2012; de Jonge and Thomma, 2009). Bacterial transcription-activator like effectors (TALEs) from *Xanthomonas* species recognise and bind to host promoter sequences of targets known as susceptibility genes (Boch *et al*., 2014). These effectors were first discovered in *Xanthamonas* following identification of two R genes (Bs1 and Bs3) in resistant pepper (*Capsicum annuum*) cultivars, which were introduced into a susceptible background to produce near isogenic lines (Minsavage *et al.*, 1990). This allowed the identification of incompatible *Xanthamonas* strains on these pepper cultivars and the effector gene *avrBs3*, which is located on a self-transmissable plasmid in *X. campestris* pv. *vesicatoria*, was identified and cloned (Bonas *et al.*, 1989). It was later shown that AvrBs3 binds to the promoter of the basic helix-loop-helix domain transcription factor *Upa20* which regulates cell size, inducing its expression and leading to hypertrophy of mesophyll cells (Kay *et al.*, 2007). Other examples of TALE

effectors include PthXo6 from *Xanthomonas oryzae* pv. o*ryzae*, initiates the transcription of a bZIP transcripton factor and following interaction with secondary targets leads to leaf curling in the host, which favours bacterial proliferation (Boch *et al*., 2014).

Effectors from other pathogens can have highly contrasting modes of action, through manipulation of the host at a protein rather than genetic level. For example, AVR3a from *P. infestans* suppresses host cell death in *Nicotiana benthamiana* through stabilising an E3 ubiquitin ligase CMPG1, favouring the survival of the hemibiotrophic pathogen (Bos *et al*., 2010). Alternatively, *P. syringae* uses HopX1 to initiate signalling of the plant hormone jasmonic acid through promoting degradation of the Jasmonate ZIM-domain (JAZ) repressors in *Arabidopsis* (Gimenez-Ibanez *et al*., 2014). These stimulated jasmonic acid pathways antagonise salicylic acid signalling, which are crucial in host defence against the pathogen (Gimenez-Ibanez *et al*., 2014). Overall, investigations examining individual effectors have produced detailed insights into the diversity of effectors and their host targets.

1.2.3.2 Oomycete RXLR effectors

It has been over a decade since the first *Hpa* effector *Arabidopsis thaliana* Recognised (*ATR*) 13 was cloned and the interaction of its protein product characterised with the host resistance protein RPP13 (Allen *et al*., 2004). The identification of additional *Hpa* (ATR1) and *Phytophthora* (including AVR3a and AVR1b-1) effectors, enabled initial peptide sequence alignment, which identified a highly conserved motif termed RXLR for simplicity (followed by a dEER motif; Armstrong *et al*., 2005; Rehmany *et al*., 2005; Shan *et al*., 2004; Whisson *et al*., 2007). Furthermore, a comparison of these cloned effector sequences to the completed genomes of two *Phytophthera* species (*P. sojae* and *P. ramorum*) identified 700 putative avirulence genes (Govers and Gijzen, 2006; Tyler, 2006). Analysis of these candidate avirulence genes alongside the originally cloned oomycetes effectors also revealed this common RXLR-dEER motif (Govers and Gijzen, 2006; Tyler, 2006). This motif has since been identified in several hundred effector candidates in *Phytophthora* species including 550 in *P. infestans* (Yu *et al*.,

2012). A role in translocation was initially hypothesised due to similarity to a motif for cross membrane transport of proteins into human erythrocytes from the malaria parasite (Rehmany *et al*., 2005; Tyler, 2006). This was experimentally demonstrated for the oomycete RXLR motif by the autonomous transport of the GFP::RXLR-dEER construct (cloned from Avr1b-1) into soybean root cells (Dou *et al*., 2008). In general, the RXLR-dEER motif is preceded by a signal peptide for translocation of the effector from the host and followed by an effector domain, which carries out the functional host interactions in the host (Figure 2).

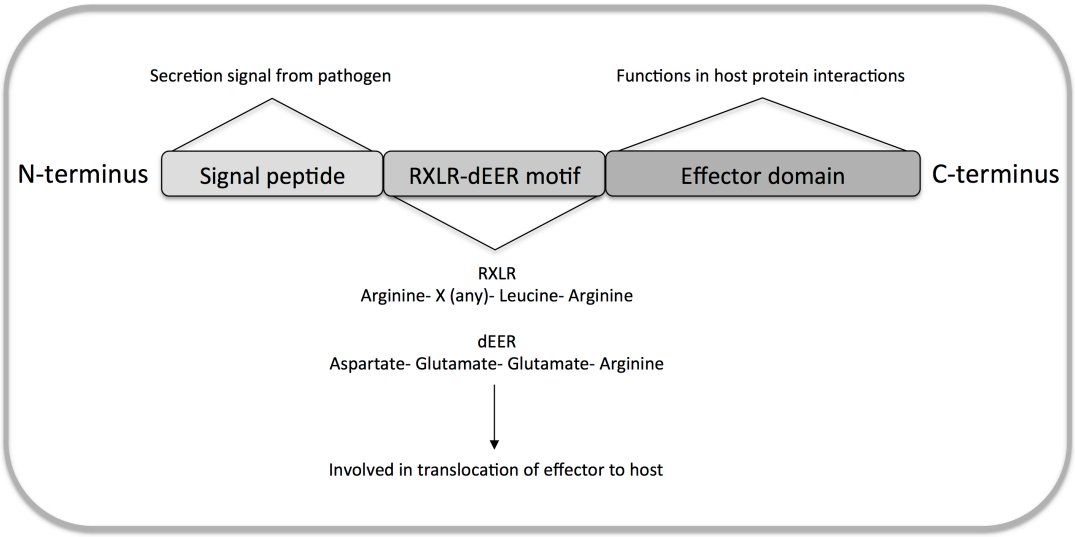

Figure 2. The general structure of an oomycete RXLR-dEER effector protein. These effectors are generally characterised by three domains with specific functions as illustrated.

The identification of the RXLR-dEER motif has been key to the prediction of further effector candidates from oomycete genome sequences leading to further insights into their function (Baxter *et al*., 2010; Coates and Beynon, 2010). The completion of the genome sequence of *Hpa* isolate Emoy2 facilitated the prediction of at least 134 putative effectors and more detailed genetic comparisons of oomycetes pathogens and RXLR effectors (Baxter *et al*., 2010). Analysis of these putative effectors highlighted the contrasting evolutionary pressures on oomycetes RXLR effectors. It was shown that only 36% of these *Hpa* effectors had significant similarity (i.e. greater than 30%) to any of the *Phytophthora* species (Baxter *et al*., 2010; Jiang *et al*., 2008). Despite this apparent low level of similarity at a genetic level, it has since been demonstrated that these effectors could have structural relatedness at a protein level. For instance, the effector AVR3a11 (*Phytopthora*) and a domain from ATR1 (*Hpa*) were independently shown in separate studies to have similarity to a cyanobacterial four bundle helix protein (Boutemy *et al*., 2011; Chou *et al*., 2011; Win *et al*., 2012b).

Overall, the large RXLR family of oomycete effector proteins provides a wealthy resource to examine their function, host interactors and the role of these targets in host immunity. Since their identification, many of these oomycetes effectors have been confirmed and characterised with alternative techniques such as investigating their effect on hypersensitive response (HR) -like cell death in *Nicotiana benthamiana* (Anderson *et al*., 2012). Large-scale yeast two-hybrid screens with oomycete effectors alongside contrasting bacterial effectors (*P. syringae*) revealed an overlap in the plant protein interactors with repeatedly targeted hubs, despite varying lifestyles and evolutionary distance (Mukhtar *et al*., 2011). This suggests that despite the apparent diversity of effectors, common patterns are likely to unify effector interactions. Therefore, insights from the study of oomycete RXLR-dEER effectors have potential applications for a better knowledge of the infection process of economically significant oomycetes pathogens and towards enhanced understanding of the plant immune network.

1.2.4 Effector-triggered immunity (ETI)

Effectors may enhance host susceptibility without host detection, although plants have evolved receptors for detection of these pathogenic proteins, triggering an immune response. The ETI response is of a higher magnitude than PTI and often induces a hypersensitive response (HR) leading to cell death (Figure 2; Jones and Dangl, 2006). This is beneficial in the context of defence against biotrophic invaders in which case tissue death limits the course of infection. Plants detect effectors with resistance (R) proteins (Dangl and Jones, 2001; Jones and Dangl, 2006; van der Biezen and Jones, 1998). These proteins often show a cytoplasmic localisation and a large class comprise of nucleotide binding (NB) and LRR domains similar to PTI receptors (Dodds and Rathjen, 2010). These NB-LRR proteins (also referred to as nucleotide-binding adaptor shared by APAF-1, R proteins, and CED-4 or NB-ARC) are a subclass of the STAND (signal transduction ATPases with numerous domains) superfamily, which combine varied functions as receptors, switches and response factors (Takken and Goverse, 2012). Upon detection of a pathogen effector or disruption to a host target, these proteins have been demonstrated to move from an auto-inhibited closed to open state (Gabriëls *et al*., 2007; Takken and Goverse, 2012). This initiating MAPK signalling cascades similar to those stimulated by PTI receptors and which may be interlinked (Gabriëls *et al*., 2007; Takken and Goverse, 2012).

A subgroup of NB-LRR proteins are characterised by an N-terminal Toll interleukin receptor (TIR) domain, which is similar to the Toll receptors identified in *Drosophila* (Figure 3; Sinapidou *et al*., 2004). These TIR-NB-LRR proteins include RPP1 in *Arabidopsis* which recognises the *Hpa* effector ATR1 (Sinapidou *et al*., 2004). The functions of Toll and Toll-like receptors (TLRs) in *Drosophila* include innate recognition and immune signalling response to pathogenic gram-positive bacteria and fungi, as well as developmental patterning (Valanne *et al*., 2011). An alternative NB-LRR subgroup is characterised by a coiled-coil (CC) domain, which is also observed in *Hpa* effector recognition receptors in *Arabidopsis* proteins including RPP8 (Figure 3; Sinapidou *et al*., 2004). It has been shown that the LRR domain is involved in the detection of effectors or their interactions, as mirrored by the function

of this domain in RLK-LRRs for recognition of MAMPs (Michelmore and Meyers, 1998; Staskawicz *et al*., 1995; Zipfel *et al*., 2004).

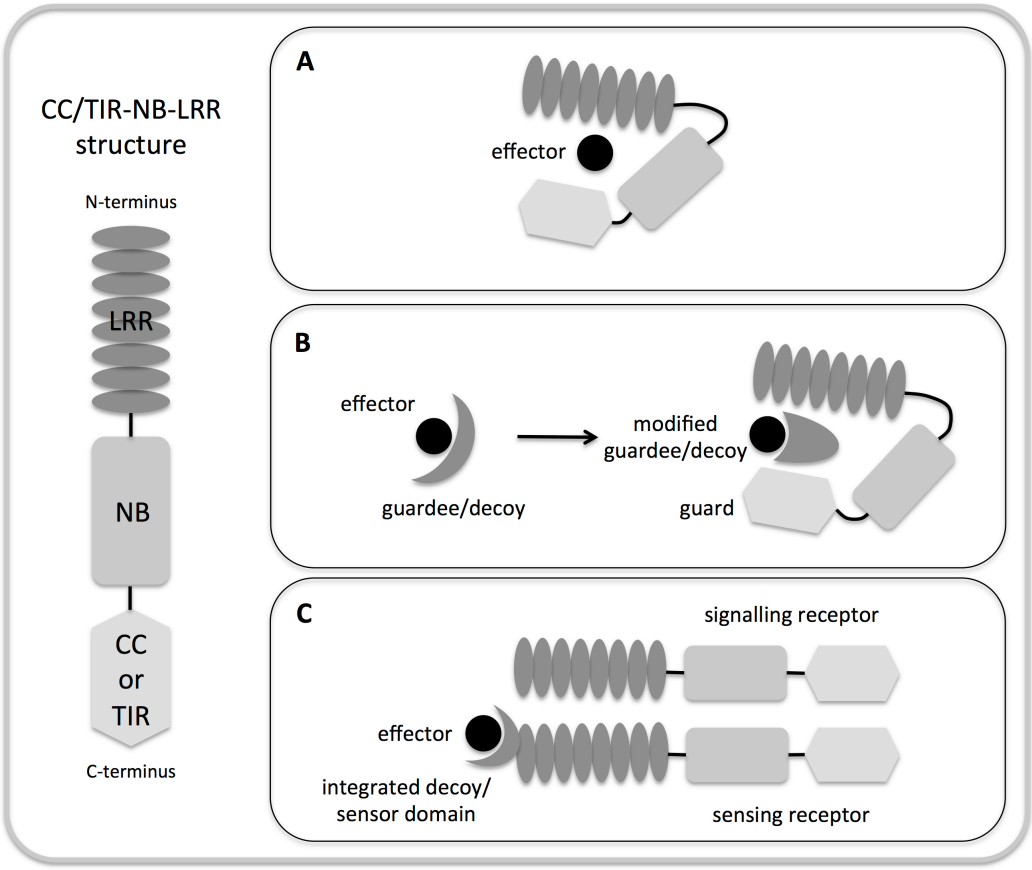

Figure 3. The structure and binding of a Toll interleukin receptor (TIR)/ coiled coil (CC) domain nucleotide binding leucine rich repeat (NB-LRR) protein. Four models of CC/TIR-NB-LRR receptor interactions with effectors are illustrated (two are summarised in **B**). **A** The effector may interact directly with the receptor. **B** The receptor may detect the interaction of the effector with another host target protein, which is a "guardee" or a "decoy" depending on the nature of its origin. **C** A sensing receptor has an "integrated decoy" or "sensing domain" which activates a signalling receptor.

Three models of effector interactions with R proteins have been proposed, each accounting for specific observations (Figure 3). The simplest model involves the direct perception of an effector by NB-LRRs often referred to as the gene-for-gene hypothesis (Keen, 1990). This is exemplified by *Xanthamonas campestris* pv. *vesicatoria* effector AvrBs2 (detected by BS2 in *Capsicum* spp.) which occurs across strains of the pathogen, the loss of which significantly reduces fitness of the pathogen leading to robust host resistance (Staskawicz *et al*., 1995). Alternatively, the "Guard Hypothesis" (as previously mentioned) explains interactions which do not occur directly between the NB-LRR and effector but rather the NB-LRR detects the presence of the effector through its disruption of an effector target in the host (Dangl and Jones, 2001). A key example of this model is the interaction between type III effector AvrRpt2 from *P. syringae* pv. *tomato* DC3000 which cleaves membrane associated protein RIN4 in *Arabidopsis* (Axtell *et al.*, 2002; Chrisholm *et al.*, 2004). RIN4 has a key role in regulating H^+-ATPase activity and hence stomatal aperture in response to infection (Liu *et al.*, 2009). The cleavage of RIN4 through the proteolytic activity of AvrRpt2 is detected by NB-LRR RPS2 triggering an immune response (Axtell *et al.*, 2002; Chrisholm *et al.*, 2004). A contrasting model suggests that effectors may also interact with a decoy protein that primarily acts as a mimic of the effector target (van der Hoorn and Kamoun, 2008). A new model has since been developed termed the "Integrated Decoy" and more recently streamlined as the "Sensor Domain" hypothesis (i.e. implying that the biochemical function of the domain may be retained), which proposes that a decoy or sensor domain could be an effector target fused to an NB-LRR protein, where a second is required to trigger signalling (Cesari *et al*., 2014; Wu *et al*., 2015). For example, it was recently shown that a WRKY transcription factor domain in the *Arabidopsis* NB-LRR RRS1-R is acetylated by *Ralstonia solanacearum* effector PopP2, which results in DNA disassociation (Le Roux *et al.*, 2015). RRS1-R is proposed to act as an integrated decoy, triggering activation of RPS4 mediated immunity via a receptor recognition/signalling complex formed through the TIR domains of these two NB-LRRs (Williams *et al.*, 2014; Le Roux *et al.*, 2015).

The interactions between effectors and R proteins has driven an evolutionary arms race between pathogens and hosts, as effectors may structurally evolve to avoid detection, while host R protein must also adapt to reflect these shifts (Figure 1;

Anderson *et al*., 2010). The *Arabidopsis* R gene *RPP13* was the most polymorphic gene identified in *Arabidopsis* at the time of discovery, highlighting the significant evolutionary pressure on immune related genes (Rose *et al*., 2004). It has been suggested in the birth-and-death model that R genes, which may be clustered at a genetic level, are "reservoirs of variation" and can be redundant or rapidly evolving depending on various factors, including the nature of the pathogen population (Michelmore and Meyers, 1998). This is reflected in the redundancy that is observed in large oomycetes effector repertoires (Birch *et al*., 2008). Therefore, effector evolution in *Phytophthora* species with multiple hosts is likely to be characterised by gene duplication events and rapid mutation rates, in order to subvert detection and ETI.

1.2.5 Hormones and the plant immune system

The plant immune system has close links with hormone signalling. Plant hormones (also known as phytohormones) regulate a broad diversity of processes, providing a network of host responses to invasion determined by the type of pathogen recognised. The following sections discuss the roles phytohormones in disease, although these are extensive and not limited to the specific hormones and examples described here.

1.2.5.1 Salicylic acid (SA)

SA has a key role in defence signalling and plants deficient in the hormone have a much higher susceptibility to a range of pathogens (including viruses, bacteria and fungi; Delaney *et al*., 1994). During an ETI response to biotrophic pathogen effectors, each subclass of NB-LRR receptors induces biosynthesis of SA through two largely distinct pathways (Vlot *et al*., 2009). As a general rule, these signal transduction pathways involve non-race specific disease resistance 1 (NDR1) with CC-NB-LRRs or enhanced disease susceptibility (EDS) 1 with TIR-NB-LRRs (Aarts *et al*., 1998; McDowell *et al*., 2000; Rustérucci *et al*., 2001). This is demonstrated by *Arabidopsis* RPP2 mediated resistance to *Hpa* isolate Cala2 (Aarts *et al*., 1998). The resistance was strongly suppressed in *eds1* lines but not with *ndr1* lines, although

exogenous application of SA could rescue this susceptible state (Aarts *et al*., 1998). This highlights the fact that these pathways act upstream of SA signalling during response to the *Hpa* infection in *Arabidopsis*, although it is unclear as to how EDS1 controls the biosynthesis of SA (Janda and Ruelland, 2015).

During pathogen recognition there is also an increase in intracellular calcium triggered by PRRs and R proteins (Seyfferth and Tsuda, 2014). This stimulates a calcium dependent signalling response, leading to the transcription of WRKY transcription factors, which in turn up-regulates key SA biosynthetic enzyme Isochorismate Synthase (ICS) 1 (Seyfferth and Tsuda, 2014). Additional regulators of SA during defence include MAPK cascades and interaction with other hormone pathways including but not limited to jasmonic acid (JA), abscisic acid (ABA) and ethylene (ET; Vlot *et al*., 2009). The pathways which link increased cytosolic SA during immunity to transcriptional response are mainly dependent on SA-induced conversion of oligomerized (i.e. a complex of four) non-expresser of pathogenesis related (NPR) 1 to a monomer (Janda and Ruelland, 2015). The monomerized NPR1 crosses the nuclear membrane and induces transcription of defence genes (Janda and Ruelland, 2015).

As well as having a central role in local immunity, SA synthesised at an infection site is transported in the phloem as mobile signals including methyl SA (meSA) and azelaic acid, increasing expression of SA associated genes such as Pathogenesis Related (PR) 1 in distal structures (Jung *et al*., 2009; Park *et al*., 2007; Spoel and Dong, 2012; Vlot *et al*., 2009). This systemic acquired resistance (SAR) has been shown to be a long lasting primed state which defends the plant against further pathogen attack (Vlot *et al*., 2009).

1.2.5.2 Jasmonic Acid (JA)

JA is also involved in the coordination of host response to pathogens with a close association to SA and ET. JA is associated with resistance to necrotrophic pathogens and defence against wounding caused by pests, such as herbivorous insects (Carvalhais *et al*., 2013). In a similar way to SA, there are several routes from

infection to production of JA. These pathways involve production of intracellular calcium via PTI and ETI receptors as previously described (Gao *et al*., 2014b). This signalling acts antagonistically to SA and the relative balance of each hormone is important in determining which type of response is favoured (Glazebrook, 2005). For example, *P. syringae* strains can secrete phytotoxin coronatine, which acts as a mimic of active jasmonate and competes for binding with the receptor complex system (Bender *et al*., 1999; Katsir *et al.*, 2008). Coronatine stimulates JA associated pathways and contributes to the suppression of SA signalling, which is crucial for host resistance to this biotrophic pathogen (Bender *et al*., 1999).

JA is synthesised through multiple steps involving enzymes including lipoxygenase (LOX) and allene oxide synthase (AOS) in the chloroplasts and 12-oxophytodienoate reductase 3 (OPR3) in the peroxisome (Schaller and Stintzi, 2009). The genes associated with the biosynthesis of JA are up-regulated during exogenous application, which suggests that JA biosynthesis is characterised by a positive feedback loop as with SA (Browse, 2009; Acosta and Farmer, 2010). However, an associated increase in JA is currently not supported by experimental evidence and there is likely to be post-translational modification of these JA biosynthesis proteins (Scholz *et al*., 2015). This means that increased expression of JA biosynthesis proteins does not necessarily lead to higher cellular JA levels.

The active (+)-7-iso-jasmonoyl-isoleucine (JA-Ile) form is able to interact with receptor coronatin insensitive 1 (COI1) to regulate the JAZ family of proteins (Browse, 2009). Under normal conditions, the JAZ repressor complex inhibits transcription at the promoters of these JA responsive genes (Kazan and Manners, 2012). The JAZ proteins interact generally with basic helix-loop-helix (bHLH) family transcription factors including MYC2 (Pauwels and Goossens, 2011). The JAZ proteins in turn recruit Novel interactor of JAZ (NINJA) and TOPLESS, which act as co-repressors (Robert-Seilaniantz *et al*., 2011). A high level of JA-Ile leads to the targeting of the JAZ proteins for degradation by the 26S proteasome via the SCF-COI1 E3 ubiquitin ligase complex (Robert-Seilaniantz *et al*., 2011). This causes the de-repression of JA associated transcription factors inducing a transcriptional response. The JAZ repressor complex is an additional level at which antagonism and convergence is observed between hormone the pathways (Kazan and Manners,

2012). For instance, JAZ proteins also inhibit the ET associated ETHYLENE INSESITIVE3 (EIN3) and EIN3-Like (EIL) proteins which are key regulators of ethylene associated genes including those associated with developmental, salt, light and defence responses (Song *et al*., 2014 & 2015). These EIN3/EIL proteins are critical in regulation of ET responsive genes such as ETHYLENE RESPONSE FACTOR1 (ERF1) through binding to regulatory elements including the EIN3-binding site (EBS; Song *et al*., 2014 & 2015).

1.2.5.3 Abscisic Acid (ABA)

ABA has a key function in coordinating plant development including germination and flowering, as well as response to abiotic stresses such as drought (Finkelstein, 2013). The hormone was identified in various contexts including from cotton in a cotyledon abscission assay and from sycamore extract, which acted as an embryo germination inhibitor in wheat (Cornforth *et al*., 1965; Cutler *et al*., 2010; Ohkuma *et al*., 1963). In the past half century ABA has become well established as a growth regulator in plants (Cutler *et al*., 2010). A large part of ABA biosynthetic pathways occurs in the chloroplast via carotenoids and the final oxidative steps in the cytosol through abscisic aldehyde (Finkelstein, 2013). It is thought that the vascular tissue is the main site of ABA biosynthesis during a dehydration response, with ABA being transported in the xylem and phloem to the sites of action (Seo and Koshiba, 2011). A study using ABA-responsive promoters fused to luciferase (LUC) –based reporters, showed radiation from the vascular tissue during water stress response towards guard cells in leaves (Christmann *et al*., 2005). The regulation of ABA is also known to depend on catabolic enzymes, which allow recovery following stress (Srivastava, 2002). The 8'-hydroxylation of ABA by cytochrome P450 CYP707A is a key step during catabolism, which is thought to occur in the ER (Endo *et al*., 2014).

The ABA agonist pyrabactin successfully identified candidate ABA receptors, known as the pyrabactin resistance 1/PYR1-like/regulatory components of ABA receptors (PYR/PYL/RCAR; Park *et al*., 2009; Santiago *et al*., 2012). These receptors bind to ABA via a pocket and in turn inhibit the protein phosphatase type 2C (PP2C) family which negatively regulate ABA pathways via sucrose non-

fermenting-1-related 2 (SnRK2) proteins (Ma *et al*., 2009; Park *et al*., 2009; Santiago *et al*., 2012). For example, the SnRK2 open stomata 1 (OST1) regulates slow anion channel 1 (SLAC1), which is associated with stomatal closure during dehydration (Mustilli *et al*., 2002).

The hormone has varied significance in the context of plant defence. These roles may generally arise from the links of the hormone to stress response and developmental processes, which may in turn have consequences during infection. There are some clear examples of direct links between ABA induced responses and pathogen defence. For example, ABA and the FLS2 induced pathways converge on OST1 during a PTI response promoting stomatal closure (Melotto *et al*., 2006). The stomata are a major route of entry into the leaf tissue meaning that their closure acts as a barrier to infection (Melotto *et al*., 2006). Furthermore, callose deposition is promoted by the PP2Cs ABA insensitive (ABI) 1 and 4 (Finkelstein, 2013). The signalling routes via these PP2Cs results in the accumulation of callose at the site of infection, which has a negative effect on fungal pathogens such as *Pythium irregulare* (Adie *et al*., 2007; Finkelstein, 2013). This callose matrix strengthens the cell wall and is often associated with accumulation of hydrogen peroxide, phenolics and antifungal compounds (Flors *et al*., 2005). This is similarly important during infection of *Arabidopsis* with *P. syringae* pv. tomato DC3000 with a sharp rise in ABA levels by 18 hours post infection in the host, which is also associated with attenuated callose deposition (de Torres-Zabala *et al.*, 2007). Furthermore it was shown that expression of the *P. syringae* effector *avrPtoB in planta* resulted in a substantial rise in ABA levels suggesting a clear link between the hormone and bacterial infection (de Torres-Zabala *et al.*, 2007).

Further roles of the hormone in defence arise from the cross talk between ABA and other phytohormone pathways. For instance, during a wounding response both JA and ABA target the transcription factor MYC2, synergistically promoting a transcriptional response (Koornneef and Pieterse, 2008). A close link between ABA and JA is also supported by their mirrored accumulation in *Arabidopsis* leaves infected with *P. syringae* pv. *tomato* DC3000, with a contrasting initial rise followed by a sharp decrease in SA (Fan *et al*., 2009). Therefore, the role of phytohormones is also likely to be variable over the course of infection.

1.2.6 Co-expression of hormone-related genes

Hormone-related genes show extensive co-regulation and co-expression, as these are commonly regulated by key transcription factors which may be antagonised by multiple hormones (Kuppusamy *et al*., 2009). These large groups of genes show similar expression profiles during response to biotic and abiotic stress. The DELLA proteins are regulated largely by gibberellin (GA) and interact with various transcription factors, acting as nuclear localised transcriptional regulators of broad processes such as root growth and response to necrotrophic fungi (Marín-de la Rosa *et al*., 2015). Therefore, there could be an additional theme to pathogen interference with hormone-related genes potentially at a level of spatially unified gene regulation (Beynon, pers. comm., 2012).

1.3 Transcription factory theory

Considerable recent evidence suggests that gene transcription is a collaborative rather than isolated process in prokaryotic and eukaryotic cells. Initial observations identified centres of concentrated DNA in bacteria using DNA staining and microscopy and these were termed “nucleoids”, reflecting their role similar to that of the eukaryotic nucleus (Eltsov and Zuber, 2006; Piekarski, 1937). Varied studies have provided evidence consistent with compartmentalisation of transcription, including observations of viral infection of eukaryotic cells, which are discussed in section 1.3.1. Model systems have included *Drosophila*, yeast and mammalian cell culture, although plant systems have since emerged in the context of application of these insights (Feng *et al*., 2014; Grob *et al*., 2013; Louwers *et al*., 2009; Schubert and Weisshart, 2015; Schubert *et al*., 2014). A crucial study focussed on RNA polymerase II (RNAPII), which transcribes mRNAs and small nuclear RNAs in eukaryotic cells (Wansink *et al*., 1993; Cramer *et al*., 2008). The localisation pattern of labelled nascent transcripts of RNAPII identified over 100 foci (Wansink *et al*., 1993). This highlighted a discrepancy between the number of actively transcribed genes and the distribution of RNAPII within the nucleus, which appeared to be inconsistent with a model of independent transcription of these genes (Wansink *et al*., 1993). Transcription factory theory proposes that genes are translocated to sites

of preassembled transcriptional components, which may contain roughly 30 active polymerases, as opposed to independent assembly onto active promoters throughout the nucleus (Cook, 1994; Jackson *et al*., 1998; Xu and Cook, 2008). In *Arabidopsis* nuclei, super-resolution microscopy showed that these RNAPII was concentrated in reticulate structures referred to as "transcription networks" (Schubert and Weisshart, 2015; Schubert *et al*., 2014).

The concept draws parallels to the nucleolus, in which RNA from nucleolar organiser regions (NORs) across multiple chromosomes is transcribed by RNAPI in a structured but non-membrane bound compartment (Osborne, 2014). While transcription factories are not defined by the same scale or composition as the nucleolus, it has been suggested that these are held on a nuclear substructure or nucleoskeleton indicating a more fixed rather than transient existence (Sutherland and Bickmore, 2009). This is exemplified by immunofluorescence experiments with mouse foetal cells, which showed that following heat shock (inhibiting transcription) the focal appearance of RNA polymerase I remained stable (Mitchell and Fraser, 2008). This further suggests that these locations of concentrated active RNAPII are not merely transient aggregations on actively transcribed promoters (Mitchell and Fraser, 2008). Despite potentially existing as relatively stable structures, transcription factories are thought to be dynamic centres in which microenvironments of transcription factors define the genes present (Figure 4; Schoenfelder *et al*., 2010). An illustration of a transcription factory is shown in Figure 4.

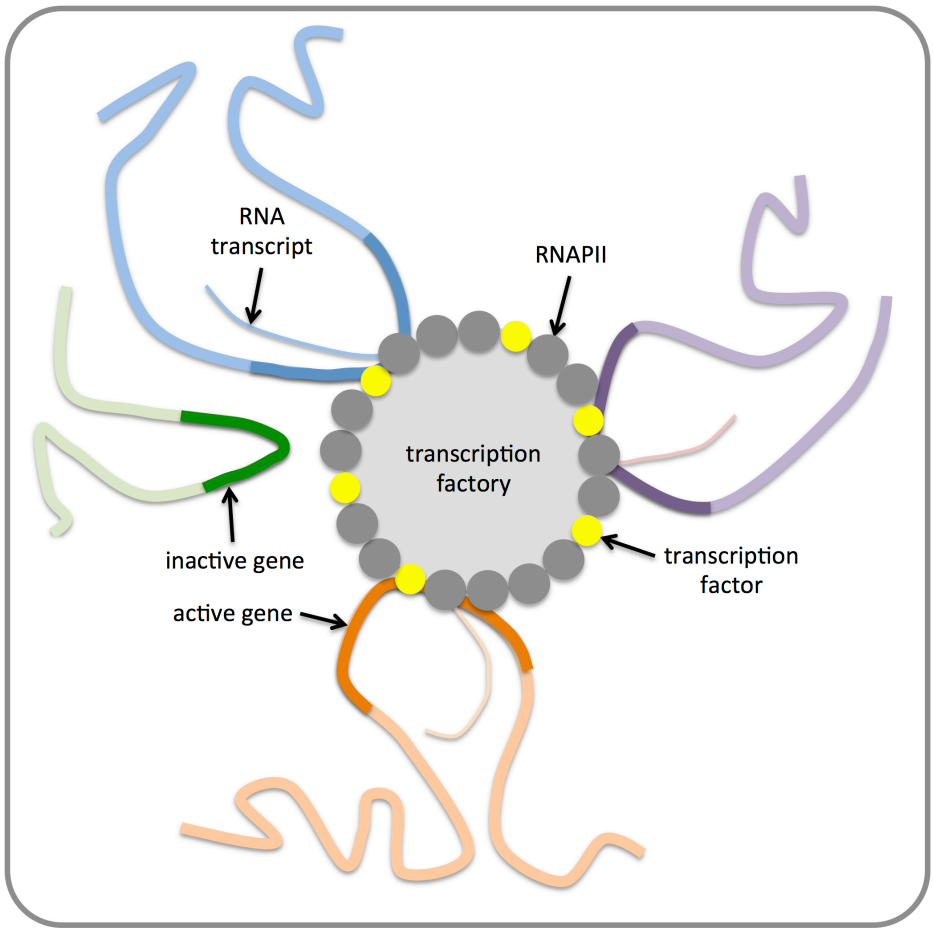

Figure 4. The key features of a transcription factory. Chromatin may form loops as genes associate with transcription factories. These transcription factories contain transcription factors, RNA polymerase II (RNAPII) and the active genes. These genes are thought to reel through RNAPII as the transcription factory is anchored to a nuclear substructure. The association of genes with the transcription factory may be transient as illustrated by active and inactive genes.

1.3.1 Evidence for transcription factories from diverse techniques

As previously mentioned, a wealth of cell biology investigations have analysed the mechanisms of transcription deduced from biochemical studies in an *in vivo* context. This led to varied observations that are not consistent with a theory of active transcription occurring independently throughout the nucleus. For instance, a study which investigated viral replication in the eukaryotic nucleus showed highly focussed sites of transcription within the host nucleus, which were termed factories (Cairns, 1960; Cook, 2010). Replicating DNA during infection of HeLa cells with vaccinia virus was labelled with H^3-Thymidine and visualised with autoradiography and showed that each viral particle initiates a unit of synthesis of viral DNA, which progressively grows over time (Cairns, 1960). A possible explanation for this observation is that the host transcriptional machinery is not evenly dispersed within the nucleus. Therefore, the observation of these discrete units during viral replication is an artefact of host transcriptional organisation and architecture.

These techniques for visualisation of transcription by labelling and microscopy were similarly applied directly to HeLa cells, giving rise to fundamental research that assisted in consolidating transcription factory theory. Early techniques in HeLa cells involved immobilising, H^3-uridine labelling the nascent RNA, followed by digestion and removal of DNA, which revealed a network of retained RNA in a structure consistent with transcription factories (Chakalova and Fraser, 2010; Jackson and Cook, 1985). This was optimised in further studies which aimed to minimise disturbance to the cell during the procedure (Chakalova and Fraser, 2010). A system was developed to encapsulate and bathe S phase cells with biotin-11-dUTP during transcription, followed by immunolabelling and visualisation by microscopy (Hozák *et al*., 1993). This found approximately 150 sites of transcription per cell, which complemented the findings of the previous study which directly visualised RNAPII (Hozák *et al*., 1993; Wansink *et al*., 1993).

Another style of technique has focussed on characterising the observed looping structures that have been suggested to be a key feature of chromatin during active gene transcription (Palstra, 2009). Chromosome conformation capture (3C) and associated technologies have become core techniques for studying individual gene

interactions, through to chromosomal arrangements (Dekker *et al*., 2002). The technique is based on the fixation of chromosome arrangement using formaldehyde, which creates a snapshot of transcription through interlinking genes physically close potentially due to their co-localisation at transcription factories (Dekker *et al*., 2002). Insights that have arisen from 3C technology include defining interactions that occur between the locus control region (LCR) that controls expression of the T helper cell 2 (Th2) cytokine genes in mice (Spilianakis and Flavell, 2004). These cytokines are spaced over 120 kilobases and have also been shown to involve interaction between genes on separate chromosomes (Spilianakis *et al*., 2005). This highlights the specificity of interactions that occur at transcription factories, which may involve intra or inter-chromosomal contacts. Since the development of the technique a vast array of studies have adopted the method to address various questions relating to gene associations and chromosomal arrangements. The 3C technique and related methodologies are described in more detail in Chapter 4 of this thesis.

1.3.2 Specialisation of transcription factories?

It has been suggested that groups of genes that are functionally related may be transcribed at the same transcription factories (Xu and Cook, 2008). However evidence to support this hypothesis is currently inconsistent (Sutherland and Bickmore, 2009). It is well established that prokaryotic and eukaryotic chromosomes are characterised by enhancer and insulator regions that may be separated by large physical distance from their associated gene promoters, which is particularly the case in animal models (Blackwood and Kadonaga, 1998; Dandanell *et al*., 1987; Krivega and Dean, 2012; Liu *et al*., 2001; Sipos and Gyurkovics, 2005). The chromatin-looping model suggests that intervening chromatin regions are physically moved aside during enhancer and promoters interactions (Krivega and Dean, 2012). This highlights a possible role for specialised transcription factories at which related genes and associated genetic elements physically associate.

Similarly to the Th2 region, studies have analysed the haemoglobin subunit beta (*Hbb*) genes and associated LCR in mice, generally suggesting that these genes may preferentially localise to the same transcription factories upon activation (Palstra,

2009). A particular study adopted methods including enhanced-circularized chromosome conformation capture (4C; for analysis of global physical chromatin interactions from a defined locus) and RNA fluorescent *in situ* hybridisation (FISH) to analyse the association of *Hbb* genes (Schoenfelder *et al*., 2010). The Kruppel-like factor 1 (also referred to as erythroid Kruppel-like factor (EKLF)) mutant *klf-1* was shown to have low expression of *Hbb* genes, consistent with the role of the transcription factor in controlling their expression (Nuez *et al*., 1995; Schoenfelder *et al*., 2010). A consistent overlap in fluorescence was observed for probes specifically hybridising to *Hbb* genes in RNA FISH (Schoenfelder *et al*., 2010). Furthermore, physical contacts were observed in enhanced 4C between the *Hbb* genes and others previously found to be regulated by Klf-1 (Schoenfelder *et al*., 2010). It was hypothesised that specialisation of transcription factories could be a logical mechanism of controlling transcription of co-regulated genes. As previously mentioned, a balance of transcription factors may form a microenvironment for controlling transcription (Schoenfelder *et al*., 2010; Sutherland and Bickmore, 2009). This could enable fine-tuning of gene regulation of groups of specialised genes (Edelman and Fraser, 2012). This may promote efficient cellular response to environmental fluctuations for groups of related genes and would facilitate rapid and unified response to specific stimuli.

1.4 Hormone induced chromatin rearrangements in mammalian cells

Currently there is some evidence to suggest that hormones induce chromatin reorganisation in mammalian cells on a large scale. Chromatin has been shown to arrange in highly looped structures based on active or inactive status (Cheutin and Cavalli, 2014). These are known as topologically active domains (TADs), within which loci most frequently interact (Dekker *et al*., 2013). A study in human mammary epithelial cells (HMEC) found a rapid estradiol-induced association of genes thought to co-localise to interchromatin granules, in which transcriptional elongation and pre-mRNA splicing factors are concentrated (Hu *et al*., 2008). However, a subsequent investigation using 3D FISH with probes for hormone associated genes in HMEC and cancer cells found no evidence of spatial association (Kocanova *et al*., 2010). A more recent investigation suggested that the activation of

TADs by hormones resulted in the induction of a large-scale change in chromatin conformation and higher frequency of contacts between loci within these domain (Le Dily *et al*., 2014). Furthermore, the activation of these TADs during treatment increased DNase I sensitivity suggesting that the chromatin state shifted to a more open form, which was also correlated with a relative change in interaction frequency as observed with Hi-C (an enhanced 3C method; Le Dily *et al*., 2014). Overall, this evidence suggests that hormones could have a significant effect on spatial gene regulation and gene interactions.

1.5 A potential role for effectors in targeting transcription factories?

Investigations focussing on pathogen effector interactions have identified targets at the level of the host transcriptional machinery. For example, it has been shown that a *Hpa* effector can interact with the mediator complex subunit MED19a, in order to manipulate the balance between JA and SA to favour pathogen survival (Caillaud *et al*., 2013). Mediator (MED) subunits form a complex acting as an interface between specific transcription factors and basal transcriptional machinery assembled on a promoter, facilitating either activation or repression of target genes (Mathur *et al*., 2011). Specific combinations of these MED subunits (of which there are thought to be 34 in plants) are required for genes involved in related processes although individual subunits can have overlapping roles (Mathur *et al*., 2011). For instance, MED2, MED14 and MED16 are involved in cold response in *Arabidopsis*, although MED16 also has a role in dark associated genes with a different group of MED subunits (Hemsley *et al*., 2014).

Therefore, specialisation of transcription factories could provide a framework to explain the impact of targeting individual elements of the transcriptional machinery on the expression of host immune-related genes. The transcriptional machinery in plants involves the cooperation of various different cofactors, the mediator complex, RNAPII and transcription factors (Samanta and Thakur, 2015). However, few studies at the beginning of this project had focussed on understanding chromatin arrangements and transcription factories in plants (Hövel *et al*., 2012). If further evidence supports a model of the spatially co-ordinated expression of related genes,

then this could raise many questions as to the relevance of this in a pathological context. During PTI, the host recognises fundamental features of potential pathogens and capitalises on their inadaptable nature. Therefore, the tables may have been turned and pathogens could hijack a core feature of eukaryotic gene transcriptional regulation in order to favour infection.

1.6 Scope of this project

The project aimed to investigate the interaction of a putative *Hpa* effector with the host immune network. The effector HaRxL14 has been shown to have multiple targets in yeast two-hybrid screens (which identify protein-protein interactions). This effector structurally comprises of an N-terminal signal peptide, RXLR-dEER domain and a C-terminal effector domain. A specific interaction has been confirmed by yeast two-hybrid with the host protein phosphatase type-2CA (PP2CA; AT3G11410; Steinbrenner, Braun and Beynon, pers. comm., 2013), which is involved in ABA and metabolic signalling. Characterising this interaction was a potentially interesting line of investigation, given previously reported results suggesting that ABA could have an important role in host defence.

Additionally, the project focussed on optimising a Hi-C related method (sequence capture of multiple regions interacting with bait loci; SCRIBL) for use with *Arabidopsis*, in which interacting regions of chromatin are enriched and identified using next generation sequencing (courtesy of Stefan Schoenfelder and Peter Fraser, Babraham Institute, University of Cambridge). During the initial stages this project, *Arabidopsis* had recently become subject to 3C-type analysis. During the course of the project, the publication of Hi-C in *Arabidopsis* gave insights into the overall chromosome conformation in plants (Schubert *et al*., 2014). This project aimed to optimise SCRIBL to determine whether response to hormones in plants could involve changes in the physical environment and the spatial association of co-regulated genes. An observed physical association of hormone-related genes could indicate a role for specialised transcription factories in plants. This could have relevance to both immune networks and in the context of pathogen effector targets.

1.7 Overall project aims

- To confirm and characterise the interaction of *Hpa* effector HaRxL14 with a putative *Arabidopsis* host target PP2CA (AT3G11410), which is involved in ABA and metabolic signalling.

- To optimise SCRIBL for use with *Arabidopsis* in order to examine the effect of hormone induction on spatial gene interactions.

2 Materials and methods

2.1 Plant materials and maintenance

2.1.1 Growth and maintenance of *Arabidopsis*

Arabidopsis seeds were sown at a high density onto Intercept® (Everris) treated compost and stratified at 4 °C for 2 to 4 days. Trays were transferred to a growth room with lids to maintain a high humidity, under light conditions of 100 μmol m^{-2} s^{-1} at 20 °C and 10 hour light cycles. Seedlings were transplanted into individual modules at approximately 10 days post germination.

The following previously generated *Arabidopsis* T-DNA homozygous insertion lines were used in these experiments (Table 1).

Table 1. The sources of the *Arabidopsis* T-DNA insertion lines used for analysis.

***Arabidopsis* T-DNA insertion lines**	**Background**	**Supplied/Generated by**
pp2ca-1	Col-0	Julian Schroeder
pp2ca-2	Col-0	As above
35S::*PP2CA*	Col-0	As above
35S::*HA*::*GFP*	Col-4	Jens Steinbrenner, Matthew Watson, Tina Payne
35S::*HA*::*HaRxL14* (line 1)	Col-4	As above
35S::*HA*::*HaRxL14* (line 2)	Col-4	As above
35S::*HA*::*HaRxL14* (line 3)	Col-4	As above
35S::*HaRxL14*	Col-4	As above
fls2	Col-4	Nottingham *Arabidopsis* Stock Centre (NASC)
eds1	Ws-0	As above

2.1.2 Maintenance of *Arabidopsis* cell suspension culture

2.1.2.1 Preparation of *Arabidopsis* cell suspension culture media

Arabidopsis cell suspension culture (from *Landsberg erecta* callus) was a kind gift from Dr. Alessandra Devoto (Royal Holloway, University of London) and was maintained with a hormone-supplemented culture medium (Table 2).

Table 2. Materials required for preparation of a litre of *Arabidopsis* cell suspension culture medium.

Component	**Amount per litre**
Murashige and Skoog basal salts with minimal organics (Sigma-Aldrich)	4.4 g
Sucrose (Sigma-Aldrich)	30 g
1-Naphthylacetic acid 1 mg/mL (Sigma-Aldrich)	500 µL
Kinetin 1 mg/mL (Sigma-Aldrich)	50 µL

The components specified in Table 2 were dissolved in 900 mL deionised (DI) water and the pH was adjusted to 5.6 to 5.7 at 22 ^{o}C with 1 M NaOH. The final volume was adjusted to a litre with DI water and autoclaved. The media was cooled rapidly and stored at 4 ^{o}C.

2.1.2.2 Growth and sub-culturing of *Arabidopsis* cell suspension culture

The *Arabidopsis* cell suspension culture was sub-cultured after periods of 7 days of growth. In a laminar flow cabinet, 15 mL of 7-day-old culture and 100 mL of *Arabidopsis* cell suspension culture medium (as described in section 2.1.2.1) were transferred into a pre-autoclaved 250 mL Erlenmeyer flask sealed with a quadruple layer of foil. The opening of the flask and foil cover were sterilised with a flame during the sub-culturing procedure. The cells were cultured under constant light, a temperature of 22 °C and shaking at 115 rpm.

2.1.2.3 Methyl Jasmonate (MeJA) induction of *Arabidopsis* cell suspension culture

In a laminar flow cabinet, a 10-day-old culture was sub-cultured with 45 mL of culture and 300 mL *Arabidopsis* cell suspension culture medium (as described in section 2.1.2.1). This was divided into aliquots of 24 mL in 50 mL Erlenmeyer flasks, ensuring the cells were homogenised by gentle swirling between taking each aliquot. The flasks were sealed with a quadruple layer of foil. The cultures were maintained under identical conditions to those previously stated in section 2.1.2.2 with the exception of shaking speed, which was increased to 125 rpm to maintain a homogenous distribution of the cells in the smaller flasks.

After 3 days, the *Arabidopsis* cells were treated with a filter sterilised stock preparation of 10 mM MeJA (Sigma-Aldrich) in absolute ethanol for a final concentration of 50 μM MeJA, according to conditions described for microarray experiments in Louwers *et al*. (2009). Mock treatments were carried out with the same volume of sterile water in lieu of MeJA in absolute ethanol. The cultures were harvested at 0 and 7 hours post MeJA and mock treatment. A sample of 4 mL was taken for RNA extraction, which was filtered through a double layer of miracloth (Merck Millipore) and flash frozen on liquid nitrogen. The remaining 20 mL was fixed with formaldehyde for analysis of chromatin interactions (section 2.7).

2.2 Nucleic acid methods

2.2.1 RNA

2.2.1.1 RNA extraction

2.2.1.1.1 *Arabidopsis* cell suspension culture

Arabidopsis cells were ground with liquid nitrogen in a pre-chilled pestle and mortar, which were sterilised at 180 °C for at least 4 hours. The RNA was extracted from 100 to 150 mg of ground cells with 1 mL TRIzol® (Life Technologies), which was mixed with a vortex mixer for twenty seconds, followed by incubation at room temperature for five minutes. This process was repeated following the addition of

200 µL chloroform. The phases were separated by centrifugation at 21,000 x g for 15 minutes at 4 °C. The upper phase was carefully removed and mixed with an equal volume of 70% (v/v) ethanol. This mixture was applied to an RNeasy® spin column (Qiagen) and purified according to the manufacturer's protocol. An on-column DNase treatment was performed and the RNA was eluted in 40 µL nuclease-free water, which was reapplied to the column to concentrate the eluted RNA. The RNA concentration was determined with a UV-Vis spectrophotometer (NanoDrop, Thermo Scientific) and stored at -80 °C.

2.2.1.1.2 *Arabidopsis* seedlings and mature leaves

Arabidopsis leaves were frozen on liquid nitrogen and ground using a bead beating method with two 5 mm glass beads per microfuge tube. This consisted of two bursts at a frequency of 25 hz for 30 seconds with chilled adapters in a mixer mill (Retsch). The beads were prepared by baking at 180 °C for at least 4 hours and were chilled with liquid nitrogen. The RNA was extracted from the ground leaf material using the TRIzol® method previously described in section 2.2.1.1.1.

2.2.1.2 Synthesis of cDNA

The extracted RNA was diluted to a concentration of 1 µg/µL for the reverse transcription reaction. A reaction with 1µg of RNA was set up for gDNA removal, followed by cDNA synthesis using the QuantiTect Reverse Transcription Kit (Qiagen) according to the manufacturer's protocol. The synthesised cDNA was stored at -20 ^{o}C.

2.2.2 NimbleGen Microarrays

2.2.2.1 Preparation of samples

Two week-old *Arabidopsis* seedlings were grown for this microarray experiment according to section 2.1.1. Three replicate modules of seedlings were grown and harvested with liquid nitrogen for T-DNA insertion *Arabidopsis* lines according to

the experimental design in section 3.7.1 without treatment (Table 1). RNA was extracted according to section 2.2.1.1.2. The quality of the RNA was verified using an RNA 6000 Nano kit (Agilent) with an Agilent Bioanalyser.

2.2.2.2 Amplification and labelling cDNA

A dilution of 50 ng/µL was prepared for each RNA sample. An input volume of 1 µL was used for the generation of first and second strand cDNA. Single primer isothermal amplification (SPIA) amplification and modification was performed using the Ovation® Pico WTA System (Nugene). The amplified SPIA cDNA was purified using QIAquick columns (Qiagen). The cDNA was loaded onto the columns, washed twice with 80% (v/v) ethanol and eluted with 30 µL nuclease-free water. The cDNA concentration was determined with a UV-Vis spectrophotometer (NanoDrop, Thermo Scientific).

Labelling reactions with cyanine dye Cy3 were prepared for the two-stranded cDNA using the NimbleGen one-colour DNA labelling kit (Roche) as described in the manufacturer's protocol. This process was carried out under low light conditions and the cDNA pellets were dried using a SpeedVac™ (Thermo Scientific). These cDNA pellets were rehydrated in 25 µL PCR grade water and the concentration determined by UV-Vis spectrophotometer (NanoDrop, Thermo Scientific). Aliquots were prepared equivalent to 4 µg of labelled cDNA sample and these were dried as previously described and stored at -20 ^{o}C.

2.2.2.3 Preparation and scanning of microarrays

The hybridisation system was equilibrated to 42 ^{o}C and the Cy3-labelled cDNA pellets were rehydrated in 3.3 µL water (VWR) and prepared for hybridisation onto two 12X135K array slides according to the manufacturer's protocol (Roche). The Cy3-labelled samples were incubated on the arrays for 16 to 20 hours.

The slides were washed using the NimbleGen Wash Buffer Kit (Roche). The slides were detached from the mixer while immersed in wash buffer I at 42 ^{o}C and the

remaining washes were carried out as described in the manufacturer's protocol (Roche). The slides were spun dry with a Microarray Dryer (Arrayit) for 30 seconds. The dried slides were loaded into a NimbleGen MS 200 Microarray Scanner (Roche) and scanned according to the manufacturer's protocol.

2.2.3 DNA

2.2.3.1 Polymerase chain reaction (PCR)

The relative gene expression was examined between biological replicates under different treatment conditions semi-quantitatively by PCR. This was used to determine whether a transcriptional response to MeJA treatment was detectable in *Arabidopsis* cell suspension culture.

Table 3. The primer sequences for genes tested for relative gene expression by PCR for MeJA induction experiment with *Arabidopsis* cell suspension culture[1].

Name	Gene ID	Orientation	Sequence (5'-3')
ACT2	AT3G18780	Forward	TGTCGCCATCCAAGCTGTTCTC
ACT2	AT3G18780	Reverse	ATCACCAGAATCCAGCACAATACCG
JAZ1	AT1G19180	Forward	TGGAGATCTGAGCTTAGGAATGGC
JAZ1	AT1G19180	Reverse	ATGGTTGTTGTCGGCTGACGTG
JR1	AT3G16470	Forward	CCTGTCCTTGGAAGTGATCAT
JR1	AT3G16470	Reverse	TCATCTGGTCCAAGCACAAAC
OPR3	AT2G06050	Forward	TACTTCACGTGGGAACCATCGG
OPR3	AT2G06050	Reverse	GGACGTGCTTCTCATGCAGTGTATC
PR1	AT2G14610	Forward	TACGCTGCGAACACGTGCAATG
PR1	AT2G14610	Reverse	GCACATCCGAGTCTCACTGACTTTC
VSP1	AT5G24780	Forward	ATGGGCTGATTTGGTTGAGGA
VSP1	AT5G24780	Reverse	TGAAATGGATACAAGGGGACA

[1] The forward and reverse primers for each are transcript specific and designed to amplify cDNA synthesised from mRNA. These primers were designed using QuantPrime software available online (Arvidsson *et al.*, 2008). The primers for amplification of JR1 and VSP1 were designed using this software by Jens Steinbrenner.

The PCR reactions were set up with the primers in Table 3. A master mix was prepared with the following components per reaction: 1 µL $MgCl_2$ (Invitrogen), 2 µL PCR buffer (Invitrogen), 13.25 µL sterile water, 0.25 µL Taq polymerase (Invitrogen), 1 µL template cDNA, 0.5 µL dNTPs (Invitrogen) with 1 µL of each primer at 10 µM in sterile water.

The general PCR conditions were as follows: 95 ^{o}C for 5 minutes (initialisation), 95 ^{o}C for 30 seconds (denaturation), 57-62 ^{o}C for 30 seconds (annealing), 72 ^{o}C for 1 minute per kilobase depending on the insert size (elongation), 72 ^{o}C for 5 minutes (final elongation).

2.2.3.2 Cloning

For expression in *Nicotiana benthamiana*, *Arabidopsis* genes were cloned using the Gateway® system (Life Technologies). These genes were initially amplified with gene specific primers for addition of partial AttB1 and AttB2 sites. With *PP2CA*, a library of *Arabidopsis* cDNA was used as template. In the case of *HaRxL14*, template cDNA derived from PCR reactions which amplified effectors from genomic DNA isolated from *Hpa* isolate Emoy2 (Fabro *et al*., 2011). Jens Steinbrenner performed these PCR reactions for *PP2CA* and *HaRxL14*.

These reactions were cleaned-up with a PCR Purification Kit (Qiagen) and a second PCR reaction was set up with the primers shown in Table 4 for the addition of the full AttB sites for cloning into Gateway pDONR™/Zeo vector. Following amplification with incorporated AttB sites, the PCR reactions were run on an agarose gel (percentage agarose dependent on the fragment length) and the product of the predicted size was isolated by excision and cleaned using a column based gel purification kit (Qiagen). These PCR reactions and gel purifications were also performed by Jens Steinbrenner.

Table 4. The primer sequences for cloning *PP2CA* (AT3G11410) into the Gateway® system and for amplication of AttB1 and 2 sites. The AttB sites are required for cloning into the Gateway® pDONR™/Zeo vector. The *PP2CA* primer sequences were previously published (Lim *et al*., 2014). These PCR reactions were carried out by Jens Steinbrenner.

Primer	**Orientation**	**Sequence (5'-3')**
PP2CA	Forward	CACCATGGCTGGGATTTGTTGCGG
PP2CA	Reverse	TTAAGACGACGCTTGATTATTCCTC
AttB1	Forward	GGGGACAAGTTTGTACAAAAAAAGCAGGCT
AttB2	Reverse	GGGGACCACTTTGTACAAGAAAGCTGGGT

The gene with AttB sites was then transferred into an entry pDONR™/Zeo vector in a BP reaction with Gateway® BP clonase II enzyme mix according to the manufacturer's protocol (Life Technologies). The products of this reaction were transformed into *Eschericia coli* as described in section 2.3.1.1 and the plasmid purified according to section 2.3.3.

A second reaction using Gateway® LR clonase II enzyme mix was used to transfer the gene into the destination vector according to the manufacturer's protocol (Life Technologies; Table 5). The product of this reaction was transformed into *E. coli* as described in section 2.3.1.1 and the plasmid purified according to section 2.3.3. The purified vector was then transformed into *Agrobacteria tumefaciens* as described in section 2.3.1.2.

Table 5. Gateway® destination vectors for expression of tagged *Arabidopsis* proteins in *N. benthamiana*. Full details are given of promoter, tag, bacterial resistance and a reference for their source.

Gateway® Destination Vector	**Promoter / Tag**	**Bacterial Resistance**	**Reference**
pK7FWG2	35S / N-terminal GFP	Spectinomycin	(Karimi *et al*., 2002)
pK7RWG2	35S / N-terminal RFP	Spectinomycin	As above
pEarlygate201	35S / N-terminal *HA*	Kanamycin	(Earley *et al*., 2006)
BIFP1	35S / C-terminal eYFP (N-terminus)	Spectinomycin	François Parcy, University of Grenoble, France
BIFP2	35S / N-terminal eYFP (N-terminus)	Spectinomycin	As above
BIFP3	35S / N-terminal eYFP (C-terminus)	Spectinomycin	As above
BIFP4	35S / C-terminal eYFP (C-terminus)	Spectinomycin	As above

2.3 Microbial techniques

2.3.1 Bacterial transformations

2.3.1.1 Transformation of *E. coli*

Chemically competent *E. coli* strain DH5α cells (Bioline) were transformed by heat shock. The cells were incubated on ice with vector DNA for 30 minutes, followed by a heat shock at 42 °C for 30 seconds. After a 10 minute incubation on ice, 9X volume of Super Optimal broth with Catabolic repression (SOC) medium was added to the reaction and the bacterial cells were incubated for one hour at 37 °C (Table 6). The transformation reactions were spread onto Lysogeny Broth (LB) agar plates with appropriate antibiotics and incubated overnight at 37 °C (Table 6).

Table 6. The composition of media for culturing *E. coli* and *A. tumefaciens.*

Component	**Amount (/L)**
LB	
Tryptone	10 g
Yeast extract	10 g
Sodium chloride	10 g (or 5 g for low salt)
SOC	
Yeast extract	5 g
Tryptone	20 g
Sodium chloride	0.584 g
Potassium chloride	0.186 g
Magnesium sulphate	2.4 g
Glucose 20% (w/v)	20 mL
YEB	
Sucrose	5 g
Peptone	5 g
Beef extract	5 g
Yeast extract	1 g
Magnesium sulphate heptahydrate	0.049 g
pH adjusted to 7.2	
Microbiological agar	15 g

A single colony was isolated and transferred into a liquid culture of LB with an appropriate antibiotic and cultured overnight at 37 °C with shaking at 220 rpm. An aliquot of 500 µL of culture and 500 µL 80% (v/v) glycerol were mixed in a microfuge tube and stored at -80 °C as a stock.

2.3.1.2 Transformation of *A. tumefaciens*

Destination vectors were transformed into *A. tumefaciens* strain GV3101 by chemical transformation. An aliquot of 100 µL of *A. tumefaciens* strain GV3101 was incubated with 1 µg of the purified destination vector on ice for 5 minutes. The transformation reaction was heat shocked by incubation on liquid nitrogen for 5 minutes, followed by incubation at 37 ^{o}C for 5 minutes. The cells were incubated on ice for 2 minutes followed by addition of 900 µL of YEB media (Table 6). The reactions were incubated at 28 ^{o}C with shaking for 2 to 3 hours, followed by centrifugation at 900 x g for 30 seconds. The cells were resuspended in 10 µL of supernatant and spread onto YEB plates (Table 6) containing appropriate antibiotics and incubated at 28 ^{o}C for at least 16 hours.

A single colony was isolated and transferred into a liquid culture of YEB media with appropriate antibiotics and cultured for approximately 20 hours at 28 °C with shaking at 220 rpm. An aliquot of 500 µL of culture and 500 µL 80% (v/v) glycerol were mixed in a microfuge tube and stored at -80 °C.

2.3.2 Colony PCR

A small scrape of cells (using an inoculation loop) was suspended in 75 µL sterile water. The cells were incubated at 95 ^{o}C for 20 minutes. A PCR mix was prepared as follows: 10 µL Biomix Red (Bioline), 1 µL of each AttB1 and AttB2 primers (Table 4), 5 µL cell suspension mix, 3 µL sterile water. The conditions for the PCR reactions are given in section 2.2.3.1.

2.3.3 Plasmid Purification

Plasmid DNA from a 5 mL overnight culture of transformed *E. coli* was purified using the GeneJET plasmid purification kit (Thermo Scientific) and eluted in 30 µL of sterile water. The DNA concentration was quantified using a UV-Vis spectrophotometer (NanoDrop, Thermo Scientific). The eluted DNA was stored at -20 °C prior to further analysis.

2.4 Cell biology methods

2.4.1 Infiltration of *A. tumefaciens* into *N. benthamiana*

A glycerol stock (as prepared in section 2.3.1.2) of transformed *A. tumefaciens* and a stock harbouring p19 (a silencing suppressor) were streaked onto YEB agar plates with appropriate antibiotics (Voinnet *et al*., 2003). A single colony was isolated to prepare a culture in liquid YEB media with appropriate antibiotics. The bacteria were cultured for approximately 20 hours at 28 °C with shaking at 220 rpm.

The bacterial cells were collected by centrifugation at 3,500 x g for 10 minutes and the supernatant was removed. The bacterial pellet was gently resuspended in half the original culture volume of infiltration buffer (10 mM MES, 10 mM magnesium chloride pH 5.7). The optical density (OD) of the resuspended cells was measured at 10X dilution in infiltration buffer, using a cell densitometer (Biowave C0800). The culture mixtures were prepared at an appropriate infiltration density according to the experiment, with 0.1 final OD of p19 culture and 0.1% (v/v) acetosyringone (Sigma Aldrich).

2.4.2 Localisation of fluorescently tagged proteins by confocal microscopy

After two days of transient expression of protein constructs in *N. bethamiana*, 7 mm leaf discs were prepared by infiltration with water for mounting and imaged using a Zeiss LSM710 microscope (Carl Zeiss).

2.5 Protein methods

2.5.1 Total protein extraction and Bradford Assay

Total protein was extracted from *Arabidopsis* seedlings and mature leaves using bead beating as described for RNA extraction (section 2.2.1.1.2). Ground leaf material was diluted with 1X SDS sample buffer (50 mM Tris-HCl pH 6.8, 2% (w/v) SDS, 10% (v/v) glycerol, 1% (v/v) 14.7 M β-mercaptoethanol, 12.5 mM EDTA, 0.02% (w/v) bromophenol blue) and boiled at 95 °C for 5 minutes. The protein

concentration was calculated using a Bradford Assay with Bradford Ultra reagent (Expedeon), which was used to determine the volume to load onto an SDS PAGE gel for an equivalent amount of protein between samples.

2.5.2 Co-immunoprecipitation (Co-IP) in *N. benthamiana* with nuclear enrichment

N. benthamiana leaves which had been infiltrated with constructs appropriate for each experiment were ground on liquid nitrogen. The ground tissue was resuspended in chilled freshly prepared nuclear isolation buffer (NIB) supplemented with an appropriate dosage of cOmplete™ Protease Inhibitor Cocktail Tablets (Roche) as shown in Table 7, with 4 mL buffer per gram of ground tissue. The tube was inverted and held on ice until the frozen ground tissue thawed, inverting every few minutes. This suspension was filtered through two layers of miracloth (Merck Millipore) into a chilled 50 mL tube on ice. The miracloth was washed with 3 mL of chilled NIB, which was applied directly to the residual material. The following nuclear isolation protocol is based on that described for 3C analysis with plant material (Louwers *et al*., 2009).

Table 7. The components of nuclear isolation buffer (NIB). The buffer is described in a protocol for 3C analysis with plant material (Louwers *et al*., 2009).

Component	**Final Amount**
Sucrose	250 mM
HEPES pH8	20 mM
Potassium chloride	5 mM
Magnesium chloride	1 mM
PMSF	0.1 mM
Glycerol	40% (v/v)
Triton X-100	0.25% (v/v)
2-mercaptoethanol	0.1% (v/v)
Protease inhibitor	cOmplete™ Protease Inhibitor Cocktail Tablets (Roche) Dosage according to manufacturer's guidelines

The suspension was centrifuged at 3,000 x g for 15 minutes to form a nuclear pellet. The supernatant was carefully decanted and the nuclear pellet was resuspended by gentle pipetting in 2 mL chilled NIB. This suspension was transferred into 2 mL microfuge tubes (Eppendorf). The suspension was centrifuged at 1,900 x g for 5 minutes at 4 ^{o}C. The supernatant was carefully removed by pipetting and 1 mL of chilled NIB was added. The nuclei were resuspended by gentle pipetting and centrifuged as with the previous wash step. These washes were repeated four times, at which point the pellet should be white with little if any green debris at the surface and the supernatant should be very light green to colourless.

The nuclear pellet was resuspended by gentle pipetting in 2 mL lysis buffer: 10 mM Tris pH7.5, 0.5 mM EDTA, 1 mM PMSF, 150 mM sodium chloride, 0.5% (v/v) Igepal and an appropriate dosage of cOmplete^{TM} Protease Inhibitor Cocktail (Roche) according to the manufacturer's protocol. The nuclei suspension was incubated on ice for 5 minutes. The nuclear debris was collected by centrifugation at 21,000 x g for 10 minutes at 4 ^{o}C. The supernatant was transferred to a chilled 2 mL microfuge tube (Eppendorf). A 60 µL sample was taken as input and mixed with 20 µL 4X SDS sample buffer (see section 2.5.1 for buffer composition) and stored at -20 ^{o}C.

An aliquot of 5 µL (or volume according to the experimental conditions specified) of GFP-binding agarose beads (Chromotek) was equilibrated per Co-IP reaction in a 1.5 mL microfuge tube (Eppendorf). The beads were resuspended in 500 µL of wash buffer (10 mM Tris pH7.5, 0.5 mM EDTA, 150 mM sodium chloride) and incubated on ice for 5 minutes followed by centrifugation at 21,100 x g for a few seconds at 4 ^{o}C. All but approximately 50 µL of the wash buffer was removed and the process was repeated for 3 washes in total. After the final wash, the beads were resuspended in the 50 µL of remaining wash buffer and this was transferred to the 2 mL microfuge tube containing the lysed nuclear proteins. The Co-IP was carried out with end-over-end mixing on slow speed for 2 hours.

The reactions were centrifuged at 500 x g for 5 minutes at 4 ^{o}C and 1 mL was removed to leave approximately 1 mL of supernatant in which the beads were resuspended by gentle pipetting. This was transferred to a chilled 1.5 mL microfuge tube and centrifuged as previously described during the wash steps for the beads. The

supernatant was removed to leave approximately 50 µL of supernatant. The beads were resuspended in 1 mL wash buffer and incubated on ice for 5 minutes followed by collection by centrifugation. This process was repeated in the same way as during the equilibration of the beads for five washes in total. Following the final wash, the supernatant was removed leaving approximately 20 µL. An equal volume of 2X SDS sample buffer was added and mixed with the beads. The Co-IP products were stored at -20 ^{o}C.

The input and Co-IP samples were prepared for SDS PAGE by boiling at 95 ^{o}C for 10 minutes from frozen. An aliquot of 15 µL of input and Co-IP samples were run on duplicate SDS PAGE gels and transferred onto nitrocellulose membranes as described in section 2.5.3. The antibody and exposure conditions were varied between experiments.

2.5.3 SDS PAGE and Western Blot

The proteins were separated on an SDS-PAGE gel with NuPAGE® MOPS SDS running buffer (Life Technologies) and Spectra™ Multicolour Broad Range Protein Ladder (Thermo Fisher Scientific). These were transferred to a nitrocellulose membrane (Amersham Hybond, GE Healthcare) in a XCell II^{TM} Blot Module (Life Technologies) for 2 hours at 25 V with transfer buffer (20 mM Tris, 150 mM glycine, 20% (v/v) methanol) surrounded by water with ice.

The membrane was blocked overnight with gentle shaking in TBST (Tris Buffered Saline with 0.1% (w/v) Tween-20) or PBST (Phosphate Buffered Saline with 0.1% (w/v) Tween-20) with 1% (w/v) BSA or 5% (w/v) Skimmed Milk Powder at 4 °C overnight, depending on the antibody (Table 8). The following day the membrane was incubated for 2 hours with the antibody specific conditions shown (Table 8).

Table 8. The conditions used for each antibody for the detection of GFP and HA tags by western blot.

Antibody	Blocking buffer	Dilution	Supplier
Anti-HA high affinity rat monoclonal (Primary)	TBST with 1% (w/v) BSA	1 in 2,000	Roche
Goat anti-rat IgG (secondary)	TBST with 1% (w/v) BSA	1 in 10,000	Abcam
Anti-HA-HRP	PBST with 1% (w/v) BSA	1 in 5,000	Miltenyi Biotech
Anti-GFP-HRP	PBST with 1% (w/v) BSA	1 in 5,000	Miltenyi Biotech
Anti-GFP-HRP	TBST with 5% (w/v) Skimmed milk powder	1 in 5,000	Santa Cruz

The membrane was treated with the Amersham ECL primer western blotting detection reagents (GE healthcare) according to the manufacturer's protocol and scanned with an imaging system (ImageQuant LAS 4000).

2.6 Pathology screens

2.6.1 Reactive oxygen species (ROS) assay

Leaf discs were harvested from four-week-old *Arabidopsis* plants and suspended in 150 µL sterile water in a 96-well plate. These leaf discs were incubated in the dark overnight.

The water from each of the wells was removed under low light conditions. A mixture of luminol, horseradish peroxidase and flg22 was then added to each of the wells and measurements of photons was taken over 30 minutes with a photon detection camera (Photek; Table 9).

Table 9. The reaction components for each ROS assay added to the leaf discs in each well of a 96-well plate.

Component	**Volume per well (µL)**
Sterile water	11
Peroxidase (10 mg/mL in water)	22
Luminol (17 mg/mL in DMSO)	22
flg22 (100 µM)	11

2.6.2 Maintenance of *Hpa* and infection of *Arabidopsis* seedlings for screens

A live stock of *Hpa* was maintained by sub-culturing spores from infected seedlings at 7 day intervals. The aerial parts of two-week-old seedlings at 7 days post infection were harvested in 10 mL pre-chilled water. This was shaken vigorously to release the spores and filtered through Miracloth (Merck Millipore). The spore density was estimated with a haemocytometer and diluted to approximated 100,000 spores per mL. A nursery of one-week-old *Arabidopsis* Columbia (Col) -0 and Wassilewskija (Ws) *enhanced disease susceptibility* (*eds*) 1 mutant Ws-*eds1* were each sprayed with the spore suspension in every orientation and incubated in propagators with sealed lids at 18 ^{o}C, with 10 hours light and 60% humidity. Infection of seedlings for scoring of asexual sporangiophores was carried out as previously described (Tomé *et al*., 2014).

2.7 Sequence capture of regions interacting with multiple bait loci (SCRIBL)

Adaptations are presented here for the analysis of chromatin interactions in *Arabidopsis*, based on an original protocol for SCRIBL in mammalian cells developed by P. Fraser and S. Schoenfelder (unpublished). The SCRIBL technique is an enhancement of Hi-C (a method for examining genome-wide chromatin interactions) adding specificity with the use of biotinylated probes for regions of interest.

2.7.1 Preparation of RNA baits

2.7.1.1 Growth of bacteria from JAtY clone library

E. coli with *Arabidopsis* ecotype Col-0 chromosome fragment insertions selected from the JAtY clone library (Genome Enterprise Limited) were streaked onto LB kanamycin plates (50 µg/mL) from agar stab cultures stored at 4 ^{o}C (see Table 6 for LB recipe). The plates were incubated at 37 ^{o}C overnight.

2.7.1.2 Bacterial artificial chromosome (BAC) extraction

Single colonies were picked and cultured initially in a 5 mL LB kanamycin (50 µg/mL) starter culture at 37 ^{o}C with orbital shaking at 220 rpm for 8 hours. From these cultures 1 mL was transferred into a larger scale 500 mL LB kanamycin (50 µg/mL) culture with the same growth conditions for 16 hours. The bacterial cells were collected at 4,000 x g for 15 minutes at 4 ^{o}C. The supernatant was removed and the BAC DNA was isolated as described in the large-construct DNA isolation kit (Qiagen) protocol with the following adaptations:

1. The column eluate was distributed into 2 mL microfuge tubes (Eppendorf) prior to the final isopropanol precipitation.

2. Following the ethanol wash of the DNA pellets, these were dried for five minutes and the tubes were centrifuged briefly to collect residual ethanol, which was removed by pipetting.

3. The DNA pellets were dissolved in 21 µL of sterile water per microfuge tube and the concentration was determined for 1 µL by UV-Vis spectrophotometer (NanoDrop, Thermo Scientific).

2.7.1.3 Digestion of BAC DNA

A reaction mixture for restriction digest was prepared with an equimolar amount of up to five individual BACs, with 200 units of *Eco*RI restriction endonuclease and NEBuffer 2 (New England Biolabs) in a total volume of 250 µL. The total quantity of BAC DNA should be a maximum of 25 µg. The reaction was incubated overnight at 37 ^{o}C with shaking at 900 rpm.

The digestion efficiency was tested with 2.5 µL of the BAC digestion reaction on a 0.8% (w/v) agarose gel with TAE buffer.

To assist removal of the upper from the lower phases, MaXtract high-density columns (Qiagen) were prepared with centrifugation according to the manufacturer's protocol. A phenol-chloroform extraction was performed on the BAC digestion reaction with one volume of phenol-chloroform (Fisher Scientific) then one volume of chloroform (Fisher Scientific). The columns were shaken for 20 seconds and centrifuged at 16,000 x g for 5 minutes after each addition of phenol-chloroform and chloroform. The aqueous layer was then transferred to a 2 mL microfuge tube (Eppendorf).

The BAC DNA was precipitated with 0.1V 3M sodium acetate pH 5.2 and 2.5X volume absolute ethanol for at least 2 hours at -20 ^{o}C.

The precipitated DNA was centrifuged at 21,000 x g for 30 minutes at 4 ^{o}C. The DNA pellet was washed with 70% (v/v) ethanol and allowed to air-dry briefly. To dissolve the DNA, 5 µL 10 mM Tris pH 7.5 per BAC and an additional 1 µL (for DNA concentration determination) was applied to the pellet then incubated at 4^{o}C overnight. The concentration was determined by UV-Vis spectrophotometer (NanoDrop, Thermo Scientific).

2.7.1.4 Annealing T7 promoter adapters

LuoT7 *Eco*RI adapters were prepared by mixing 100 µL of each LuoT7 *Eco*RI and LuoT7 *Eco*RI reverse oligos (100 µM in sterile water, Table 10) with 300 µL oligo annealing buffer (10 mM Tris, pH 8.0; 50 mM sodium chloride; 1 mM EDTA), which was split into 50 µL individual reactions.

Table 10. The primer sequences for LuoT7 *Eco*RI oligos, which were annealed to generate adapters. These adapters were ligated to digested BAC DNA, as each have complementary *Eco*RI overhangs. A 5' phosphate group (allowing ligation) is represented by [Phos] and a 3' spacer (which prevents elongation) by [SpcC3].

Primer	**Sequence (5'-3')**
LuoT7 *Eco*RI	TCTAGTCGACGGCCAGTGAATTGTAATACGACTC ACTATAGGGCGA
LuoT7 *Eco*RI reverse	[Phos]AATTTCGCCCTATAGTGAGTCGTATTACAA TTCACTGGCCGTCGACTAGA[SpcC3]

The adapters were annealed at 95^{o}C for 5 minutes and the temperature was then decreased by 1^{o}C every minute to a minimum of 14^{o}C. The annealed adapters were stored at -20 ^{o}C.

2.7.1.5 Ligating T7 promoters to *Eco*RI overhangs in digested BAC DNA

The ligation reaction was prepared with the following components in a 1.5 mL microfuge tube (Eppendorf): 25 µL purified BAC DNA mixture (complete volume following determination of concentration), 6.2 µL LuoT7 *Eco*RI adapters, 15 µL 10X T4 DNA ligase buffer (New England Biolabs), 2.4 µL T4 DNA ligase (New England Biolabs) and 102.4 µL sterile water. The reaction was incubated at 16^{o}C overnight. The reaction was heat inactivated at 65^{o}C for 10 minutes and transferred immediately to ice.

2.7.1.6 Sonication of digested BAC DNA with ligated T7 promoters

The reaction was diluted to a total volume of 270 µL with sterile water. For quality assessment, a 10 µL aliquot was taken for analysis by gel electrophoresis (as described in section 2.7.1.3) and the remaining volume was split into two 130 µL aliquots in 0.5 mL Bioruptor® Microtubes (Diagenode).

In order to generate fragments with an average size of 200 base pairs, the DNA was sonicated (Bioruptor®, Diagenode) with six 10-minute cycles of 30 seconds on and 30 seconds off with low power. The ice was replenished in the water bath after every 10-minute cycle. To test the sonication efficiency a 4 µL aliquot of the reaction mixture post-sonication was run alongside the pre-sonication sample on a 3.5% (w/v) agarose gel with TAE buffer.

2.7.1.7 End repair of fragments and size selection of fragments

The post-sonication samples should be approximately 130 µL and were made up to this volume with sterile water where necessary. A reaction mixture was prepared with 17 µL 2.5 mM mixed dNTPs (Invitrogen), 9.5 µL 10X ligase buffer (New England Biolabs), 6 µL T4 DNA polymerase (New England Biolabs), 6 µL polynucleotide kinase (New England Biolabs) and 1.5 µL Klenow (large fragment; New England Biolabs) in a total volume of 170 µL. This reaction was incubated at room temperature for 30 minutes. To purify the filled in fragments, the reaction was split into two aliquots, which were purified using a PCR purification kit (Qiagen) according to the manufacturer's protocol. The purified DNA was eluted in 50 µL of sterile water from each column, which was mixed to give a total reaction volume of 100 µL for the subsequent steps.

Double-sided Solid Phase Reversible Immobilisation (SPRI) was used to select for DNA fragments between 180 and 300 base pairs. The SPRI beads (Agencourt AMPure XP beads) were vortexed to ensure complete homogenisation and mixed with the BAC-T7 promoter DNA at a concentration of 0.7X the input reaction volume. This reaction was incubated at room temperature for 10 minutes and placed

on a magnetic rack to separate the beads from the supernatant (containing fragments in the required size range), which was transferred to a fresh microfuge tube. An aliquot of 110 μL of SPRI beads was then concentrated by placing on the magnetic rack and removing 30 μL of supernatant. The beads were resuspended in the supernatant and 30 μL of beads were then added to the supernatant from the previous size selection. The reaction was incubated at room temperature for 10 minutes and the supernatant was removed following magnetic separation. The beads, which were bound to the DNA in the desired fragment size range, were resuspended in TLE buffer (10 mM Tris, 0.1 mM EDTA) and incubated at room temperature for 5 minutes. The beads were collected on a magnetic rack and the supernatant which at this point contains the size selected DNA, was transferred to a fresh tube. The DNA concentration was determined with a UV-Vis spectrophotometer (NanoDrop, Thermo Scientific).

2.7.1.8 Generation of RNA baits by *in vitro* transcription with biotin labelled UTP

The T7 promoters ligated at the restriction sites are utilised for the transcription of RNA baits. The T7 MegaScript Kit (Ambion) was used with biotin labelling mix (Roche) to prepare the reaction mixture given in Table 11. The reactions were incubated at 37 ^{o}C for 12 to 16 hours.

Table 11. Reaction mixture for the generation of biotinylated RNA based on components from the T7 MegaScript Kit (Ambion) and Biotin Labelling Mix (Roche).

Component	**Volume**
DNA template	Variable (100 to 500 ng)
Biotin labelling mix	6 μL
Enzyme mix	2 μL
10X buffer	2 μL
RNase-free water	Variable
TOTAL	20 μL

2.7.1.9 Purification of biotinylated RNA baits

The reaction was treated with 1 µL Turbo DNase (Life Technologies) for 15 minutes at 37 ^{o}C to remove the template DNA.

The RNA baits were purified using the Ambion MEGAclear kit according to the manufacturer's protocol. The purified RNA was eluted in a final volume of 50 µL and rapidly split into 5 to 10 µL aliquots and stored at -80 ^{o}C. The yield was determined with a UV-Vis spectrophotometer (NanoDrop, Thermo Scientific) and should be between 20 and 50 µg.

2.7.2 Preparation of a Hi-C library from *Arabidopsis* cell suspension culture

2.7.2.1 Fixation of *Arabidopsis* cell suspension culture

The *Arabidopsis* cell suspension culture from the experiment described in section 2.1.2.3 were split into two aliquots of 10 mL. Each aliquot was processed separately.

The *Arabidopsis* cell suspension culture was fixed in 50 mL tubes with the addition of 39% (v/v) formaldehyde with the final concentration of formaldehyde depending on the experiment. The tubes were inverted gently and regularly to ensure constant mixing for 10 minutes. To quench the formaldehyde, 1 M glycine (Sigma Aldrich) was added to a final concentration of 0.125 M and the tubes were inverted gently for 10 minutes as previously. Finally the cells were filtered through two layers of miracloth (Merck Millipore), flash frozen in foil in liquid nitrogen and stored -80 ^{o}C.

2.7.2.2 Nuclear extraction for *Arabidopsis* cell suspension culture

The frozen formaldehyde fixed *Arabidopsis* cell suspension culture cells were ground in a sterile pestle and mortar with liquid nitrogen. The ground tissue was transferred into a pre-chilled 10 mL tube and stored on liquid nitrogen. The ground tissue was resuspended in chilled freshly prepared nuclear isolation buffer (NIB) supplemented with an appropriate dosage of cOmplete^{TM} Protease Inhibitor Cocktail

(Roche) as shown in Table 7 (7 mL per 10 mL *Arabidopsis* cell suspension culture) and incubated on ice with inversion until the tissue thawed. The tissue was filtered and prepared in the same way as described in section 2.5.2 for isolation of nuclei.

Following two washes with 1 mL chilled NIB in 2 mL microfuge tubes the nuclei pellet should be white and the supernatant colourless. The supernatant was removed by careful pipetting and the nuclei were resuspended in 500 µL 1.2X NEBuffer 2 (New England Biolabs) and the centrifugation was repeated as described in section 2.5.2. Finally the supernatant was removed and the pellet was resuspended in 400 µL 1.2X NEBuffer 2 (New England Biolabs). The nuclei were incubated on ice before the next steps of the Hi-C protocol.

2.7.2.3 Digestion of chromatin

Prior to the digestion of the chromatin in the purified nuclei, the nuclei were permeabilised with a final concentration of 0.75% (v/v) SDS to allow access to the restriction enzyme. This reaction was incubated at 65 ^{o}C with shaking at 900 rpm. A final concentration of 1.8% (v/v) Triton X-100 was added to quench the SDS and was incubated for 1 hour at 37 ^{o}C with shaking at 900 rpm.

An appropriate volume of restriction enzyme was added according to the experiment. The restriction digest reactions were incubated overnight at 37 ^{o}C with shaking at 900 rpm.

2.7.2.4 Generation of blunt-end chromatin fragments

Following the restriction digest reaction, the overhangs were filled in with dNTPs including biotin-14-dATP (Roche). The reaction components are given for biotin fill-in (Hi-C) and an unbiotinylated (control) fill-in reactions (Table 12). The reactions were incubated with DNA Polymerase I, Large (Klenow) Fragment (New England Biolabs) at 37 ^{o}C for 1 hour with pipetting up and down gently approximately every 10 minutes (unless otherwise specified for specific experimental conditions). An

additional 3C control (i.e. without blunt ends) was rested on ice during this time with an equivalent volume of water.

Table 12. The components of biotin (biotin-14-dATP) and control fill-in reactions with DNA Polymerase I, Large (Klenow) Fragment.

Component	**Volume (µL) for biotin fill-in reaction**	**Volume (µL) for control fill-in reaction**
10X NEBuffer 2	6	6
Water	0	40
Biotin-14-dATP	40	0
dATP 10 mM	1.6	1.6
dCTP 10 mM	1.6	1.6
dGTP 10 mM	1.6	1.6
DNA Polymerase I, Large (Klenow) Fragment	10	10

The enzyme was inactivated for all reactions with a final concentration of 0.4% (v/v) SDS and incubated at 65 ^{o}C with shaking at 950 rpm for exactly 30 minutes.

2.7.2.5 Ligation of blunt-end chromatin

In order to quench the SDS, the nuclei were transferred into a pre-ligation reaction mixture containing the following components: 381 µL 20% (v/v) Triton X-100, 768 µL 10X ligation buffer (New England Biolabs), 82 µL 10 mg/mL BSA and 5.769 mL water. This reaction was incubated for 1 hour at 37 ^{o}C with occasional mixing by inversion.

The reactions were ligated with T4 DNA Ligase (New England Biolabs) at 16 ^{o}C for 5 hours (or overnight depending on the experiment). The reactions were mixed with inversion at 15 to 30 minute intervals.

2.7.2.6 Reversal of chromatin cross-linking and removal of RNA

The chromatin cross-linking was reversed with 60 µL 10 mg/mL proteinase K (Roche) and incubation at 65 ^{o}C overnight. The samples were then incubated for 1 hour at 37 ^{o}C with 30 µL 1 mg/mL RNase A (Roche).

2.7.2.7 Purification of DNA

An equal volume of phenol-chloroform (Sigma Aldrich) was added to each reaction and then shaken gently for 20 to 30 seconds. The reactions were centrifuged at 3,000 x g for 15 minutes at room temperature. The upper phase was transferred to a new 50 mL tube with a 2.5X volume of ice-cold 100% ethanol and a 0.1X volume of 3M sodium acetate pH5.2. The reactions were precipitated overnight at -20 ^{o}C.

The overnight precipitation reactions were centrifuged at 21,000 x g for 30 minutes at 4 ^{o}C. The supernatant was removed and the pellets were washed with 1 mL 70% (v/v) ethanol (ice-cold) by centrifugation at 21,000 x g for 15 minutes at 4 ^{o}C. The ethanol was removed and the washes were repeated. The pellets were resuspended in 500 µL Tris-EDTA (TE) buffer and incubated at room temperature for 30 minutes.

An equal volume of phenol-chloroform (Sigma Aldrich) was added to the resuspended DNA in 2 mL microfuge tubes (Eppendorf) and shaken for 30 seconds. The samples were centrifuged at 16,000 x g for 5 minutes and the upper phase was transferred to a new microfuge tube. This process was repeated three times. Finally the upper phase was precipitated in the same way as described for the previous phenol-chloroform extraction and precipitated at -20 ^{o}C overnight.

The overnight precipitated samples were centrifuged at 21,000 x g for 30 minutes at 4 ^{o}C. The supernatant was removed and the pellets were washed with 1 mL 70% (v/v) ethanol (ice cold) at 21,000 x g for 15 minutes at 4 ^{o}C. These washes were repeated three times in total. The pellets were resuspended in 25 µL TE buffer and the concentration was determined with a UV-Vis spectrophotometer (NanoDrop, Thermo Scientific).

2.7.2.8 Digestion efficiency test and control PCR reactions for the Hi-C library

The libraries were examined to determine whether short-range ligation products had been generated. This involves the use of forward-forward or reverse-reverse primer combinations adjacent to restriction sites. This would not amplify a product in the absence of restriction digest and ligation that could change the relative orientation. In addition, products were amplified across the restriction junctions as an estimation of digest efficiency. These PCR reactions were carried out with the general conditions given in section 2.2.3.1 with various combinations of the following primers Table 13.

Table 13. The primer sequences for investigating restriction digestion efficiency and short-range ligation products in a Hi-C library by PCR[1].

Primer	**Orientation**	**Sequence (5'-3')**
LHCh4-1	Forward	CGAGAAGCGCAAAATATCGT
LHCh4-2	Reverse	AGTTCCGTCACGAAAGCATC
LHCh5-1	Forward	TCACAAATGTTGAGGCAAGG
LHCh5-2	Reverse	CCTGTCTGATCCATTACACGAA
LHCh6-1	Forward	AACAAAAATGATAAGCAAAGAATGG
LHCh6-2	Reverse	CATCCAAAAATCGAGAAACTGA
LHCh8-1	Forward	AGGGTATGATCGCGAGAGTG
LHCh8-2	Reverse	TTCCTGTTCCTCCAAATCCA
LHCh10-1	Forward	TCCGGTGTTGACTCCTGAAT
LHCh10-2	Reverse	TTGCTTGCAAAATGAATGGA
LHCno-1	Forward	AAACCGGTCTGGTCGAGTAGT
LHCno-2	Reverse	TGGTAATGGTTGTGGTGGTG

[1] The primers bind to the region within and surrounding the light harvesting chlorophyll a/b-binding complex (LHC) genes *Lhcb2.1* (AT2G05100) and *Lhcb2.2* (AT2G05070). These primers were designed by Polly Downton as part of an unpublished 3C experiment with *Arabidopsis*.

3 Examining a pathogen effector interaction with a host protein

3.1 Introduction

3.1.1 *H. arabidopsidis* (*Hpa*) effector proteins

As discussed in section 1.2.3.2**,** the conserved RXLR-dEER motif identified in oomycete pathogens including *Hpa*, has allowed effectors to be predicted from the Emoy2 genome sequence. Subsequently a study which cloned these putative effectors presented an opportunity to characterise their structure and interactions (Fabro *et al*., 2011). In this study, the effector detector vector (EDV) system was used to deliver these predicted *Hpa* effectors individually into various *Arabidopsis* accessions, via the type III secretion system of luciferase expressing *P. syringae* pv. *tomato* DC3000 (Fabro *et al*., 2011). The expression of luciferase allowed host susceptibility to be monitored and revealed that most effectors enhance bacterial growth. However, many of the effectors did not enhance susceptibility across all accessions suggesting that there could be at least subtle differences between the targets in each accession (Fabro *et al*., 2011). This finding highlights the role of evolutionary pressures in determining effector interactions with host proteins.

Furthermore, large-scale yeast two-hybrid screens have identified putative host targets of effector proteins from *Hpa*, as well as bacterial (*P. syingae*) and fungal (*Golovinomyces orontii*) pathogens of *Arabidopsis* (Mukhtar *et al*., 2011; Weßling *et al*., 2014). This study involved roughly 8,000 full-length proteins previously used to generate *Arabidopsis* interactome version 1 (AI-1), which were screened against 552 effector and host immune proteins (Mukhtar *et al*., 2011). Combining this new set of interactions with AI-1 formed the basis of the plant-pathogen immune network version 1 (PPIN-1; Mukhtar *et al*., 2011). This network defined interactions between effectors and host proteins, as well as the interactors of effector targets (Mukhtar *et al*., 2011). The main findings of these screens was the identification of a set of host proteins that are targeted by effectors from multiple species, which is significantly greater than predicted by chance (Mukhtar *et al*., 2011; Weßling *et al*., 2014). Furthermore these targets also have a much higher than expected degree of

connectivity (Mukhtar *et al*., 2011; Weßling *et al*., 2014). This evidence provides support for the hypothesis that highly connected and conserved elements of the host immune network play a key role in coordinating host defence (Mukhtar *et al*., 2011). The manipulation of these hub proteins by a pathogen are predicted to have a more focussed destructive impact on host immune networks (Mukhtar *et al*., 2011).

Additional interesting observations from these screens include that only two out of thirty NB-LRR proteins were directly targeted by effectors, although nearly half of their interactions were with effector targets (Mukhtar *et al*., 2011). This observation is consistent with the Guard Hypothesis described in section 1.2.4 in which the NB-LRR receptor does not directly interact with effectors but rather monitors the state of the host target. This suggests that immunity is an intricate web of interactions in which there are likely to be many indirect links to immune receptors. Furthermore, many of the effectors have several targets suggesting that immune interactions are characterised by additional dimensions of complexity (Mukhtar *et al*., 2011).

3.1.2 *Hpa* candidate effector protein HaRxL14 has multiple targets

Further to the insights into the big picture of effector-host interaction networks, these screens have also generated considerable interaction data revealing novel effector targets. Effectors had previously been thought to interact specifically with individual host proteins (Win *et al*., 2012a). However, more recent evidence suggests that single effectors may have a broad range of targets potentially involved in different processes (Win *et al*., 2012a). The redundancy of proteins within pathways and the complex nature of cascades involved in hormone signalling, makes it necessary for pathogens to manipulate various proteins to enhance susceptibility. Therefore to overcome MAMP-triggered immunity and host defences, pathogens may deliver hundreds of effectors in the case of *Phytophthora* species (Yu *et al*., 2012). Alternatively, these effectors may have several targets as with HopQ1 which interferes with multiple 14-3-3 family proteins that have previously been shown to have a role in NB-LRR signalling (Li *et al*., 2013b).

The previously described yeast-two hybrid (Y2H) screens, in addition to unpublished PPIN-3 (Steinbrenner, Braun and Beynon, pers. comm., 2013), identified multiple and diverse interactions of *Hpa* effector HaRxL14 (Mukhtar *et al*., 2011). The identified host protein targets include armadillo repeat only (ARO) 2 and 3, nucleosome assembly protein (NAP) 1 and 3, Myb domain protein (MYB) 70 and protein phosphatase type-2CA (PP2CA). These interactions have subsequently been verified with one-to-one testing (Steinbrenner, unpublished). In addition, the interactions with ARO2 and 3 have been confirmed by Co-IP and bimolecular fluorescence complementation (Steinbrenner *et al*., 2014), techniques which can provide *in planta* verification of protein complexes.

3.1.3 The role of PP2CA in the ABA response

Hormone signalling is highly interwoven with various pathways and processes, including response to biotic and abiotic stress. As previously described in section 1.2.5.3, the PP2Cs are a family of 80 proteins in *Arabidopsis* that integrate signalling in response to ABA (Singh *et al*., 2015). These are co-receptors to the PYR/PYL/RCAR ABA receptor proteins. Under normal conditions, PP2CA dephosphorylates its targets the Snf1 related protein kinases (SnRKs) 1s and 2s (Figure 5; Sheard and Zheng, 2009). This represses these signalling cascades. During the perception of ABA, PP2CA forms a complex with the PYR/PYL/RCAR receptors, which in turn activates the SnRK2s (Figure 5; Sheard and Zheng, 2009). This suggests that manipulation of PP2CA by a pathogen effector could have broad effects due to its role in signal integration.

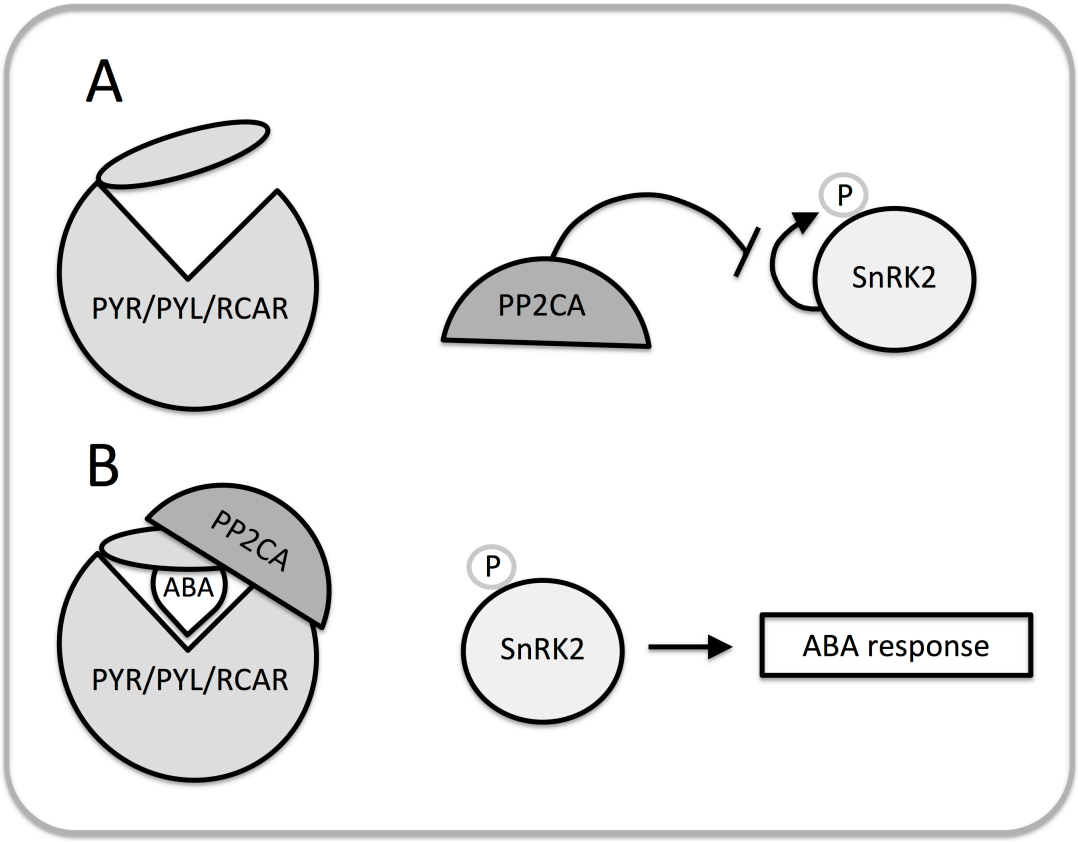

Figure 5. The role of PP2CA in ABA signalling. **A** When ABA is absent, PP2CA blocks phosphorylation of SnRK2, which inhibits the ABA signalling cascade. **B** When ABA is present, the hormone binds to the receptor proteins PYR/PYL/RCAR producing a binding site for PP2CA. This results in the activation of phosphorylated SnRK2 leading to the induction of an ABA signalling cascade. This figure is based on information presented in Figure 1 from (Sheard and Zheng, 2009). Adapted by permission from Macmillan Publishers Ltd: Nature (Sheard and Zheng, 2009), copyright (2009).

3.1.4 ABA in plant-pathogen interactions

ABA has a complex role in plant-pathogen interactions. The hormone has cross talk with other pathways involved in immunity and response to pathogens including jasmonic acid signalling (Fan *et al*., 2009; Koornneef and Pieterse, 2008). The influence of ABA induced pathways on susceptibility to pathogens is highly variable and contrasting between necrotrophs and biotrophs (Asselbergh *et al*., 2008). For instance, ABA induces the closure of stomata, which is beneficial for some pathogens but detrimental for others as described in section 1.2.5.3. *P. syringae* pv. *tomato* DC3000 T3Es induce up-regulation of ABA-related genes such as *NCED3* (encoding an ABA biosynthetic enzyme), with a corresponding endogenous rise in ABA which enhances susceptibility to the pathogen (de Torres-Zabala *et al.*, 2007). There is currently conflicting evidence relating to the effect of ABA on *Hpa* infection. For example, *Hpa* was shown to enhance ABA signalling in order to promote the lifestyle of the pathogen (Asai *et al*., 2014; Fan *et al*., 2009). More specifically, ABA deficient mutants have three-fold less sporulation when infected with *Hpa* which suggests that ABA is required for full virulence and asexual sporulation (Fan *et al*., 2009).

3.2 Aims

1. To verify the interaction of HaRxL14 with PP2CA, which integrates abscisic acid (ABA) and metabolic signalling.
2. To characterise the role of this putative effector target in host immunity.

3.3 Characterising protein localisation

3.3.1 Localisation of PP2CA and HaRxL14

The localisation of PP2CA has previously been described as nuclear and therefore the investigation initially aimed to confirm this result (Pizzio *et al*., 2013). In addition, a large number of *Hpa* effectors have also been determined to have nuclear expression (Caillaud *et al*., 2012a). Therefore it was predicted that there could be a common pattern of nuclear localisation.

To investigate the localisation of the effector and target, fluorescently tagged constructs (35S::*GFP*::*HaRxL14* and 35S::*GFP*::*PP2CA* (pK7FWG2)) transformed into *A. tumefaciens* were infiltrated and expressed in *N. benthamiana* and detected by confocal microscopy (Zeiss LSM 710) as described in section 2.4.2. This test would therefore determine whether the two proteins localised to the same cellular compartment.

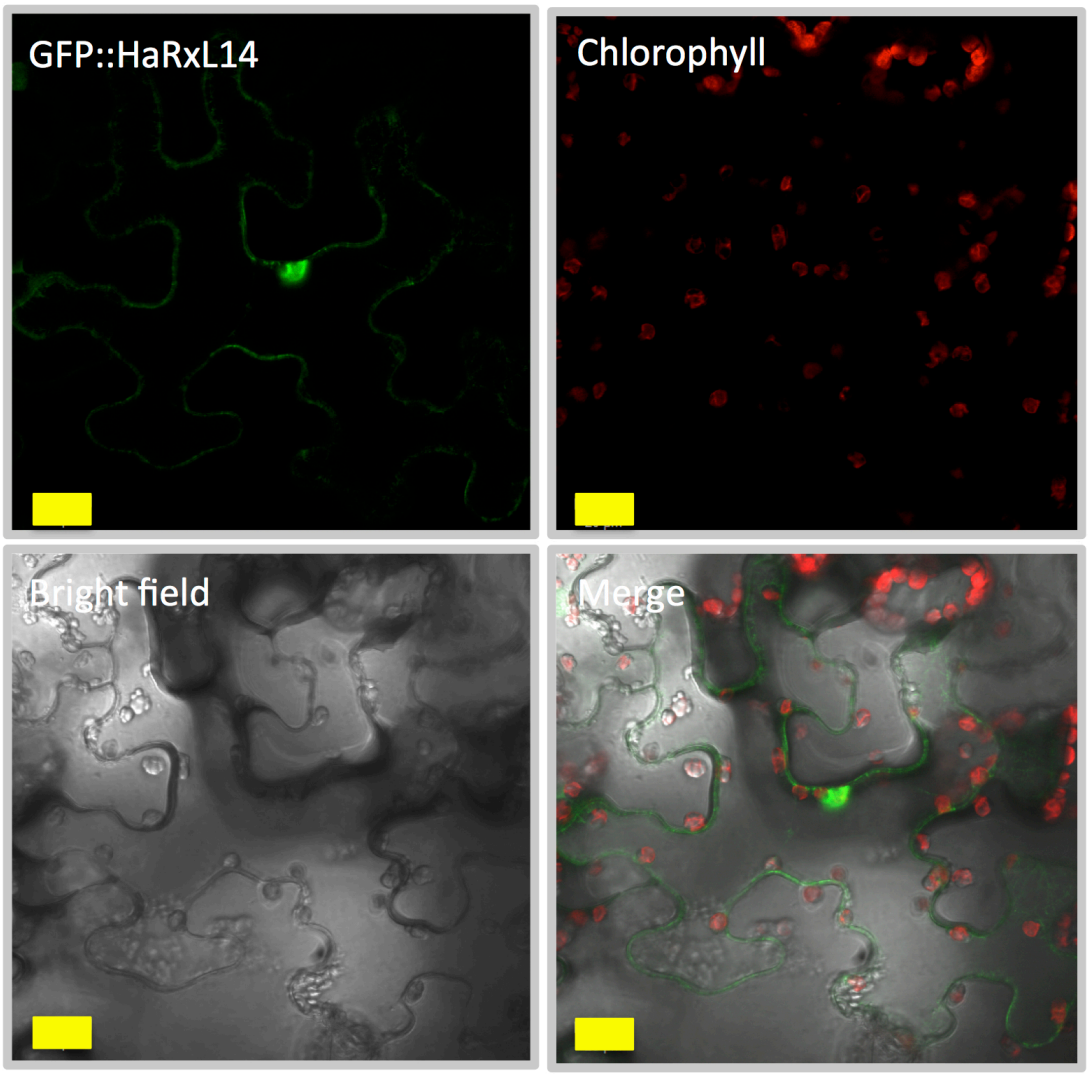

Figure 6. Localisation of 35S::*GFP*::*HaRxL14* expression *in planta* by confocal microscopy. *A. tumefaciens* harbouring the construct 35S::*GFP*::*HaRxL14* (pK7FWG2) and silencing suppressor p19 were infiltrated into 4 to 5-week-old *N. benthamiana* leaves and proteins were transiently expressed for 2 days (Voinnet *et al*., 2003). The fluorescent construct was visualised by confocal microscopy (Zeiss LSM 710). The scale bar represents 20 µm.

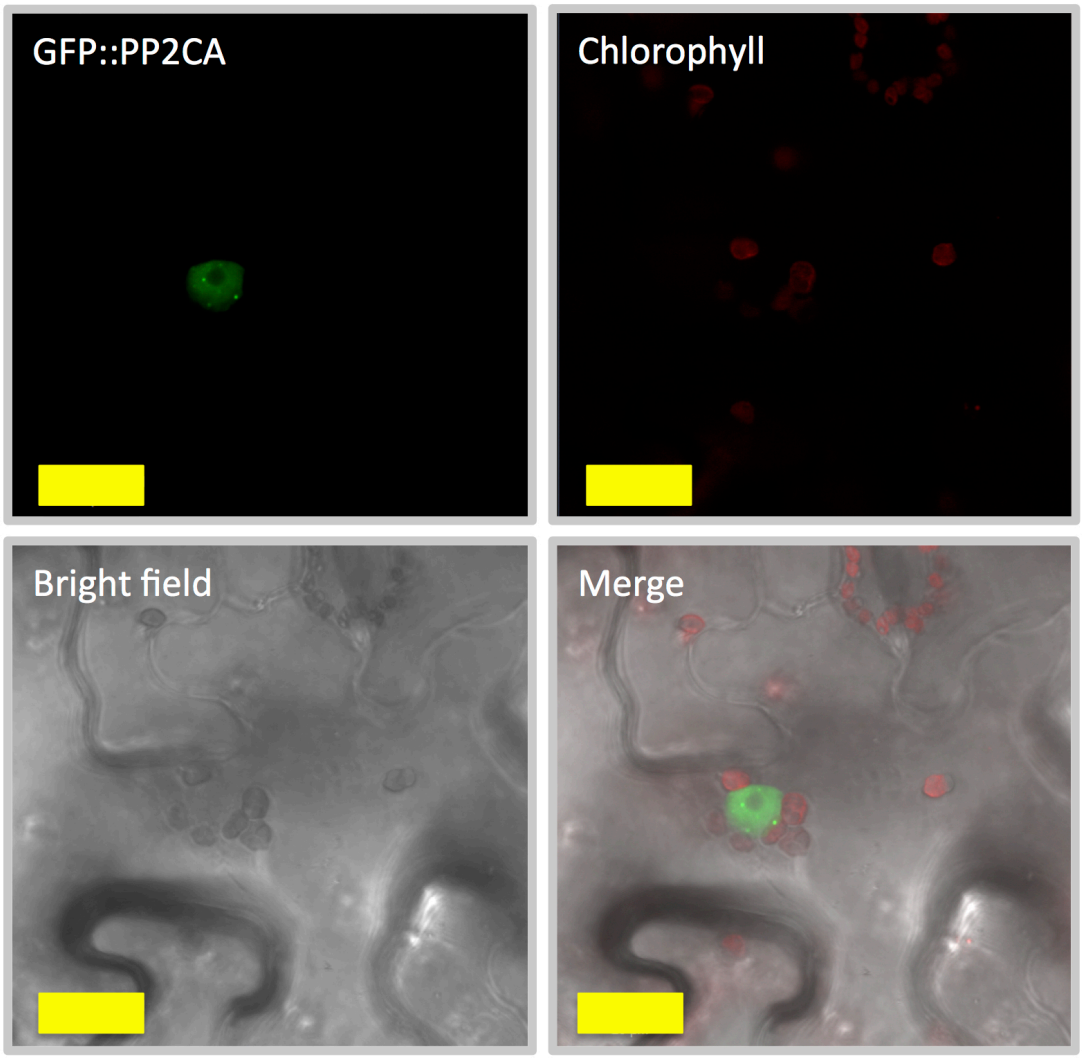

Figure 7. Localisation of 35S::*GFP*::*PP2CA* expression *in planta* by confocal microscopy. *A. tumefaciens* harbouring the construct 35S::*GFP*::*PP2CA* (pK7FWG2) and silencing suppressor p19 were infiltrated into 4 to 5-week-old *N. benthamiana* leaves and proteins were transiently expressed for 2 days (Voinnet *et al*., 2003). The fluorescent construct was visualised by confocal microscopy (Zeiss LSM 710). The scale bar represents 20 µm.

From Figure 6 and Figure 7 it is clear that both GFP::PP2CA and GFP::HaRxL14 localise to the nucleus and GFP::HaRxL14 also appears to be present in the cytosol. This supports previous finding of the location of PP2CA (Antoni *et al.*, 2012). In addition, PP2CA has a pattern of speckled bodies in the nucleus (Figure 7). This suggests that the construct could localise to sub-nuclear bodies or may be the result of aggregation due to the high level of expression.

3.3.2 Bimolecular fluorescence complementation for PP2CA and HaRxL14

From the results of the localisation of the fluorescently tagged PP2CA and HaRxL14 contructs, it appears that there is an overlap in the nucleus. Bimolecular fluorescence complementation (BiFC) technique (here split-YFP) was used to verify this locational observation and also as an alternative technique to confirm the interaction itself. The split-YFP method is based on the ability to divide YFP into N and C-terminal domains which are unable to fluoresce independently. When brought into close proximity these emit fluorescent signal (Kerppola, 2006). Therefore, the N and C-terminal YFP domains can be fused to two proteins of interest to test for a possible interaction and to identify the subcellular location. The expression of four combinations of the domain of YFP and orientation of the fusion on the protein of interest in *N. benthamiana*, was possible using the pBiFP (Gateway® compatible BiFC *in planta* vectors) system which was kindly provided by Francois Parcy (University of Grenoble, France).

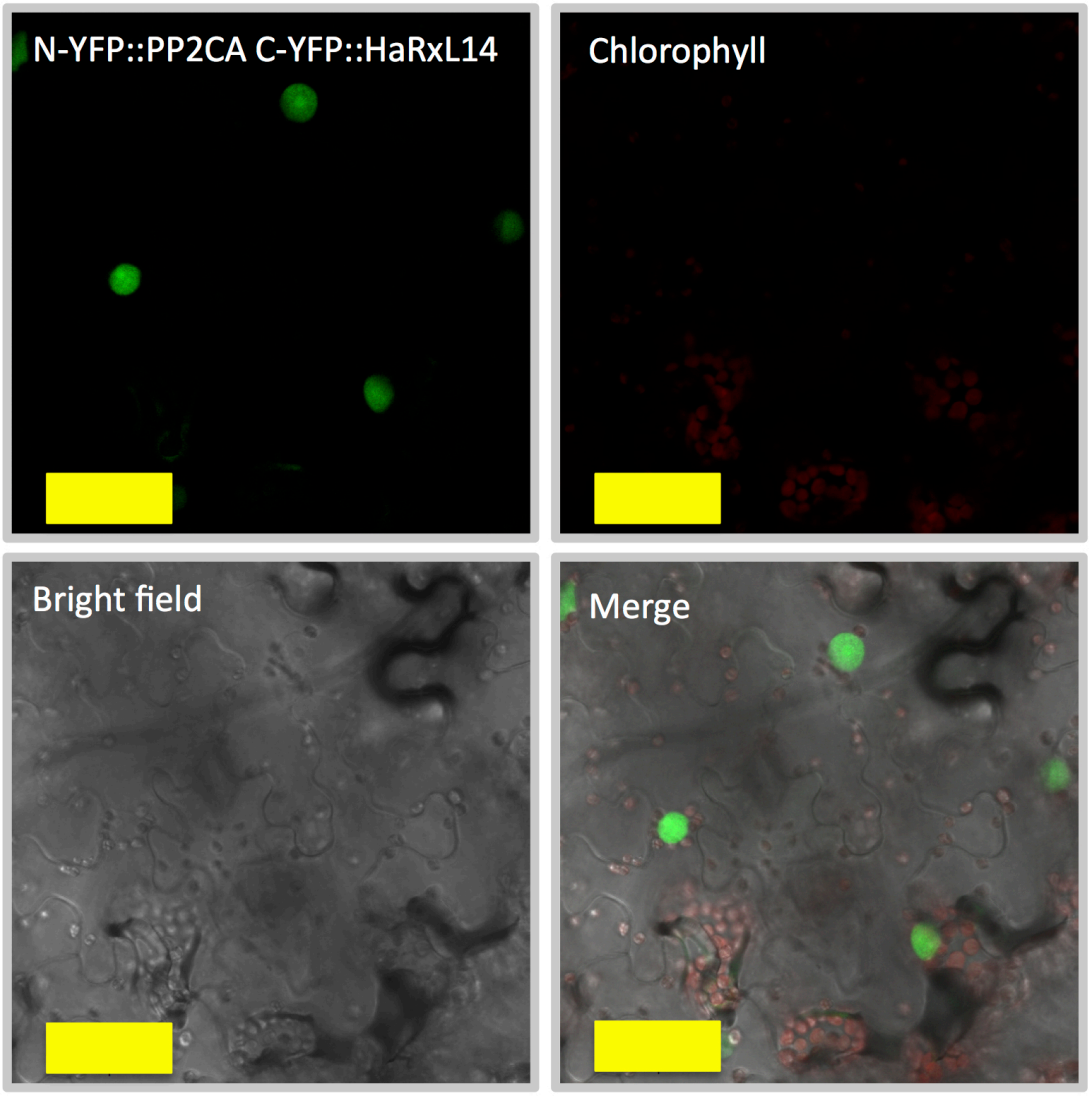

Figure 8. Bimolecular fluorescence complementation for transiently expressed 35S::*N-YFP*::*PP2CA* (pBIFP-2) and 35S::*C-YFP*::*HaRxL14* (pBIFP-3) constructs *in planta* by confocal microscopy. *A. tumefaciens* cultures individually harbouring 35S::*N-YFP*::*PP2CA*, 35S::*C-YFP*::*HaRxL14* and silencing suppressor p19 were infiltrated into 4 to 5-week-old *N. benthamiana* leaves and proteins were transiently expressed for 2 days (Voinnet *et al*., 2003). The fluorescent construct was visualised by confocal microscopy (Zeiss LSM 710). The length of the scale bar represents 50 µm.

Figure 8 indicates that the proteins interact in the nucleus, which is consistent with the previous findings described in section 3.3.1. In addition to the observed nuclear interaction, there also appeared to be fluorescent signal from the nucleolus. This contrasts to the individual localisation patterns of GFP::PP2CA and GFP::HaRxL14 in which expression appears to be excluded from the nucleolus (Figure 6 & Figure 7). This raises the question of whether there could be a functional role of the nucleolus in the interaction of these two proteins or if this observation is simply an artefact of the technique. A similar fluorescent signal in the nucleolus was also observed with the constructs 35S::*HaRxL14*::*C-YFP* (pBIFP-4) and 35S::*N-YFP*::*PP2CA* (pBIFP-2). Contrastingly, no fluorescent signal was observed with the combinations HaRxL14 in pBIFP-1 with PP2CA in pBIFP-3 and HaRxL14 in pBIFP-2 with PP2CA in pBIFP-3 (see Table 5). This suggests that the two domains of YFP are unable to assemble when fused to each protein in these orientations. This could be due to the tags causing interference with the interacting domains of the effector and target. Therefore, the two YFP domains no longer come into sufficiently close proximity to assemble and emit fluorescent signal. It may also have been beneficial to have included a second protein not known to interact with the effector as an additional control.

3.3.3 No re-localisation of PP2CA by HaRxL14

If relocalisation of one or both of the proteins is observed this would provide further evidence indicating that the interaction itself is true. This would also suggest mechanisistic insights into the nature of the interaction. There are several possible explanations for an observed relocalisation. For example, it could suggest that the effector changes the location of its target in order to protect the host protein from a wild-type function with interactors. Therefore, this could prevent these pathways being activated or repressed, promoting coniditions conducive to the survival of the pathogen.

To investigate whether the effector could change the localisation of PP2CA, 35S::*GFP*::*PP2CA* (pK7FWG2) and 35S::*RFP*::*HaRxL14* (pK7RWG2) constructs were coinfiltrated into *N.benthamiana* as described in sections 2.4.1. Confocal

microscopy was used to identify cells which were co-expressing these constructs and the pattern of localisation was captured for each (section 2.4.2).

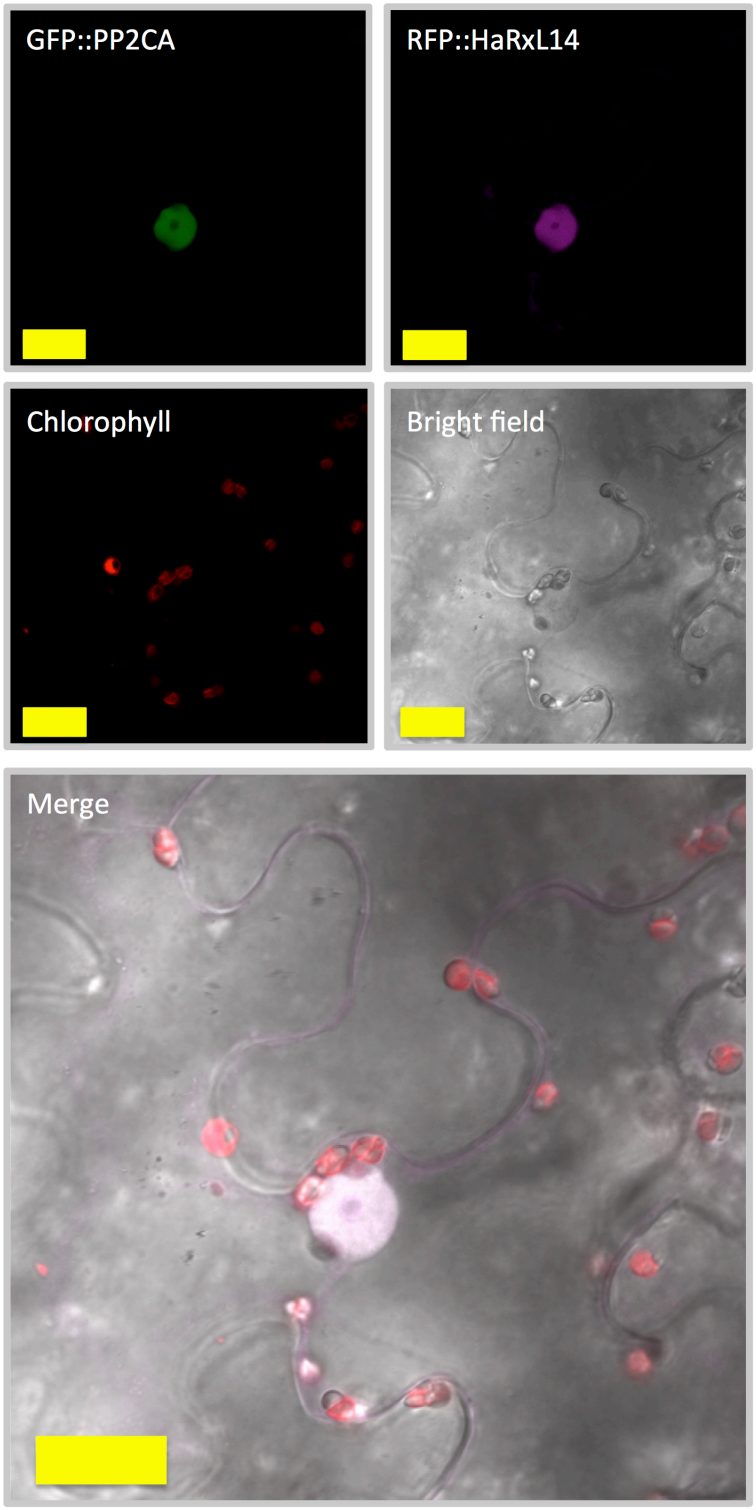

Figure 9. Co-localisation of *35S::GFP::PP2CA* and *35S::RFP::HaRxL14* expression *in planta* by confocal microscopy. *A. tumefaciens* harbouring the constructs *35S::GFP::PP2CA*, *35S::RFP::HaRxL14* in vectors (pK7FWG2 and pK7RWG2 respectively) with silencing suppressor p19 were infiltrated into 4 to 5-week-old *N. benthamiana* leaves and proteins were transiently expressed for 2 days (Voinnet *et al*., 2003). The fluorescent construct was visualised by confocal microscopy (Zeiss LSM 710). The length of the scale bar represents 20 µM.

It is clear from Figure 9 that there does not appear to be a change in the localisation of either GFP::PP2CA or RFP::HaRxL14 as a result of the co-expression of these protein constructs. There is a clear overlap in nuclear expression as indicated by the white area in the merged fields (Figure 9). This suggests that a potential functional interaction between the effector and PP2CA is not characterised by manipulation of the location of the host protein.

3.4 Co-IP with nuclear enrichment

3.4.1 HaRxL14 pull-down with GFP binding beads

A Co-IP experiment was set up to test the effector and PP2CA interaction. In this experiment, two proteins of interest are co-expressed with contrasting tags. A pull-down is then performed with beads (or another similar method) that specifically bind to one of these tags and these beads are washed several times. The purified fraction, which is bound to the beads, is separated on an SDS PAGE gel. The proteins of interest can be identified with appropriate antibodies on a western blot. A positive Co-IP will show the pulled-down protein enriched between before (input) and after (IP) the Co-IP and the same pattern for the interactor. Therefore, this result suggests a close association of the interactor with the pulled-down protein, which is not washed away during the purification steps.

As a nuclear interaction of the effector and PP2CA had been observed in split-YFP, nuclear enrichment steps were carried out prior to the pull-down. The nuclei were washed in nuclear isolation buffer in order to remove other contaminating cellular components and debris (as described in section 2.5.2) before lysing the nuclei, which produced the input for the pull-down. This nuclear enrichment can reduce background in the final IP fraction of proteins that do not interact with the enriched protein but were not removed during the washing steps. Therefore if a nuclear interaction is predicted then this can aid interpretation of the final result for Co-IP.

In this experiment, GFP binding agarose beads (Chromotek) were used to pull-down GFP::HaRxL14 to test for an interaction with HA::PP2CA. Another GFP labelled *Hpa* effector (GFP::HaRxL21) for which no interaction was detected with PP2CA in

the yeast two-hybrid screen, was included as a negative control (Mukhtar *et al*., 2011).

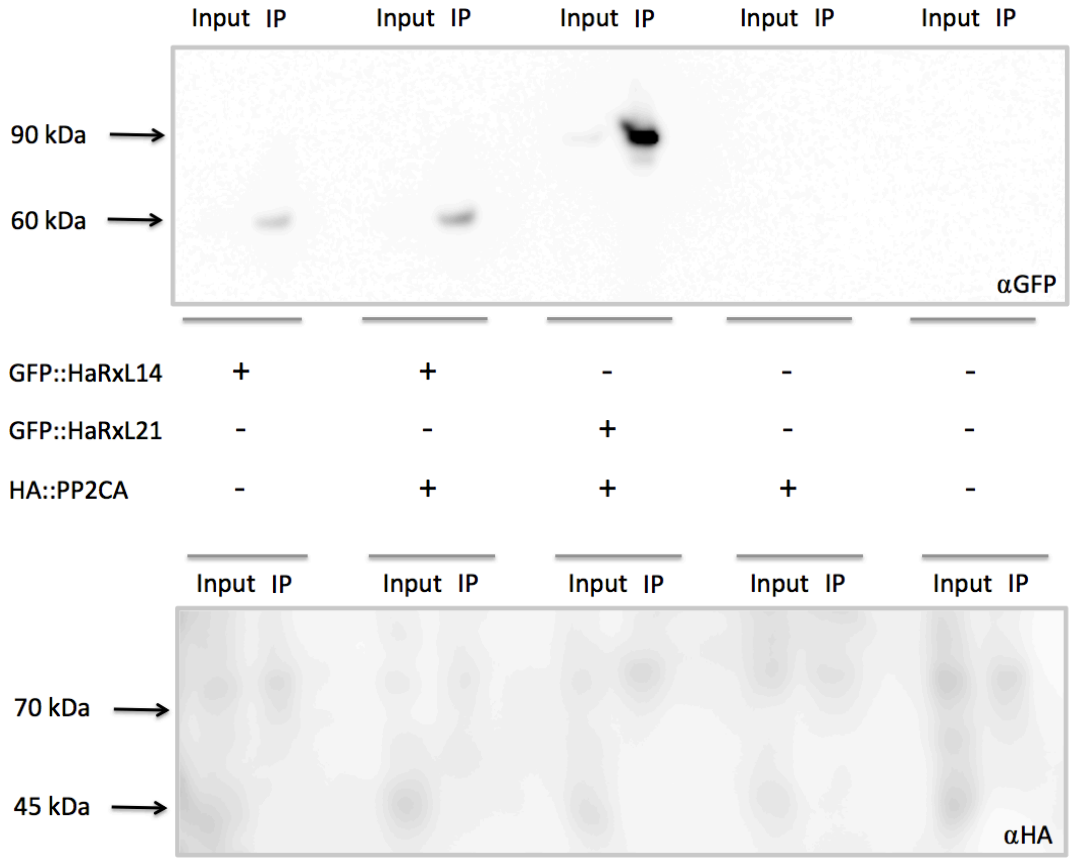

Figure 10. Co-IP to identify a potential interaction between GFP::HaRxL14 and HA::PP2CA *in planta* with GFP pull-down. The constructs 35S::*GFP*::*HaRxL14* and 35S::*HA*::*PP2CA* along with the control 35S::*GFP*::*HaRxL21*, which did not show an interaction with PP2CA in a yeast two-hybrid screen, were expressed transiently in *N. benthamiana* for 3 days, in the combinations indicated. The silencing suppressor p19 was co-infiltrated in all samples at a final OD of 0.1 (Voinnet *et al*., 2003). The membranes were probed with HRP conjugated αGFP or αHA antibody (Miltenyi Biotech). For western blot conditions see section 2.5.3 and Table 8**.**

Figure 10 shows the products of these Co-IP reactions on western blot membranes probed with GFP and HA antibodies. The αGFP membrane showed an enrichment GFP::HaRxL14 in the first two sample sets (from left to right) and GFP::HaRxL21 control in the next IP lanes (Figure 10). This indicates that the GFP bound proteins were pulled-down as expected with the beads. However, no clear enrichment of HA::PP2CA is apparent in the second set of input and IP samples which should be approximately 55 kDa (Figure 10). Therefore under these conditions an interaction between the two proteins is not detectable. It is possible that the interaction frequency between the protein could be relatively low meaning that a higher abundance of the proteins may be required in order to detect the interaction.

3.4.2 HaRxL14 pull-down with GFP binding beads and additional starting leaf material

A Co-IP experiment was set up with greater input of 8 g of starting *N. benthamiana* leaf material expressing GFP::HaRxL14 and HA::PP2CA. Additionally, samples of supernatant were taken from each of the wash steps during the nuclear enrichment. This would enable detection of any potential loss of either protein during the nuclear enrichment process. This could result in a small quantity of the putative interactor by the Co-IP steps as opposed to no apparent interaction. If loss of the interactor is detected in the supernatant then the nuclear enrichment could be hindering the experiment. In this case, Co-IP would need to be performed with total protein as input.

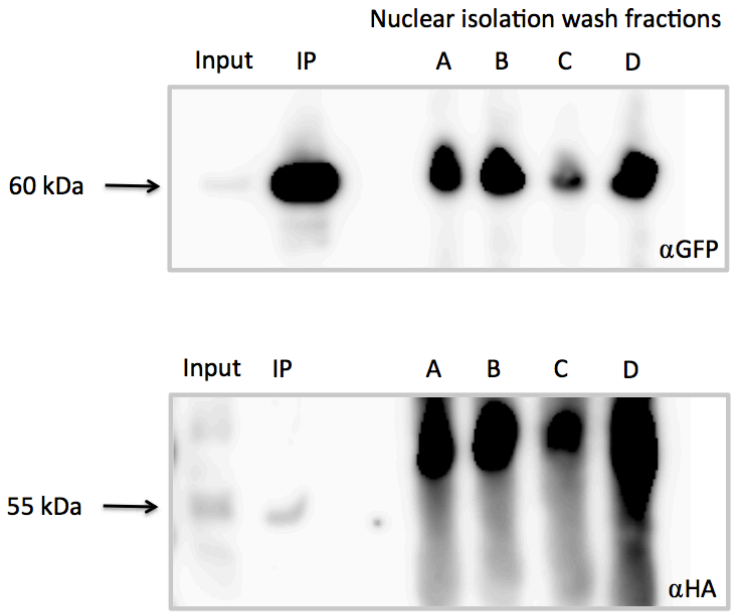

Figure 11. Co-IP to identify a potential interaction between GFP::HaRxL14 and HA::PP2CA *in planta* with GFP pull-down and wash fractions. The constructs 35S::*GFP*::*HaRxL14* and 35S::*HA*::*PP2CA* were expressed transiently in *N. benthamiana* for 3 days. The silencing suppressor p19 as co-infiltrated at a final OD of 0.1 (Voinnet *et al*., 2003). Successive wash fractions from the supernatant of the nuclear isolation process are shown in A (first), B, C and D (last) to identify potential loss of the proteins during this process. Input and IP products from the CoIP reactions following nuclear isolation and lysis are also shown. The membranes were probed with HRP conjugated αGFP or αHA antibody (Miltenyi Biotech). For western blot conditions see section 2.5.3 and Table 8.

The αGFP membrane indicates a substantial enrichment in GFP::HaRxL14 (at 60 kDa) between the input and IP (Figure 11). It is also clear that GFP::HaRxL14 is lost in the supernatant during the wash steps (A, B, C and D), although this is expected as the effector was previously shown to be present in the cytosol (Figure 6 & Figure 11).

The αHA membrane shows a band at 55 kDa, which is present in the input and IP lanes (Figure 11). This could be a positive Co-IP result as the band is of an anticipitated size in a similar region to that predicted for HA::PP2CA (although this theoretically is approximately 45 kDa). Therefore, this may be a low frequency interaction and a larger quantity of starting material may be required to detect the interaction as was the motivation for the experiment. Although, due to the similarity in size to GFP::HaRxL14 (at 60 kDa) this could be a cross-reaction of the αHA antibody due to the substantial amount of effector which was pulled down of a similar molecular weight. In the subsequent Co-IP experiment HA-binding agarose beads (Sigma Aldrich) were used to pull-down HA::PP2CA to determine whether this could make a difference to the outcome of the experiment and highlight whether these initial results were true or a false positive.

3.4.3 PP2CA pull-down with HA-binding beads

As an alternative approach to the Co-IP experiment, HA-binding agarose beads (Sigma Aldrich) were used to pull down the HA::PP2CA construct. This would give several important insights. Firstly, it would confirm that HA::PP2CA is highly expressed in *N. benthamiana* following infiltration of *A. tumefaciens* harbouring the construct into the leaves. If pull-down of HA::PP2CA is unsuccessful in this experiment then it could indicate that this vector is not expressed at the required level for detection of the protein construct by the end of the experiment.

Furthermore, it could show whether pulling down the putative host interactor as opposed to the effector could lead to a different outcome to that shown in Figure 10. Theoretically, pull-down of either protein in an interacting pair should result in a positive Co-IP result where an interaction is true. However, the stability of the

protein complex could be affected differently depending on which tag is bound to the beads during the pull-down process. This could result in the complex being detectable when the tag of one of the proteins is enriched but not with that of the other. Therefore the experiment aimed to investigate the complex through the enrichment of HA::PP2CA to determine whether this resulted in the same outcome or whether a stronger interaction is detectable.

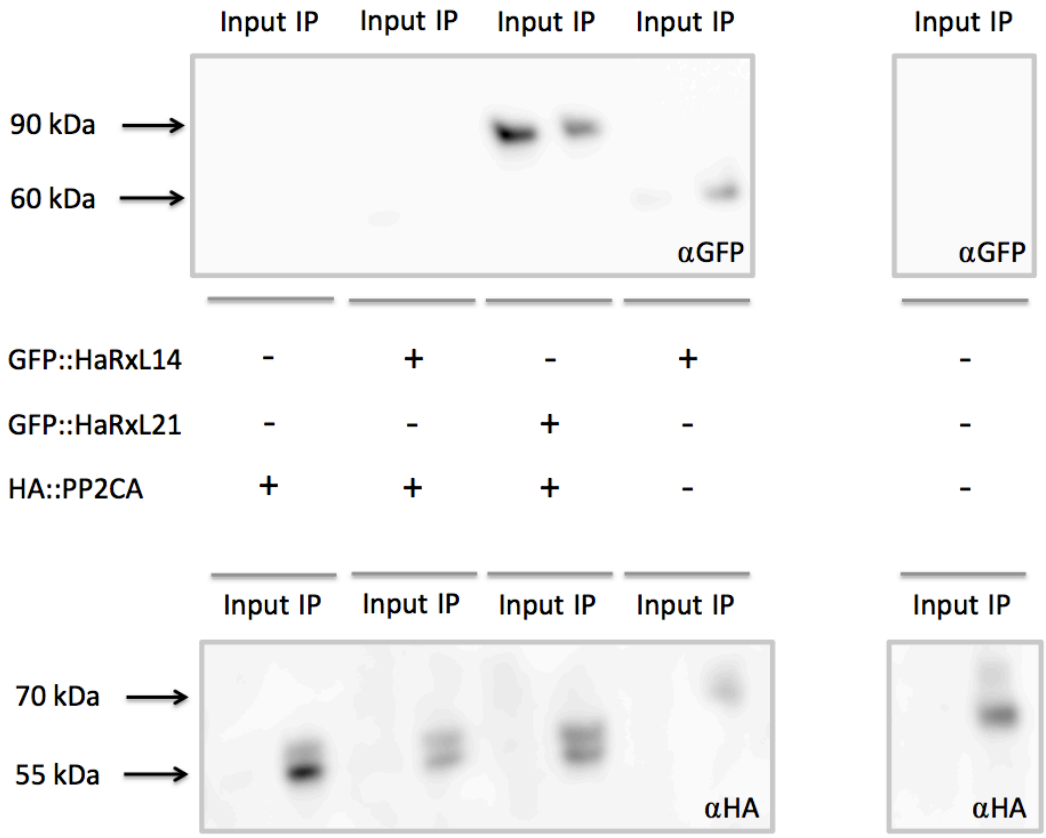

Figure 12. Co-IP to identify a potential interaction between GFP::HaRxL14 and HA::PP2CA *in planta* with HA pull-down. The constructs 35S::*GFP*::*HaRxL14* and 35S::*HA*::*PP2CA* along with control 35S::*GFP*::*HaRxL21* (which did not show an interaction with PP2CA in a yeast two-hybrid screen) were expressed transiently in *N. benthamiana* for 3 days, in the combinations indicated. The silencing suppressor p19 was co-infiltrated in all samples at a final OD of 0.1 (Voinnet *et al*., 2003). Sections are taken from the same western blot membranes. The membranes were probed with HRP conjugated αGFP (Santa Cruz) or αHA antibody (Miltenyi Biotech). For western blot conditions see section 2.5.3 and Table 8.

The αHA membrane shows bands at approximately 55 kDa in the first three sample sets (from left to right; Figure 12). This corresponds to those expressing HA::PP2CA, which as previously discussed has a predicted size of approximately 45 kDa (Figure 12). This suggests that the size of HA::PP2CA as determined by SDS-PAGE is 55 kDa, which is larger than predicted. In the light of this further evidence, it is highly likely that the partial Co-IP experiment presented in Figure 11 indicates that HA::PP2CA was pulled-down with GFP::HaRxL14. This experiment would need to be repeated with the same set of controls as presented in Figure 10 and with the larger quantity of starting material and GFP-binding agarose beads. However, the similarity in size of the two proteins constructs means that the final results are harder to distinguish by western blot. Therefore, further experiments used GFP::PP2CA and HA::HaRxL14 constructs in order to improve differentiation between the final proteins and mitigate the potential cross-reaction issue in the interpretation of the western blots.

The αGFP membrane shows unexpected results (Figure 12). The GFP-tagged effectors are detected in the anticipated input lanes. However, the presence of effector in the corresponding IP lanes is not as predicted (Figure 12). In particular, the negative control GFP::HaRxL21 appears to have been pulled-down with HA:PP2CA (Figure 12). In addition, GFP::HaRxL14 is present following the Co-IP when HA::PP2CA was not expressed (Figure 12). This raises the possibility that the HA binding beads have a tendency to bind non-specifically to the effector proteins. Therefore, in the following experiment the tags of the proteins were swapped. This resolved the issue of the size similarity of the constructs. Furthermore the GFP-binding beads did not show non-specific binding to the effector under these experimental conditions.

3.4.4 PP2CA pull-down with GFP-binding beads

This Co-IP experiment was set up in the same way as that presented in section 3.4.1 and Figure 10 with a reversal in the tags with each construct. Therefore, the constructs used in this experiment were GFP::PP2CA and HA::HaRxL14, along with HA::HaRxL21 as a negative control in the combinations shown in Figure 13. As previously described, this would identify if an interaction could be observed when pulling down PP2CA rather than HaRxL14 or if no identifiable interaction was distinguishable.

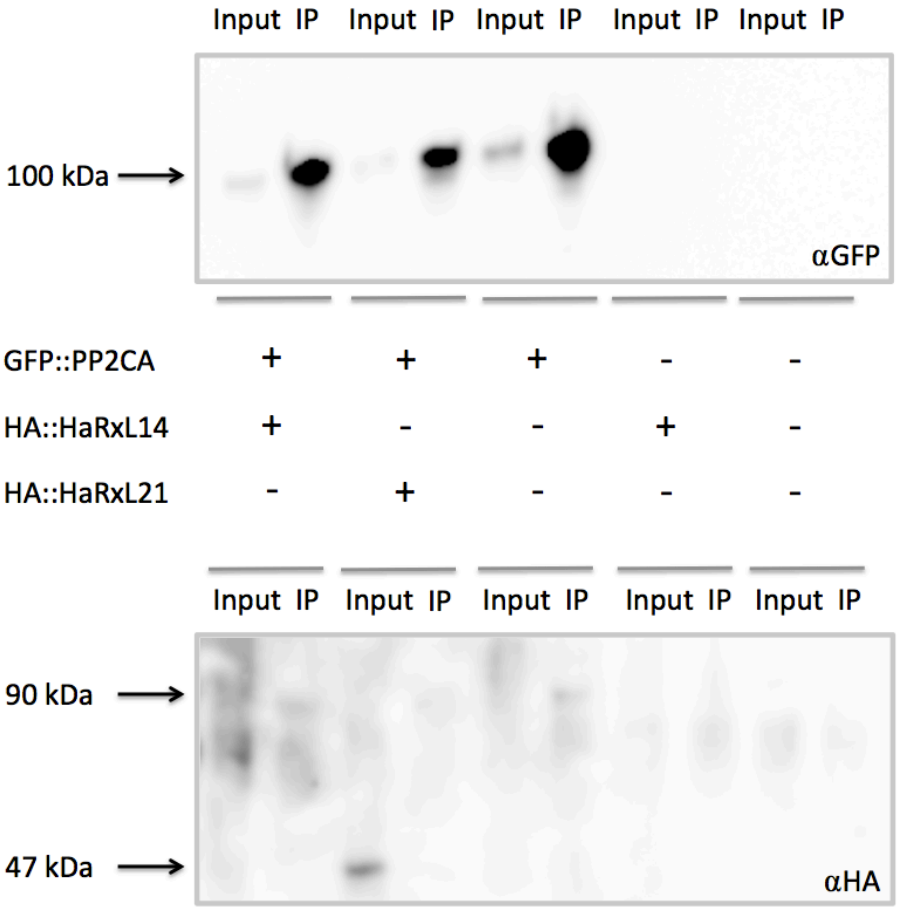

Figure 13. Co-IP to identify a potential interaction between HA::HaRxL14 and GFP::PP2CA *in planta* with GFP pull-down. The constructs 35S::*HA*::*HaRxL14* and 35S::*GFP*::*PP2CA* along with control 35S::*HA*::*HaRxL21*, which did not show an interaction with PP2CA in a yeast two-hybrid screen, were expressed transiently in *N. benthamiana* for 2 days, in the combinations indicated. The silencing suppressor p19 was co-infiltrated in all samples at a final OD of 0.1 (Voinnet *et al*., 2003). The membranes were probed with HRP conjugated αGFP or αHA antibody (Miltenyi Biotech). For western blot conditions see section 2.5.3 and Table 8.

The αGFP membrane shows input and substantial enrichment of GFP::PP2CA which has a molecular weight of 100 kDa in the predicted lanes as shown (Figure 13). The αHA membrane however does not show a positive interaction (Figure 13). There are no bands in the region of 27 kDa which is demonstrated in Figure 16 to be the actual size of HA::HaRxL14 (Figure 13). The band in the region of 47 kDa in the input channel for the second sample set (from left to right) appears to indicate expression of HA::HaRxL21 (Figure 13). However, there are no apparent bands in the first and third input channels, in which HA::HaRxL14 should be detectable (Figure 13). Therefore, it is possible that this result could be due to low or no expression of HA::HaRxL14.

3.4.5 Preliminary Co-IP test for HaRxL14 and PP2CA with ABA infiltration

An initial experiment was set up to determine whether a protein complex formed between HaRxL14 and PP2CA could be stabalised in the presence of ABA. While this was not the case in the yeast two-hybrid screen in which the interaction between the two proteins was identified, it could be a necessary condition to observe the interaction *in planta*.

In this experiment, the constructs were infiltrated into *N. benthamiana* leaves (as previously described) and 30 minutes before harvesting the leaves were infiltrated with 50 μM ABA (Sigma Aldrich) in water. During this time it was clear that the leaf showed absorption into its vasculature. In this Co-IP eperiment, GFP-binding agarose beads were used to pull down GFP::HaRxL14 in one reaction and GFP::PP2CA in the other.

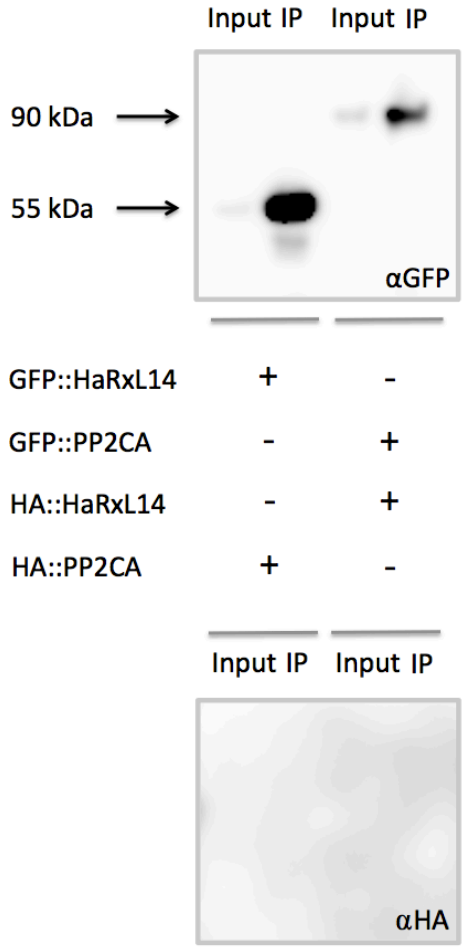

Figure 14. Co-IP to identify a potential interaction between HaRxL14 and PP2CA *in planta* with GFP pull-down with ABA infiltration. The constructs 35S::*HA*::*HaRxL14*, 35S::*GFP*::*HaRxL14*, 35S::*GFP*::*PP2CA* and 35S::*HA*::*PP2CA*, were expressed transiently in *N. benthamiana* for 2 days, in the combinations indicated. The silencing suppressor p19 was co-infiltrated in all samples at a final OD of 0.1 (Voinnet *et al*., 2003). ABA at 50 µM in water (Sigma Aldrich) was infiltrated into the leaves 30 minutes prior to harvesting. The membranes were probed with HRP conjugated αGFP or αHA antibody (Miltenyi Biotech). For western blot conditions see section 2.5.3 and Table 8.

The infiltration of 50 μM ABA into the leaves does not appear to make a difference to the outcome of the Co-IP (Figure 5). The αGFP membrane shows a clear enrichment in GFP::HaRxL14 and GFP::PP2CA between the input and IP channels (Figure 14). However, there are no clear bands indicating the presence or enrichment of HA::HaRxL14 or HA::PP2CA on the αHA membrane. This could be due to lack of expression. Alternatively, it is possible that the treatment conditions (i.e. the concentration of ABA and the duration of treatment) were not optimal. Follow up experiments could investigate whether changing these conditions may result in a different outcome to the Co-IP experiment.

3.4.6 Co-IP with determination of products by Mass Spectroscopy for HaRxL14 and PP2CA

An alterative approach was adopted in a last Co-IP experiment, in which Mass Spectroscopy (MS) was used to detect interacting proteins to increase the sensitivity of the Co-IP technique. Here GFP-binding beads were used to pull down GFP::HaRxL14 and GFP::PP2CA to confirm whether the bait protein affected the outcome as previously discussed. In addition, HA::GFP was co-expressed with GFP::PP2CA or GFP::HaRxL14 as a control to confirm that an observed interaction was unlikely to be a result of non-specific binding of the tags.

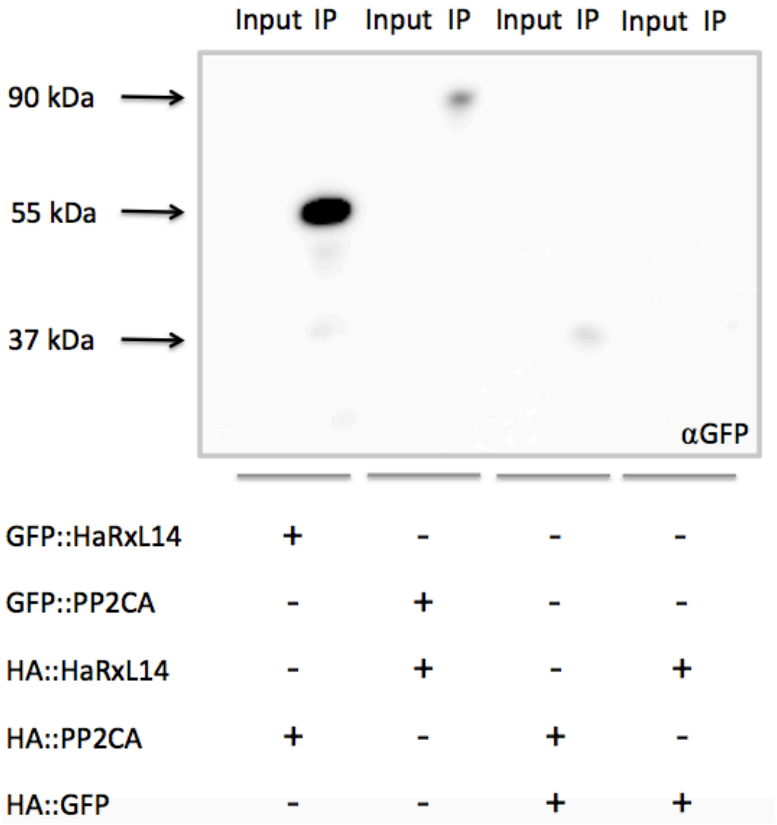

Figure 15. Verification of GFP pull-down to identify a potential interaction between HaRxL14 and PP2CA *in planta* with Co-IP by mass spectroscopy. The constructs 35S::*HA*::*HaRxL14*, 35S::*GFP*::*HaRxL14*, 35S::*HA*::*PP2CA* and 35S::*GFP*::*PP2CA* along with controls 35S::*HA*::*HaRxL21*, which did not show an interaction with PP2CA in a yeast two-hybrid screen, and 35S::*GFP*::*HA* were expressed transiently in *N. benthamiana* for 2 days, in the combinations indicated. The silencing suppressor p19 was co-infiltrated in all samples at a final OD of 0.1. The membrane was probed with HRP conjugated αGFP (Miltenyi Biotech). For western blot conditions see section 2.5.3 and Table 8.

As a quality control prior to the preparation of the reactions for MS, 10% of each input and IP sample was analysed by western blot to confirm the presence of the pulled down protein in the output of the Co-IP reactions. Figure 15 indicates that the GFP-tagged protein constructs were expressed as expected. The HA::GFP construct (molecular weight 37 kDa) has the weakest expression and is very faintly detected in the IP lane for the forth sample set (from left to right; Figure 15). A relatively larger amount of GFP::HaRxL14 and GFP::PP2CA constructs were detected following pull down (Figure 15).

Overall, the samples were determined to be acceptable for MS. Sarah Harvey prepared the samples for MS, which was run on the Proteomelab PF2D protein fractionation system (Beckman Coulter) by Cleidiana Zampronio. The results did not detect an interaction between the proteins despite the proteins individually being identified (GFP::HaRxL14 and GFP::PP2CA). This could mean that no interaction is apparent. Alternatively, it has been suggested that HaRxL14 could have a role in enhancing host susceptibility in *N. benthamiana* to *P. infestans* (Hazel McLellan, unpublished). Furthermore, it was shown that GFP::HaRxL14 has a range of interactions in *N. benthamiana* which were not apparent with GFP::PP2CA or HA::GFP. These include various chloroplast-localised proteins such as chlorophyll a-b binding proteins, which are part of the light-harvesting complex. Therefore it is possible that pathological role of the effector in *N. benthamiana* could negatively influence the ability to detect the interaction by Co-IP.

3.5 Pathology screens

3.5.1 Confirmation of effector protein over-expression in *Arabidopsis* lines

The three HA::HaRxL14 expressing transgenic *Arabidopsis* lines (see section 2.1) were confirmed for expression of the protein construct by western blot. To ensure that expression of the protein was stable through the growth stages of the *Arabidopsis* plants, analysis was carried out with 2-week-old seedlings and also with leaves collected from plants at 4-weeks growth. Transgenic *Arabidopsis* lines expressing HA::GFP were included as a positive control for expression as this has previously been confirmed (Jens Steinbrenner, unpublished). In all cases the total

protein was extracted and a Bradford Assay was performed to correct for the differences in total protein between samples as described in section 2.5.1. The protein extracted from the various lines was analysed by western blot (see section 2.5.3).

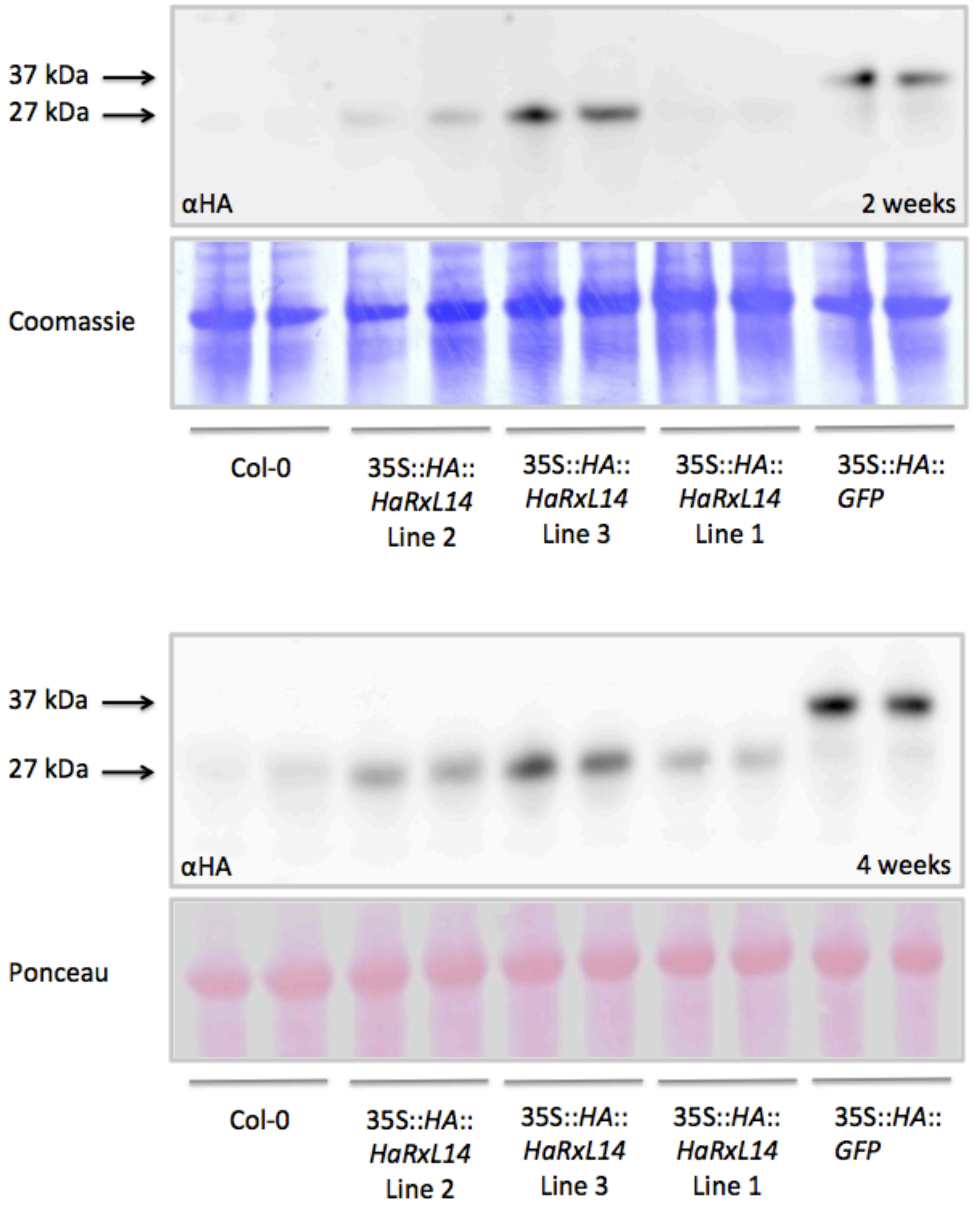

Figure 16. Relative protein expression determined by western blot in 35S::*HA*::*HaRxL14* lines with 35S::*HA*::*GFP* and Col-0 as controls in 2-week-old *Arabidopsis* seedlings and 4-week-old plants. The preparation of tissue was carried out as described in section 2.5.3. Two biological replicates were tested for each seed line. The membranes were probed with HRP conjugated αHA (Miltenyi Biotech). The membranes were stained with either Coomassie Brilliant Blue or Ponceau for loading controls as indicated. For western blot conditions see section 2.5.3 and Table 8.

The expression of HA::HaRxL14 with a molecular weight of 27 kDa can be confirmed across each of the lines but at different relative levels (Figure 16). This pattern of relative expression between the three lines is consistent when comparing the seedlings at 2 weeks and the plants at 4-weeks (Figure 16). Line 3 has the highest level of expression of the protein construct, while line 1 has the weakest expression (Figure 16). This variability of expression of HA::HaRxL14 across the lines could be useful in further analysis. For instance, it will allow investigation of how a relatively high or low level of the effector protein influences its pathological effect on the host.

3.5.2 *Hpa* screens for over-expressing HaRxL14 lines

The *Arabidopsis* transgenic HA::HaRxL14 expressing lines were screened for susceptibility to *Hpa*. This involved infection of two-week-old seedlings with *Hpa* spore suspension and counting the number of sporangiophore structures on the cotyledons and true leaves after 4-days of infection (see section 2.6.2). In these screens, Col-0 was included as a wild-type control and Col-0 expressing β-glucuronidase (GUS) as a control for transgene expression. In addition, 35S::*HaRxL14* is included a positive control, as this has previously been confirmed to have enhanced susceptibililty to *Hpa* (Fabro *et al*., 2011).

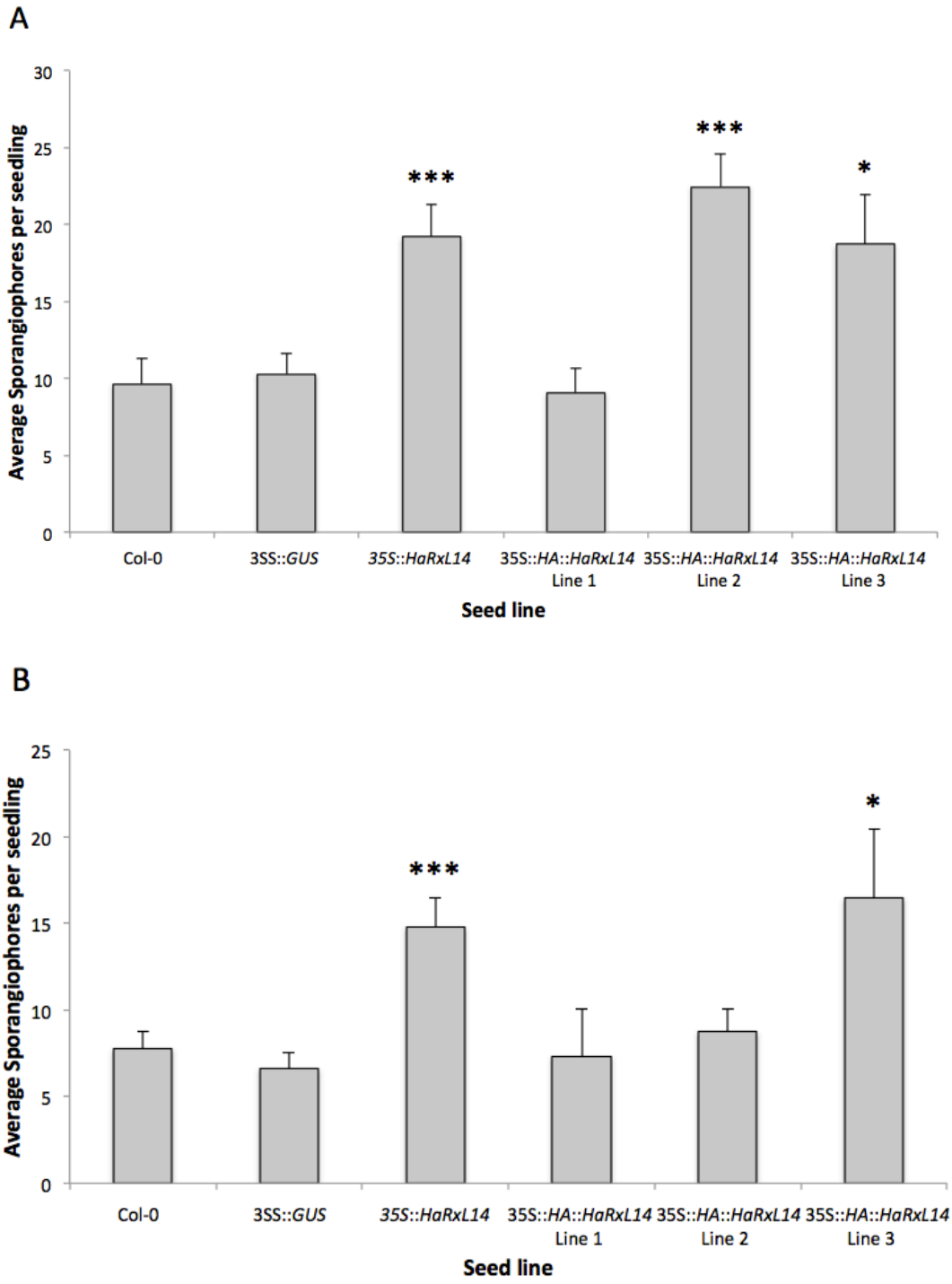

Figure 17. Sporangiophore count for *Arabidopsis* seedlings expressing 35S::*HA*::*HaRxL14* (three lines), 35S::*HaRxL14*, Col-0 (wild-type) and 35S::*GUS* following infection with *Hpa* in two independent screens (**A** and **B**). The seedlings were sprayed at 14-days with *Hpa* spore suspension of pathogen isolate Noks1 and incubated for 4 days and the total sporangiophores per seedling were counted with a stereomicroscope. The charts show the average sporangiophores per seedling and +SE. Statistically significant p-values based on t-test against Col-0 are denoted by * ≤ 0.05 and *** ≤ 0.001.

The results show that line 3 had enhanced susceptibility to *Hpa* compared to Col-0 in both screens, while line 2 had higher susceptibility in screen A but not B (Figure 17). Line 1 does not have enhanced susceptibility to *Hpa* in either screen (Figure 17). This is in agreement with the western blot results which showed that the expression of HA::HaRxL14 is relatively lower in this line (Figure 16). Overall, it appears that expression of HaRxL14 in *Arabidopsis* enhances susceptibility of the plant to *Hpa* isolate Noks1.

3.5.3 *Hpa* screens for PP2CA lines

To investigate how knocking-out and over-expressing PP2CA affects the immune response, two knock-out and an over-expressing lines were screened for susceptibility to *Hpa* (see section 2.6.2). With the role that PP2CA has in ABA signal transduction and evidence suggesting that ABA pathways are suppressed by *Hpa*, it seems likely that these *PP2CA* mutant lines could have changed susceptibility (Asai *et al*., 2014). In the same way as the previous set of screens, the lines 35S::*HA*::*HaRxL14*, Col-0, 35S::*GUS* and 35S::*HaRxL14* were included as controls.

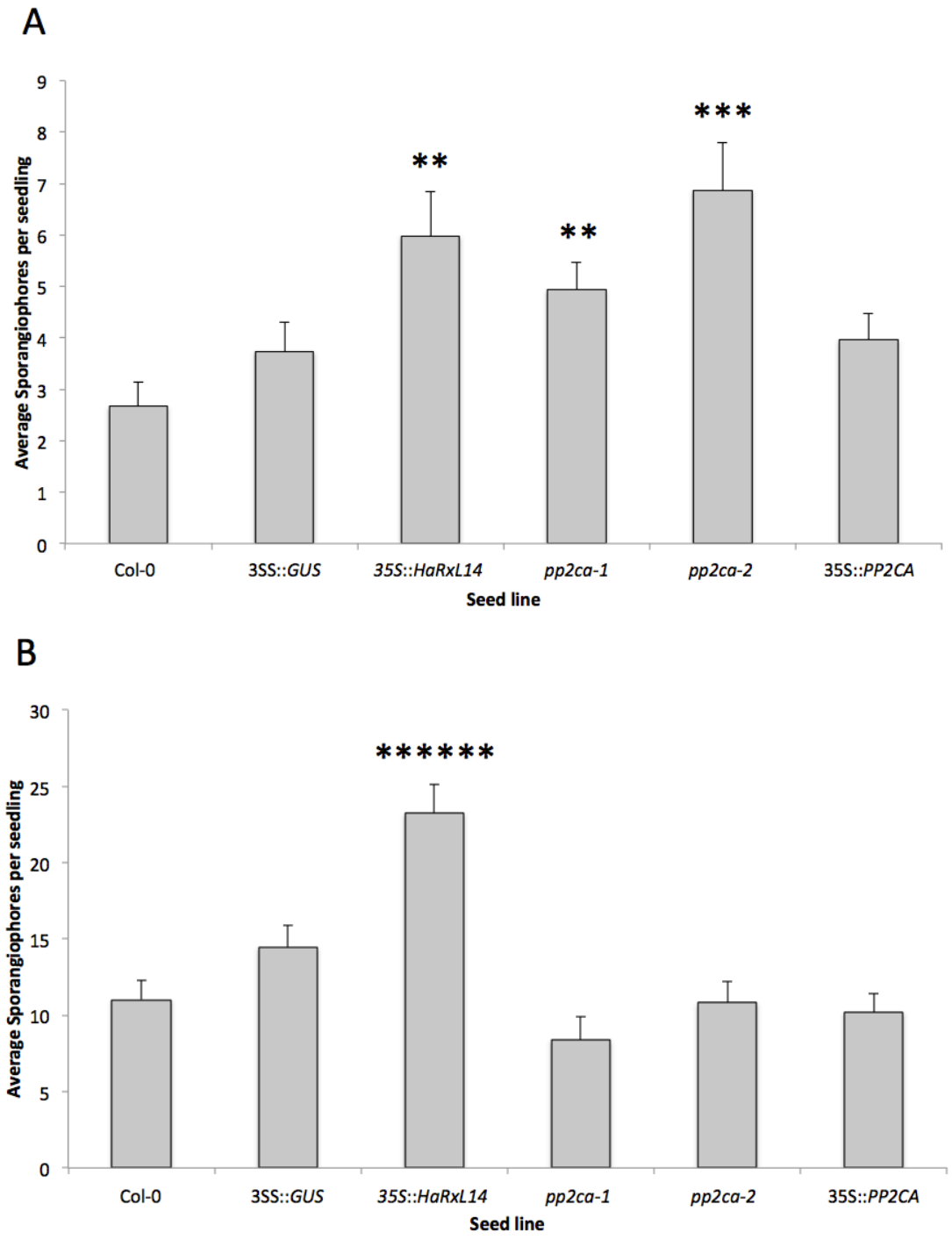

Figure 18. Sporangiophore count for *Arabidopsis* seedlings expressing 35S::*HaRxL14*, knock-outs *pp2ca-1* and *pp2ca-2*, PP2CA over-expressor (35S::*PP2CA*) Col-0 (wild-type) and 35S::*GUS* following infection with *Hpa* in two independent screens (**A** and **B**). The seedlings were sprayed at 14-days with *Hpa* spore suspension of pathogen isolate Noks1 and incubated for 4 days and the total sporangiophores per seedling were counted with a stereomicroscope. The graphs show the average sporangiophores per seedling and error bars represent +SE. Statistically significant p-values based on t-test against Col-0 are denoted by ** ≤ 0.01, *** ≤ 0.001 and ****** ≤ 0.000001.

The screens showed mixed effects on susceptibility to *Hpa* in the PP2CA lines and a further repeat will be required to verify a final result. The initial screen shown in Figure 18A indicates that the two knock-out lines have enhanced susceptibility compared to Col-0. Both *pp2ca-1* and *pp2ca-2* have a sporangiophore count significantly higher than Col-0, with p-values less than 0.01 (and less than 0.001 in the case of *pp2ca-2*; Figure 18). However, the second screen did not show a significant difference between the *PP2CA* knock-out and over-expressing lines and Col-0.

It is possible that the interaction with PP2CA alone is not sufficient to enhance susceptibility. As HaRxL14 has multiple targets, a combined effect of the interactions with these host proteins could lead to the overall enhanced susceptibility that is shown in Figure 17. However, if the results of the first screen are confirmed and knocking out *PP2CA* does improve growth of *Hpa*, then this could be due to an increased sensitivity of these lines to ABA. It has previously been shown that *Hpa* growth is improved by induction of an ABA response (Fan *et al*., 2009). Alternatively the presence of the effector may be required for the enhancement of susceptibility to the pathogen. This may be through stabilising an interaction with a particular host protein, which may not be emulated by a genetic mutation of the protein.

3.6 MAMP inducible reactive oxygen species (ROS) burst screens

To investigate whether PP2CA has a role in the MAMP-inducible ROS burst, the knock-out lines *pp2ca-1* and *pp2ca-2* along with the over-expressing PP2CA line were screened for ROS production following elicitation by the active epitope of the bacterial flagellum (flg22). During recognition of a pathogen, superoxide or hydrogen peroxide particles are released by host cells for varied purposes which may include the strengthening of the cell wall or signalling (Torres, 2010). It has previously been identified that ROS production is an outcome of ABA signalling and there is also a known interplay with the MAMP-inducible pathways (Melotto *et al*., 2006). Therefore it was hypothesised that a potential interaction of the effector with PP2CA could have an effect on the ROS burst which is induced during host defense.

Each line was screened against Col-4 and receptor kinase FLAGELLIN-SENSITIVE 2 (FLS2) knock-out (unable to percieve flg22) to determine whether an interaction of HaRxL14 with PP2CA could have an effect on MAMP-inducible ROS production.

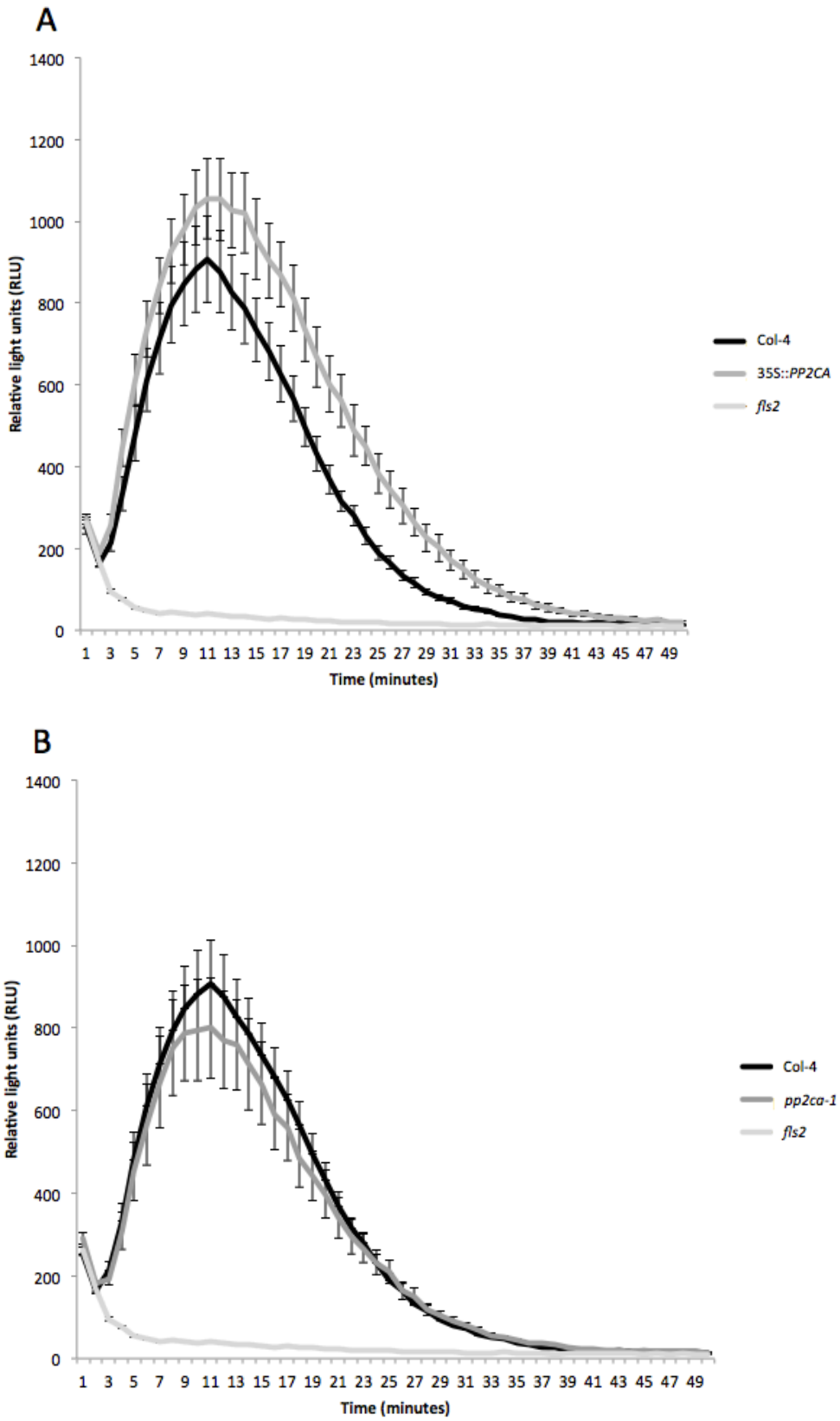
A
1400
1200
1000
800
600
400
200
0
Relative light units (RLU)
1 3 5 7 9 11 13 15 17 19 21 23 25 27 29 31 33 35 37 39 41 43 45 47 49
Time (minutes)
Col-4
35S::PP2CA
fls2
B
1400
1200
1000
800
600
400
200
0
Relative light units (RLU)
1 3 5 7 9 11 13 15 17 19 21 23 25 27 29 31 33 35 37 39 41 43 45 47 49
Time (minutes)
Col-4
pp2ca-1
fls2

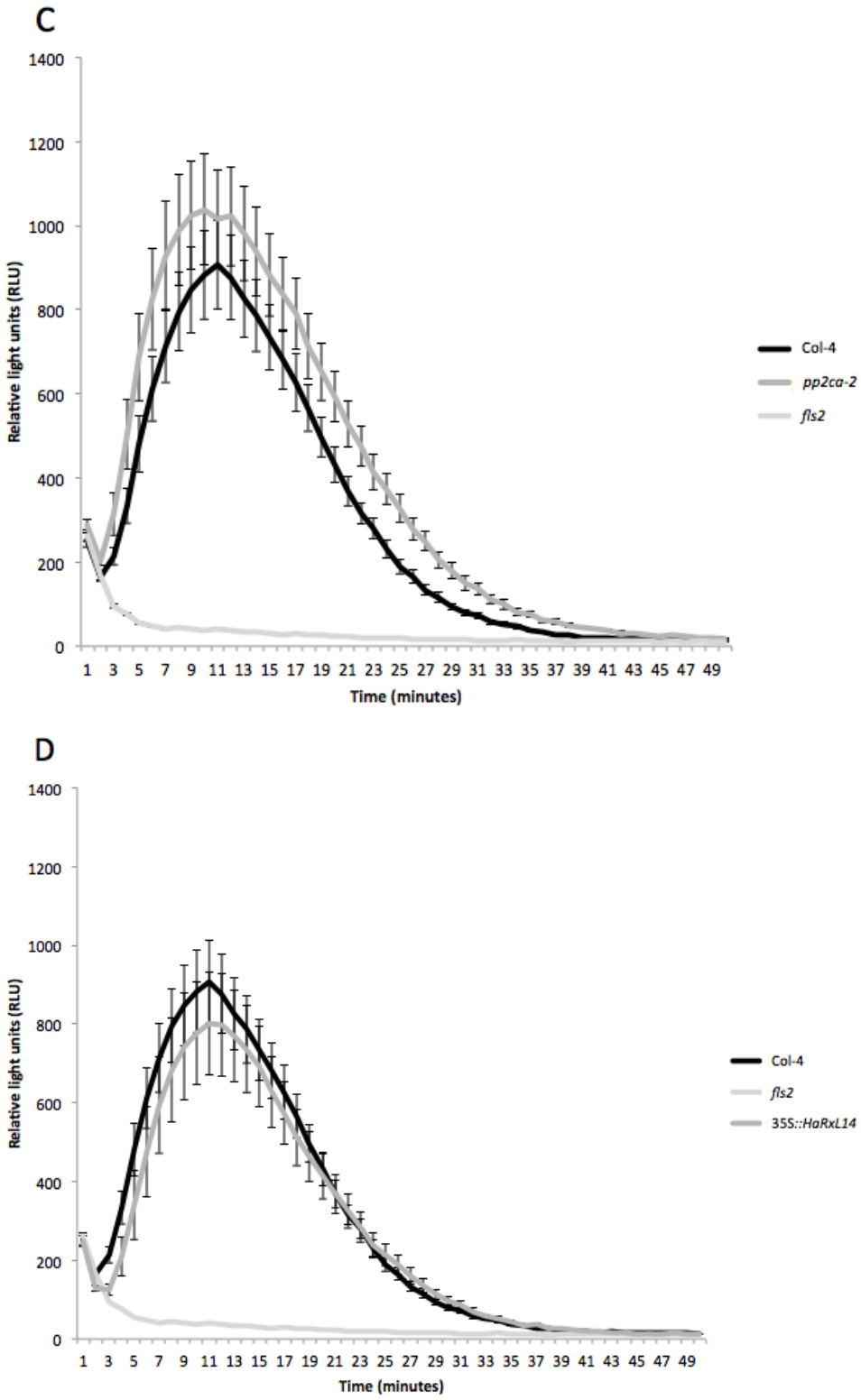

Figure 19. ROS assay for 35S::*PP2CA* (**A**), *pp2ca-1*, *pp2ca-2* (**B** & **C**) and 35S::*HaRxL14* (**D**) with *fls2* and Col-4 controls. Twelve leaf discs per seed line were taken the previous evening and suspended in water in the dark. A reaction mixture including flg22 was applied to each leaf disc and readings were taken as described in section 2.6.1. Average relative light units at each time point are shown. Error bars represent +/- SE.

The screens showed that there was no significant difference between the peaks in the production of ROS between the PP2CA mutant *Arabidopsis* lines and wild-type (Figure 19). However during the late phase in the production of ROS, there is a statistically significant difference between *pp2ca-2* and the *PP2CA* over-expressing line compared to wild-type (Figure 19). The production of ROS in the *PP2CA* over-expressor in particular remains higher for longer and becomes statistically significant by 2 minutes after the peak in ROS production (Figure 19).

It has previously been shown that the PP2C mutant *abscisic insensitive-1* (*abi-1*) is linked to ABA-induced ROS production by a down-stream signalling cascade involving slow anion channel-associated (SLAC) 1, which activates stomatal closure (Lee *et al*., 2013; Mustilli *et al*., 2002). The SLAC1 anion channel is also activated in the pathways associated with flg22 induced ROS (Guzel Deger *et al*., 2015). It has recently been found that these signalling pathways converge at OST1 (a SnRK2-type protein) which is a target of the PP2Cs and that this kinase in turn activates SLAC1 (Guzel Deger *et al*., 2015; Lee *et al*., 2013). Therefore, when the PP2C *abi-1* mutant is treated with flg22 the stomata close as with wild-type as it is upstream of OST1 (Guzel Deger *et al*., 2015). The PP2CA mutant lines therefore are expected to show a similar response based on these data. Overall, knocking out PP2CA is unlikely to have an effect on the production of ROS in response to detection of MAMPs. Although there could be an unclear mechanism behind the sustained period of ROS production in the PP2CA over-expresser or *pp2ca-2* knock-out line, a consistent trend would need to be verified in a further screen.

3.7 Gene expression analysis

3.7.1 Microarrays to examine gene expression changes in HA::HaRxL14 and PP2CA knock-out and over-expressing lines

Microarrays were performed to investigate the overall gene expression changes in the HA::HaRxL14 lines and the *PP2CA* knock-out and over-expressing lines. Figure 20 shows the experimental design used in this microarray analysis. The NimbleGen microarrays (*Arabidopsis* 12X135K arrays) which were used in the experiment ensured good reproducibility of results and meant that technical replication of samples was not necessary. This would be required in a system with high variablity between arrays. The cDNA from each biological replicate labelled with fluorescent Cy3 dye were hyridised to a single array. Three biological replicates were analysed per seed line and the seedlings were harvested at 2-weeks growth without treatment.

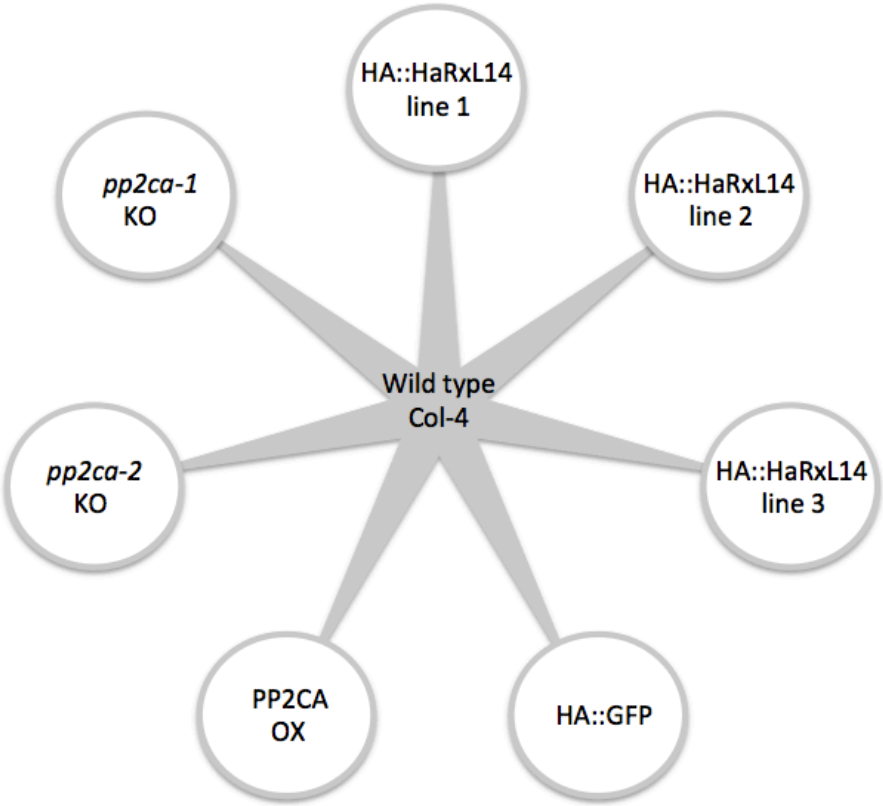

Figure 20. Experimental design for microarray experiment. The gene expression data for each of the seed lines represented in the circles were compared to wild-type *Arabidopsis* ecotype Col-4 during microarray data analysis. Three biological replicates were analysed for each of the lines.

3.7.1.1 Data normalisation

The raw intensity data were normalised using ANAIS software (Simon and Biot, 2010). This software examines the intra- and inter-array variability of dye intensity data and normalises the relative expression of each of the gene probes based on these assessments. Figure 21 shows the spread of intensity data for each array as box-plots before and after this normalisation.

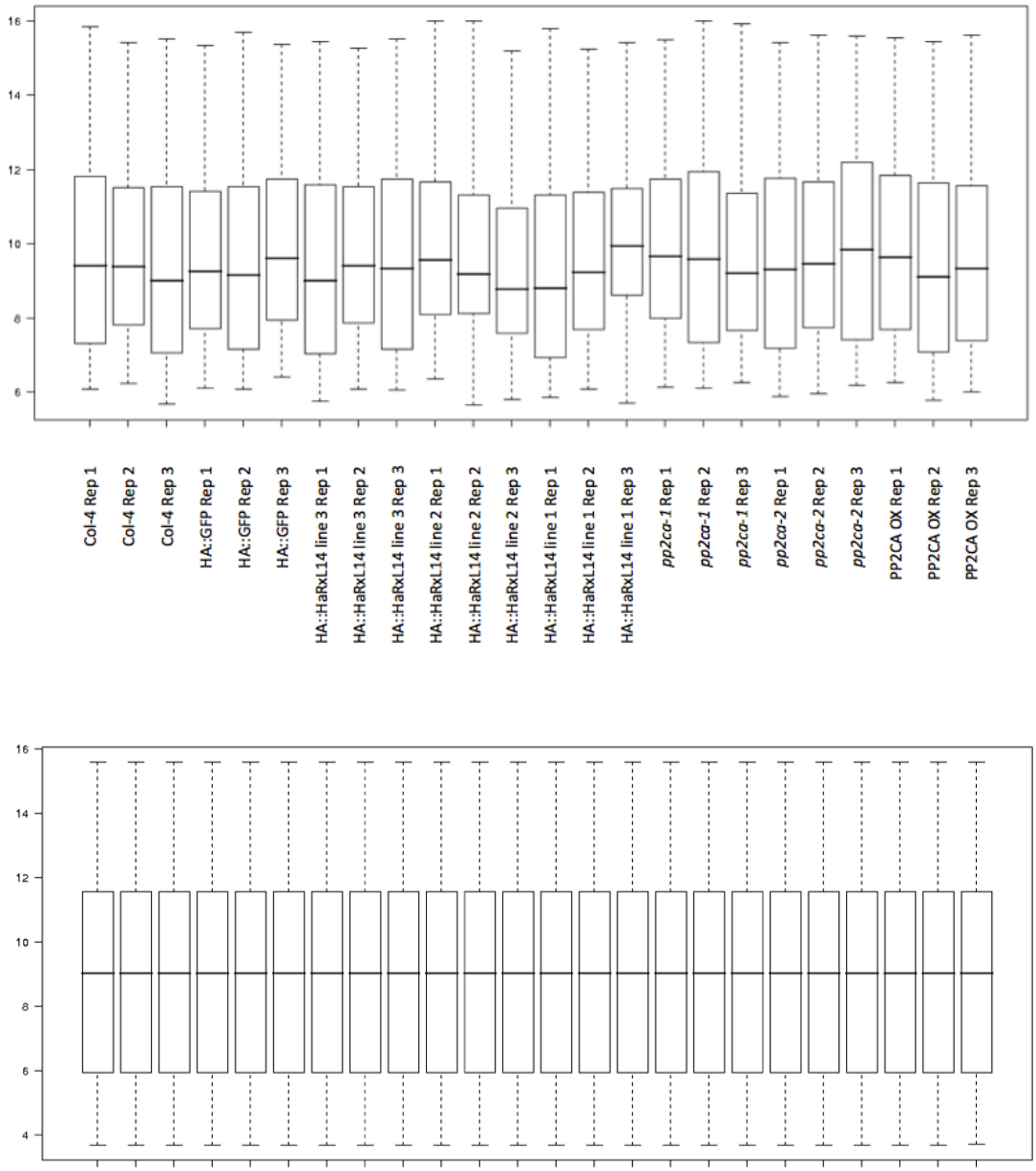

Figure 21. Microarray normalisation for each biological replicate for HaRxL14 and PP2CA knock-out and over-expressing (OX) *Arabidopsis* lines. The box-plots show the distribution of array intensity data before (above) and after (below) normalisation with ANAIS online software (Simon and Biot, 2010). The median is represented by the midpoint, the edges of the boxes are one standard deviation and the edges of the whiskers are one and a half standard deviations from the median.

3.7.1.2 Analysis of differentially expressed genes

The normalised data were analysed using LIMMA in R in which a contrast matrix was used to compare each of the lines to Col-4 (Smyth, 2005). These comparisons were used to calculate p-values for each gene and identify differentially expressed genes for each of the lines (Figure 20).

From these analyses it was determined that a large number of genes were differentially expressed in comparison to Col-4 in HA::HaRxL14 lines 1 and 2 (significant at $p<0.05$). Therefore, those which were significant at $p<0.01$ were used in further analysis (Figure 22). By contrast, HA::HaRxL14 line 3, *pp2ca-1*, *pp2ca-2* knock-outs and the PP2CA over-expressing line showed little if any differentially expressed genes in comparison to Col-4. This is likely due to the wild-type like response of the first biological replicate of line 3, as shown for the relative expression of the genes in Figure 23.

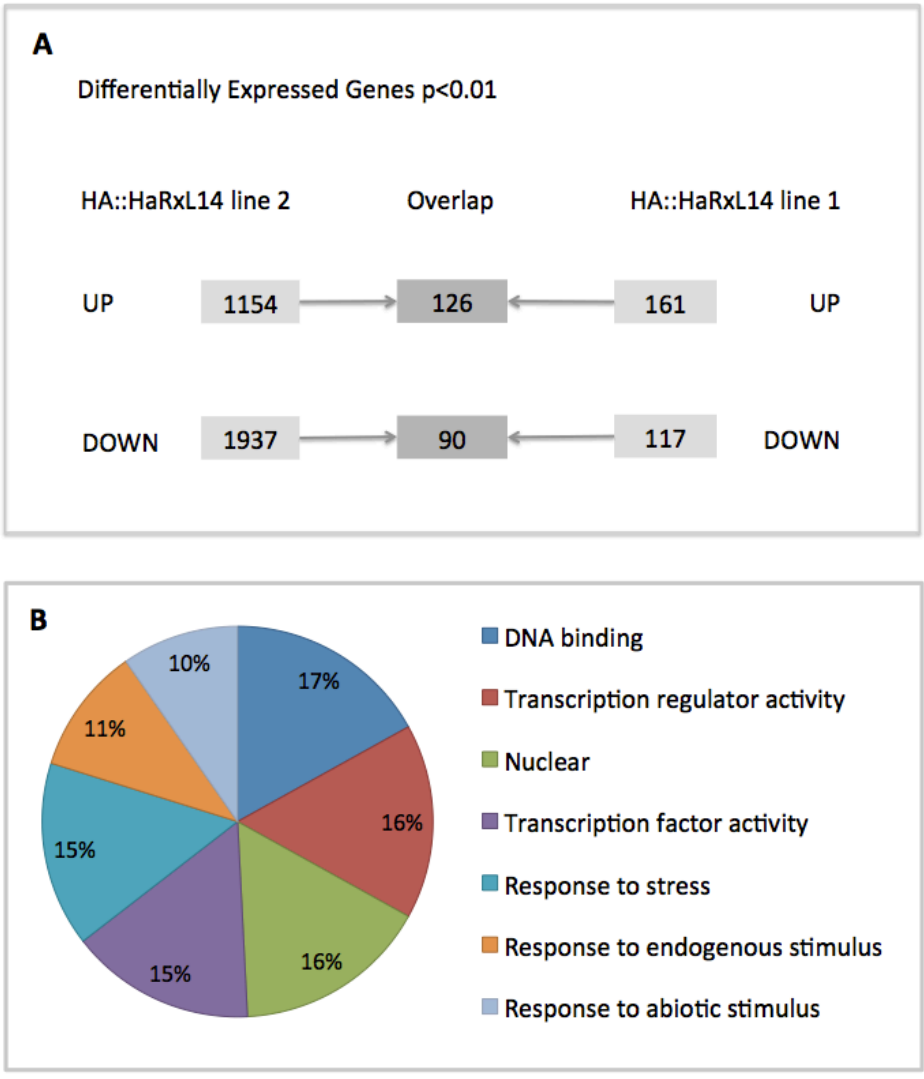

Figure 22. Analysis of differentially expressed genes ($p<0.01$ when compared to Col-4) for 35S::*HA*::*HaRxL14* lines 1 and 2. **A** The differentially expressed genes were compared between line 1 and 2 and the number of genes that were significantly up or down-regulated in both. The up-regulated genes were investigated in a gene ontology (GO) term analysis in Cytoscape plug-in BiNGO **(**GOSlim Plant; Maere *et al.*, 2005). **B** The percentages of genes in each GO category ($p<0.05$).

Analysis of the differentially expressed genes in HaRxL14 lines 1 and 2 when compared to Col-4 at $p<0.01$, showed a significant proportion of overlap between the two lines (Figure 22). The up and down-regulated genes showed 78% and 77% overlap respectively (as a proportion of genes differentially expressed in line 1; Figure 22A). The HA::HaRxL14 line 2 had the largest number of genes up and down-regulated and from Figure 16 is is clear that 2-week old seedlings have higher expression of the effector in line 2 than line 1. Another key observation from the microarray data is that despite the effector protein showing highest expression in HA::HaRxL14 line 3, this line showed only one differentially expressed gene (AT1G53480) significant at $p<0.05$. However, it is clear from the following gene expression data shown for four different genes across all lines that the first biological replicate of HA::HaRxL14 has expression comparable to that of the controls (Col-4 and HA::GFP; Figure 23). Therefore, it is likely that this result could be skewing the calculations for differentially expressed genes in this line. Analysis could therefore be repeated for this line without this replicate.

A gene ontology (GO) term analysis was used to identify the nature of the genes which were consistently up or down regulated between HA::HaRxL14 lines 1 and 2. The genes that were identified in Figure 22A as overlapping between the lines were analysed in BiNGO which is a plug-in for Cytoscape (Maere *et al*., 2005). A GOSlim Plant anaylsis was used to gain a general overall picture of the GO catergories which were significantly over-represented at $p<0.01$ and these are presented as a pie chart (Figure 22B). A GOSlim analysis of the down-regulated genes identified tropism as a single over-represented catergory. It is clear from the pie chart showing up-regulated genes that a large proportion of the GO terms fall into the catergories of response to stress, endogenous or abiotic stimulus (36% overall; Figure 22B). With further investigation of these genes it was clear that many had links to hormone pathways including ABA. Figure 23 shows relative expression across all of the seed lines and biological replicates for four ABA-related genes.

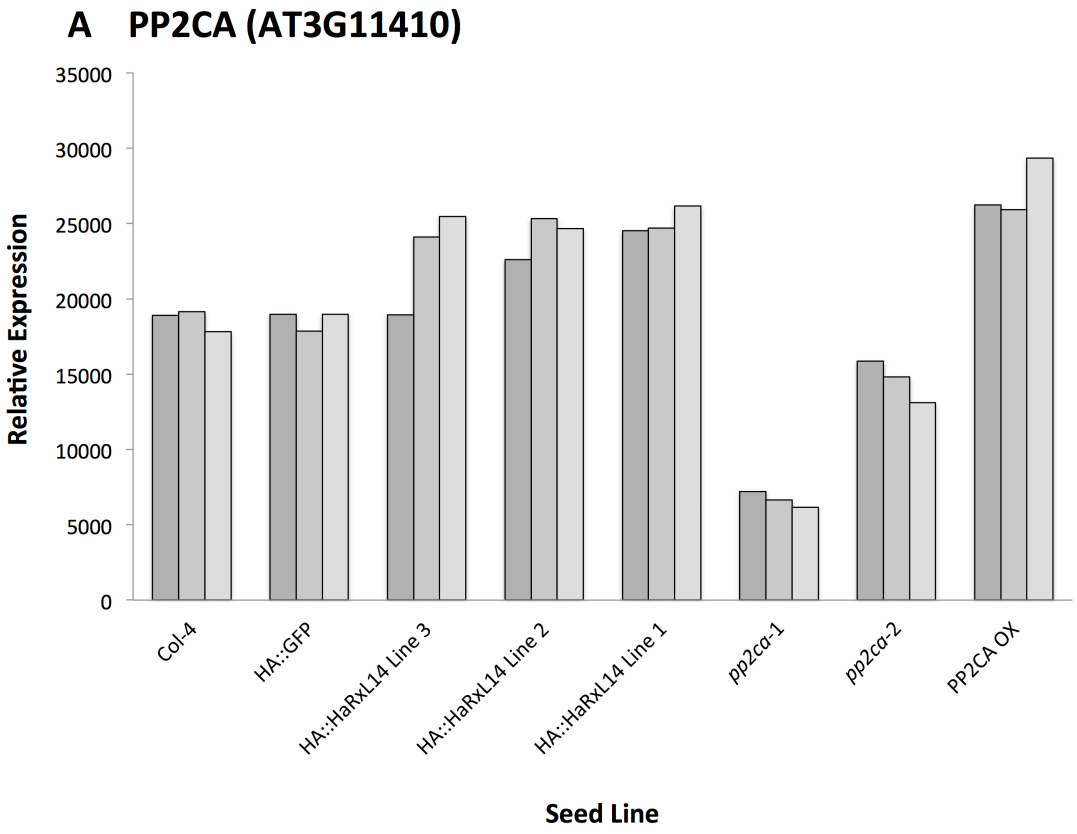
A PP2CA (AT3G11410)
Relative Expression
35000
30000
25000
20000
15000
10000
5000
0
Col-4
HA::GFP
HA::HaRxL14 Line 3
HA::HaRxL14 Line 2
HA::HaRxL14 Line 1
pp2ca-1
pp2ca-2
PP2CA OX
Seed Line

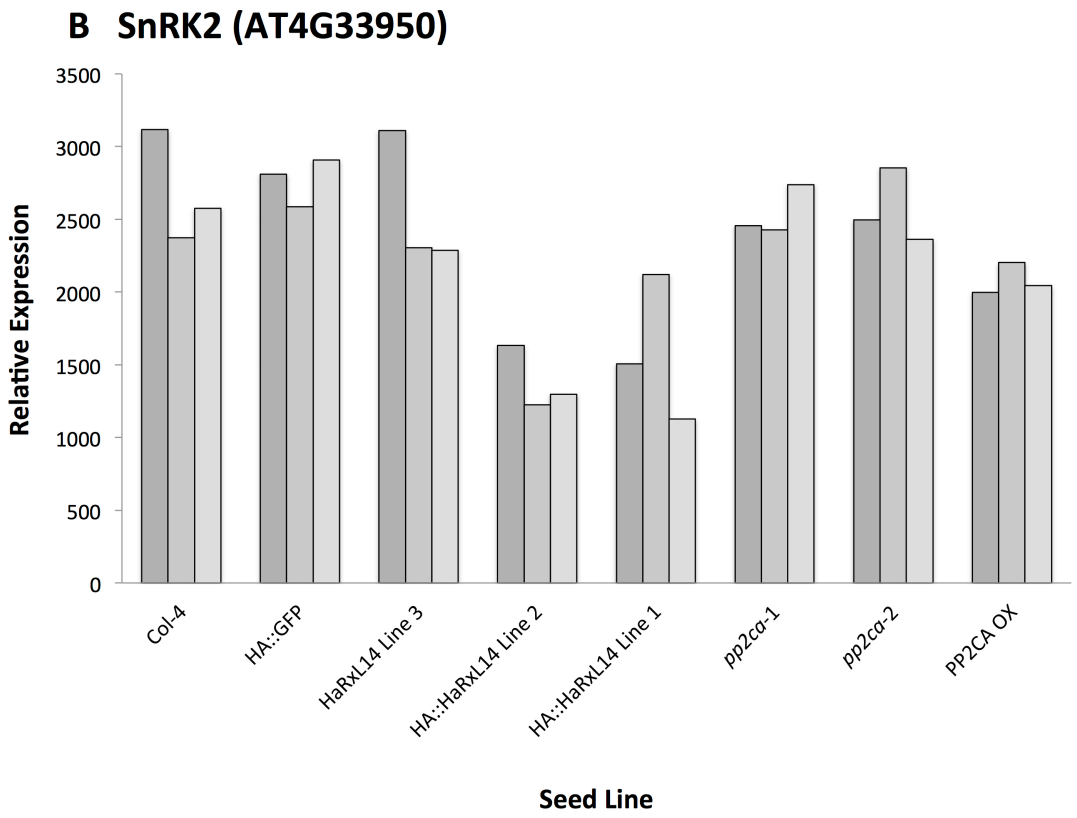
B SnRK2 (AT4G33950)
Relative Expression
3500
3000
2500
2000
1500
1000
500
0
Col-4
HA::GFP
HaRxL14 Line 3
HA::HaRxL14 Line 2
HA::HaRxL14 Line 1
pp2ca-1
pp2ca-2
PP2CA OX
Seed Line

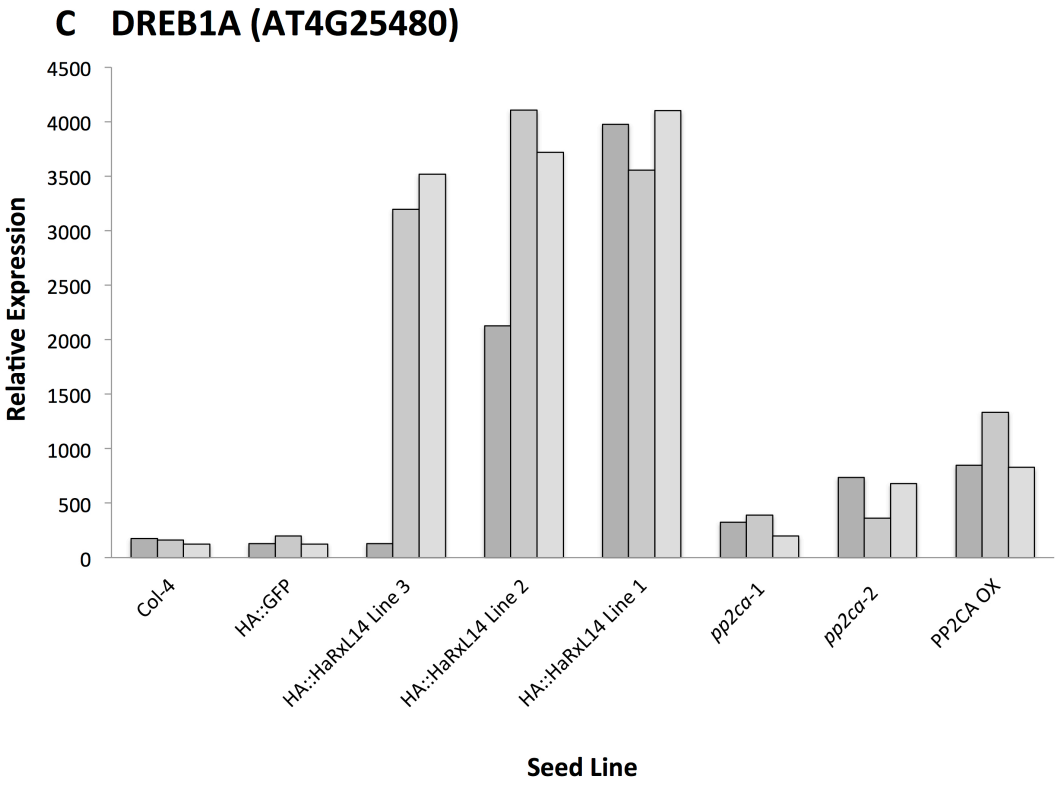

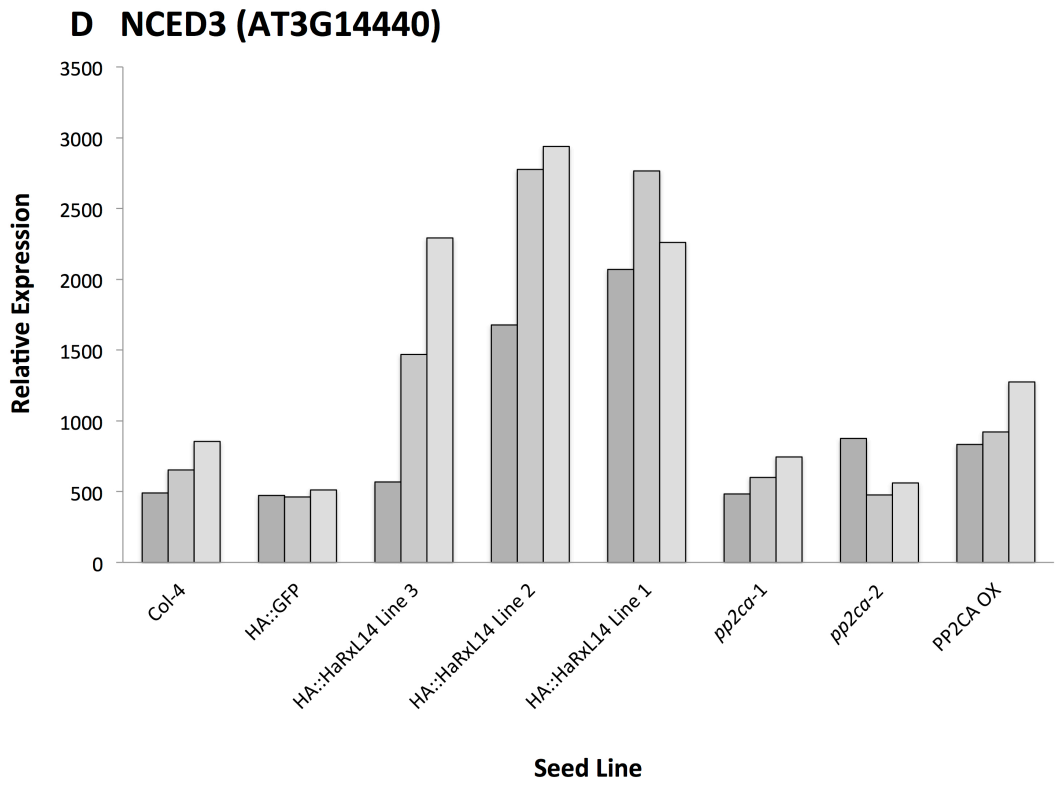

Figure 23. Relative expression of four genes differentially expressed in *HA*::*HaRxL14* lines 2 and 3 ($p<0.01$ when compared to Col-4) across all investigated lines. Each bar represents relative expression of the gene in a single biological replicate. The genes shown are involved in ABA recognition and signal transduction (**A** & **B**), transcriptional coordination (**C**) and ABA biosynthesis (**D**).

These ABA related genes which were significantly up-regulated in HA::HaRxL14 lines 1 and 2 and showed consistent patterns in expression across the lines (Figure 23). The expression of PP2CA across all of the seed lines shows an interesting pattern. As predicted, the expression of the gene is low in the knock-out lines *pp2ca-1* and *pp2ca-2* (particularly low expression in *pp2ca-1*) and has highest expression in the PP2CA over-expressing line (Figure 23A). It is also apparent that PP2CA was significantly up-regulated in HA::HaRxL14 lines 1 and 2. This increase in expression of PP2CA has been identified as a response to ABA and is also observed for other signalling components (Chan, 2012; Tähtiharju and Palva, 2001). Furthermore, DREB1A (a transcriptional regulator involved in cold response) and NCED3 (an ABA biosynthetic enzyme) are also strongly induced in these two effector over-expressing lines (Figure 23C and D). Interestingly, a 15-fold increase in *NCED3* transcripts was also observed in microarrays with *Arabidopsis* tissue infected with *P. syringae* pv. *tomato* DC3000 with T3Es (Figure 23D; de Torres-Zabala *et al.*, 2007). A significant up-regulation was also evident for several other ABA-related genes including NAC2 (AT1G01720) and NAC72 (AT4G27410), which is also consistent with the up-regulation of NAC transcription factors in response to *P. syringae* pv. *tomato* DC3000 with T3Es (de Torres-Zabala *et al.*, 2007). These results all suggest that the effector could be inducing a host response to ABA in a similar way to bacterial infection (de Torres-Zabala *et al.*, 2007).

Overall, the microarray results suggest that there are a substantial number of genes that are differentially expressed when the effector is over-expressed. A GO term analysis of consistently up-regulated genes between two effector over-expressing lines identified various ABA and other hormone-associated genes. A large number of these genes showed a distinctive pattern of up-regulation in comparison to Col-4, HA::GFP and the *PP2CA* knock-out lines as shown in Figure 23. This suggests that the effector could manipulate hormone pathways to enhance susceptibility to the pathogen.

3.8 Discussion

The experiments presented aimed to investigate an interaction identified between the *Hpa* effector HaRxL14 and the *Arabidopsis* protein PP2CA in a large-scale yeast two-hybrid screen. As previously described, PP2CA is one of a family of proteins involved in coordinating response to ABA. Furthermore, PP2CA also has a role in metabolic stress and therefore integrates various stress related signals. These investigations were aimed at verifying the interaction with alternative techniques to yeast two-hybrid. Further tests examined if and potentially how this interaction could enhance host susceptibility to the pathogen.

Localisation of the effector and PP2CA by transient expression *in planta*, showed an overlap in the expression of the two proteins in the nucleus. When co-expressed the localisation pattern of the each protein remained the same as when expressed individually. This suggests that the effector does not manipulate the location of PP2CA in a potentially functional interaction between the two proteins. Furthermore, a biomolecular fluorescence complementation (split-YFP) experiment verified these observations and showed an interaction occurring between the two proteins in the nucleus. This nuclear interaction was tested by mass spectroscopy, although it was unable to be confirmed under various conditions. As a follow up experiment, the Co-IP products were examined by Co-IP although this was unable to confirm an interaction between the two proteins. However, the effector was shown to interact with proteins in *N. benthamiana* including chlorophyll a-b binding proteins. Therefore a possible role of the protein interacting with non-host proteins could obscure a possible interaction by Co-IP.

The pathology screens showed that over-expression of the effector in *Arabidopsis* enhanced host susceptibility to *Hpa*. The *PP2CA* knock-out and over-expressing lines were also investigated for susceptibility to the pathogen and the initial result showed higher susceptibility in the two knock-out lines. However, this was unable to be reproduced in a further screen and therefore requires repeating in order to verify a final result. It is possible that the presence of the effector is required and therefore knocking-out or over-expressing *PP2CA* does not have an effect on host susceptibility to *Hpa*.

To test whether knocking-out and over-expressing *PP2CA* or the effector could have an effect on MAMP-triggered immunity, these were screened for ROS production following induction with flg22. This showed no difference for any of the lines to Col-4. It has recently been demonstrated that the interaction between the ABA signalling and flg22 response pathways converge at an SnRK2 protein (OST1) which is downstream of the PP2CAs (Guzel Deger *et al*., 2015; Lee *et al*., 2013). Therefore the results seem to support these findings and it appears that manipulation of PP2CA is unlikely to have an effect on MAMP-triggered immunity through ROS production pathways.

The microarray results showed that over-expression of HaRxL14 in *Arabidopsis* results in a large number of differentially expressed genes. GO term analysis of the up-regulated genes showed that a large proportion of genes are involved in response to stress and abiotic stimulus. These included PP2CA and other ABA-related genes such as cold stress associated *DREB1A*, which shows strong induction in two of the effector over-expressing lines. This pattern is consistent across many genes including those directly associated with ABA. This suggests that expression of HaRxL14 *in planta* can induce a response concurrent with that of ABA induction. These results show similarity to microarrays examining *Arabidopsis* tissue infected with *P. syringae* pv. *tomato* DC3000 with T3Es, which also showed a 15-fold increase in *NCED3* expression (de Torres-Zabala *et al.*, 2007). Furthermore, gene expression changes associated with HaRxL14 expression *in planta* show similarities to those observed with *P. syringae* effector AvrPtoB under control of a Dexamethasone (Dex)-inducible promoter (de Torres-Zabala *et al.*, 2007). This microarray experiment showed that the expression of AvrPto alone was sufficient for significant up-regulation of *NCED3*, consistent with the findings for HaRxL14 shown in Figure 23D, and that the elevation of ABA level impaired other immune responses such as callose deposition favouring pathogen infection (de Torres-Zabala *et al.*, 2007). Overall, these results highlight an interface between ABA and immunity, which is exploited by multiple pathogens.

There are several other experiments that could confirm a link between HaRxL14 and ABA signalling. Firstly, the differential expression of ABA marker genes in effector over-expressing lines would need to be confirmed by an alternative technique such as

qPCR. This would determine whether changes in gene expression amount to a global ABA response. This experiment could also investigate how exogenous ABA application affects these gene expression changes. If the effector causes constitutive activation of ABA pathways then endogenous application may not induce a significant difference compared to wild-type. Furthermore, a phosphorylation assay could test whether presence of the effector results in a change in the phosphorylation of PP2CA. This could indicate whether the effector induces changes in the ABA downstream signalling cascades through manipulating the interactions of PP2CA in the host and its ability to dephosphorylate its target proteins. A change in the interactions of PP2CA with the SnRK2 proteins could explain the gene expression changes that are associated with ABA perception.

Overall, the experiments suggest that there could be a functional interaction between the effector and PP2CA. This was verified by yeast two-hybrid and split-YFP, although the interaction has not as yet been shown by Co-IP. There appears to be a link between expression of the effector and an increase in ABA gene induction. However, it is also possible that this could be caused by an interaction with another host target, which has knock-on effects for various ABA pathways without these being the primary targets of the effector. However, given that *Hpa* and other pathogens such as *P. syringae* have previously been shown to enhance ABA signalling in order to promote host susceptibility, it appears likely that this interaction with PP2CA could be a key functional target of the effector (Asai *et al*., 2014; de Torres-Zabala *et al.*, 2007; Fan *et al*., 2009).

4 Investigating hormone inducible chromosome conformation changes

4.1 Introduction

4.1.1 Chromosome conformation capture (3C)

Chromosome conformation capture (3C) was developed to investigate chromatin arrangements in the nucleus, which were initially observed with microscopy (see section 1.3.1). The core stages of 3C are summarised in Figure 24. Briefly, the method uses formaldehyde cross-linking to take a snapshot of chromosomal arrangements in the nucleus (Dekker *et al*., 2002). The chromatin is fragmented by a restriction digest step, with the frequency of the cut sites determining the resolution of the interaction map (de Wit and de Laat, 2012). A ligation reaction is then performed under dilute conditions with the cross-links intact. This favours the ligation of fragments within cross-linked regions.

These hybrid ligation products form a library, which allows the identification of novel joined and interacting regions. The 3C technique relies on primer design for specific regions of interest and qPCR to determine the relative frequency of these physical interactions (Dekker, 2006). The methods used to identify these interactions have diversified considerably and have become more powerful as the technique has adapted to the lowering cost of next generation sequencing (NGS; de Wit and de Laat, 2012). This has allowed greater precision and a genome level picture to be generated from gene to chromosome level interactions (de Wit and de Laat, 2012).

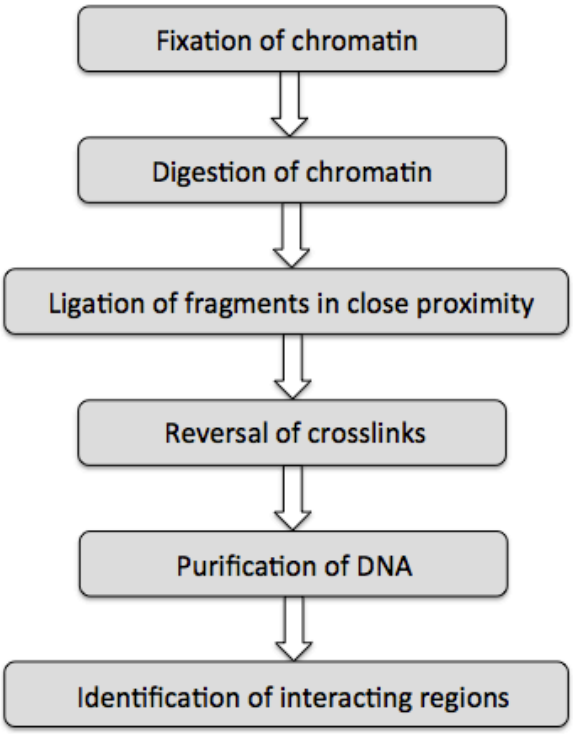

Figure 24. Key stages of chromosome conformation capture (3C) and related techniques. The steps shown here form the basis of the 3C methodologies including but not limited to circularized chromosome conformation capture (4C), chromosome conformation capture carbon copy (5C) and Hi-C, with greatest variation being represented in the last step in which the interacting regions are identified.

Hi-C is an example of a more recent methodology which uses biotin during the generation of hybrid interacting fragments (Figure 25; Lieberman-Aiden *et al*., 2009). This marks the ligation junctions which are enriched with a streptavidin pull-down before sequencing (Dekker *et al*., 2013). Chromosome maps representing the relative frequency of physical contacts between each region are generated with these data, which show a global picture of chromosome interaction domains (Lieberman-Aiden *et al*., 2009; van Berkum *et al*., 2010). It has been shown from these Hi-C based experiments that mammalian chromosomes are arranged in a fractal globule structure with structured territories in which individual chromosomes are bundled with fewer inter-chromosomal contacts (van Berkum *et al*., 2010). This contrasts to an equilibrium globule in which chromosomes are intermingled in a less ordered conformation (Dekker *et al*., 2013). Hi-C has made a significant contribution towards understanding the big picture of chromosome conformation.

4.1.2 3C and enhanced techniques in plants

An optimized approach for 3C in Maize has given initial insights into the chromatin conformation of plant cells and this has subsequently been optimized for other species including *Arabidopsis* (Louwers *et al*., 2009). From these studies it has been demonstrated that there are likely spatial interactions between genes within the FLC locus which regulates flowering time (Crevillén *et al*., 2013). Studies which have adapted Hi-C for use with *Arabidopsis* have produced an overall impression of chromosome conformation which somewhat differs from the highly structured topological domains observed in mammalian cells (Dixon *et al*., 2012). Although evidence suggests that the conformation of chromosomes in plants follows a similar overall structure and are arranged into territories based on the state of the chromatin (Grob *et al*., 2013).

These studies have given a first impression of chromosome conformation and functional interactions between genes at a spatial level. However, little is known regarding whether there are observable preferential interactions between related and co-expressed genes, as might be expected based on the hypothesis of specialized transcription factories.

4.1.3 Scope of this investigation

Hi-C has been subject to further adaptation for a more targeted experimental approach. Sequence capture of multiple regions interacting with bait loci (SCRIBL) is an adaptation of Hi-C tailored towards the capture of specific regions of interest through the use of biotinylated RNA baits, which was developed by Peter Fraser and Stefan Schoenfelder (unpublished). The stages of the technique are summarised in Figure 25. Briefly, BAC DNA is used as template to generate the biotinylated RNA baits, which are hybridised to a Hi-C library. The majority of ligation products that would otherwise form part of the Hi-C library are washed away during this process. These enriched regions of interest form a SCRIBL library, allowing a greater focus of reads compared to standard Hi-C when this is sequenced with NGS technology.

This project aimed to investigate transcription factories in *Arabidopsis* cell suspension culture using the SCRIBL methodology. An *Arabidopsis* cell suspension culture was used on the basis of the large amount of plant material required for the experiments. Therefore the rapid proliferation of cells in culture meant that this system was a practical choice for these experiments, which required optimisation at various steps. Furthermore, it was found that a more consistent hormone-induced gene expression response could be stimulated in *Arabidopsis* cell suspension culture in contrast to a whole plant-based method.

These experiments were based on hormone treatment, which was used to stimulate a genome-wide activation of various signalling, biosynthesis and other related genes. Jasmonic Acid derivative Methyl Jasmonate (MeJA) has previously been shown to induce a large-scale transcriptional response in *Arabidopsis* cell suspension culture (Pauwels *et al*., 2008) and it was verified here that these were appropriate treatment conditions. Genes were then selected on the basis of significant up-regulation in response to hormone stimulus. The SCRIBL technique is adapted in these experiments to capture the spatial environment of these genes and surrounding regions. The technique was used to test the hypothesis that the spatial environment of these genes may change as a result of hormone induction. If this is apparent then it is also possible that genes involved in related pathways translocate to the same specialised transcription factories within the nucleus, as has been observed in other

systems (Schoenfelder *et al*., 2010; Xu and Cook, 2008). Therefore, this experiment could uncover more about a spatial mechanism through which groups of related genes are co-regulated within the nucleus of plants.

Hormone pathways are also highly relevant to plant pathology given the manipulation of hormone response by many pathogens (Kazan and Lyons, 2014). The sabotage of these pathways often leads to changes in the host response conducive to pathogen survival. Therefore specialised transcription factories could be targets for host manipulation in a pathological context.

4.2 Aims

1. Confirm transcriptional response to MeJA in *Arabidopsis* cell suspension culture and select appropriate genes to be the focus of this investigation.
2. Optimise SCRIBL for use with *Arabidopsis* cell suspension culture.
3. Analyse the effect of treatment with MeJA on the nuclear environment of these genes and the arrangement of chromatin in *Arabidopsis* cell suspension culture using this technique.

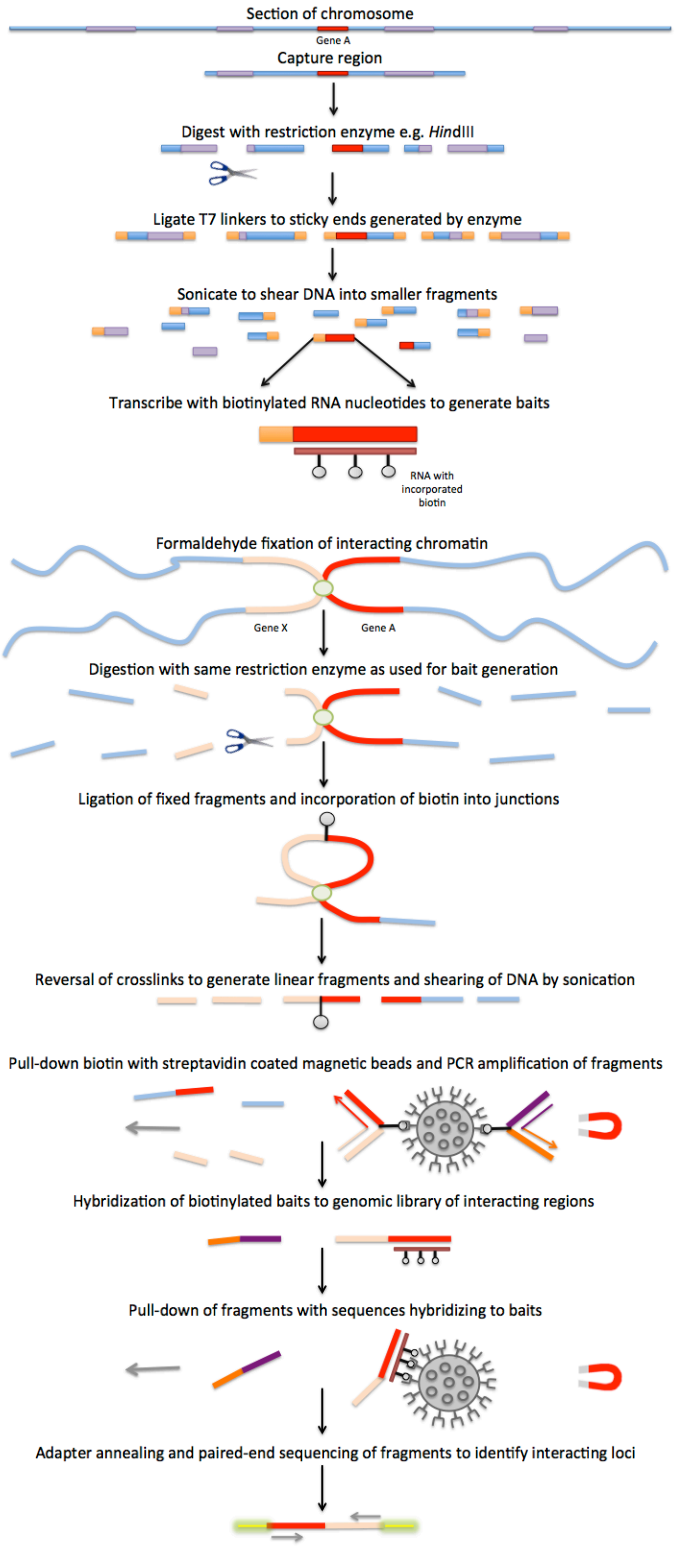

Figure 25. Schematic to show key stages in the SCRIBL methodology. This technique is based on Hi-C in which digested fragments are filled-in with biotinylated bases before ligation, marking these junctions. These Hi-C fragments are hybridised to biotinylated RNA probes generated for specific regions of interest, forming a SCRIBL Hi-C library. This higher specificity library is sequenced using next generation sequencing technology to identify the interacting loci (Stefan Schoenfelder, unpublished).

4.3 Methyl Jasmonate (MeJA) induction of *Arabidopsis* cell suspension culture

Specialisation of transcription factories could be important in coordinating the response of highly up-regulated groups of genes during response to stimulus. Hormone induction was selected based on the substantial number of genes that are involved in this type of response. In addition, hormone signalling has well-established links with pathogenesis (Denancé *et al*., 2013). Therefore, if coordinated regulation at transcription factories is apparent, then this could be a potential target for manipulation by pathogens.

A system for the induction of a hormone-associated transcriptional response with MeJA was optimised in *Arabidopsis* cell suspension culture. This *Arabidopsis* cell suspension culture originated from Landsberg erecta callus and was kindly provided by Dr. Alessandra Devoto (Royal Holloway, University of London). This was the basis for investigating the potentially dynamic association of genes and chromatin interactions in response to hormone stimulus. The selection of *Arabidopsis* cell suspension culture as an experimental system was based on several factors. These included the homogenous cell type and the small nature of the clumps of cells, which would therefore enable a relatively even exposure to formaldehyde during chromatin fixation. This followed the conditions for which the SCRIBL methodology was developed (i.e. mammalian cell culture). In addition, the single cell type means that variability in the response of different cells is minimised.

4.3.1 Experimental design

4.3.1.1 Experiment A: Time-point 7 h

To test the experimental conditions for MeJA treatment, cultures were treated with 50 μM MeJA or mock treated as described in section 2.1.2.3. This treatment was based on the final concentration in a microarray analysis of *Arabidopsis* cell suspension culture treated with MeJA as previously described (Pauwels *et al*., 2008). Samples were harvested for RNA extraction at 0 and 7 hours post treatment or mock treatment. The processes of hormone treatment and sample collection are summarised in Figure 26.

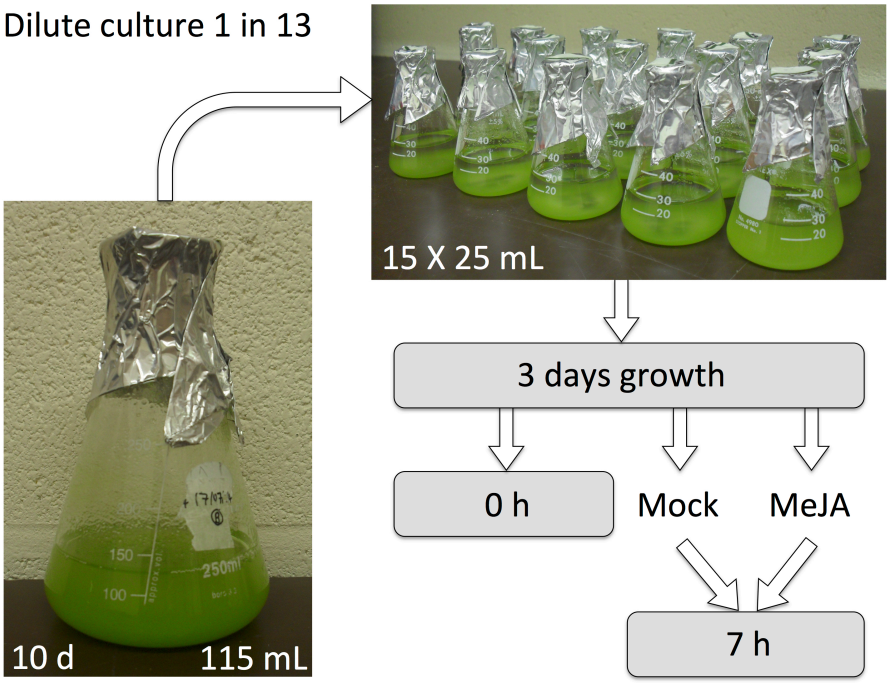

Figure 26. Experimental design for *Arabidopsis* cell suspension culture methyl jasmonate (MeJA) induction experiment. A 10-day-old culture (10 d) was diluted 1 in 13 with *Arabidopsis* cell suspension culture media to prepare fifteen 25 mL cultures. The cells were cultured for three days (into rapid growth phase) before starting the experiment. Five flasks were collected at 0 hours (0 h) for RNA extraction (4 mL) and fixation (20 mL). Five flasks were treated with MeJA at a final concentration of 50 µM MeJA (stock 10 mM in absolute ethanol) and five with an equivalent volume of water in replacement of MeJA. These flasks were incubated for 7 h with shaking and collected as previously.

The RNA was extracted from three biological replicates of 0 and 7 hours MeJA treated and mock treated samples, to assess the hormone inducible transcriptional response of the *Arabidopsis* cell suspension culture (see section 2.2.1.1.1). The mRNA was reverse transcribed and gene expression changes determined semi-quantitatively by PCR with template cDNA. Primers used for the assessment of this response were designed for a selection of JA marker genes including *JR1* and *VSP1* which showed the expected increase in expression in MeJA treated samples, in addition to a constitutively expressed actin gene (*ACT2*; see section 2.2.3.1 for primers; An *et al*., 1996; Berger *et al*., 2002; León *et al*., 1998). These genes were selected based on their well-established role in jasmonate response (Boter *et al*., 2004; Dombrecht *et al*., 2007). It was important for this experiment that there was a clear increase in expression detectable for multiple genes. This global change in expression indicates that there could be a coordinated association of these genes at transcription factories.

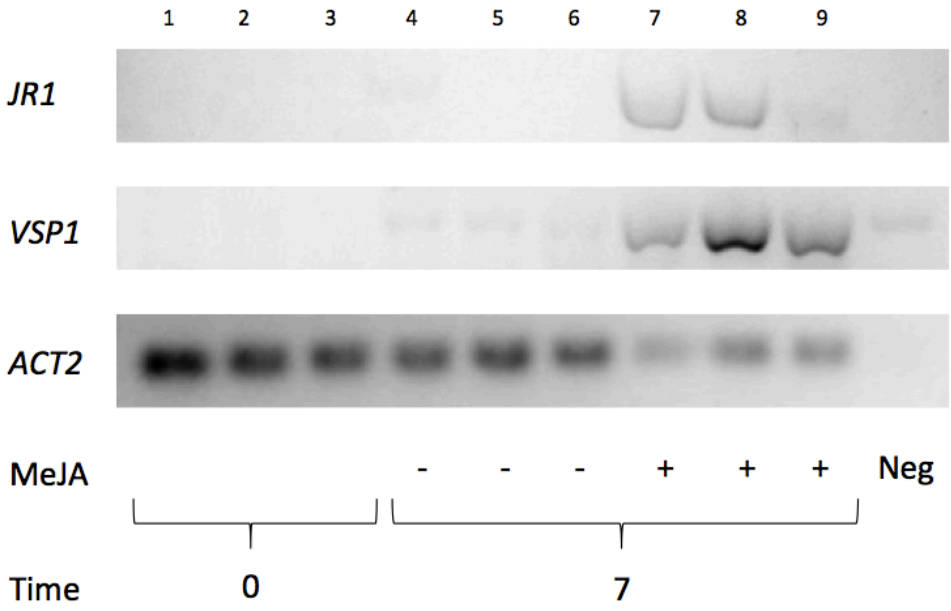

Figure 27. Relative gene expression analysed by PCR for MeJA induction experiment with *Arabidopsis* cell suspension culture (experiment A). The template cDNA was synthesised from 1 µg of RNA extracted from three biological replicates of *Arabidopsis* cell suspension culture. The cells were harvested at time points 0 hours (0 h) and 7 h following treatment with 50 µM MeJA (+) or mock induction (-). The products of PCR reactions with primers designed for *JR1*, *VSP1* and *ACT2* were separated by gel electrophoresis. A negative control without template is also shown for each gene transcript specific primer pair. Each lane labelled 1 to 9 represents an independent culture flask.

PCR amplification of these two genes indicated that a transcriptional response was induced by the MeJA treatment for both JA markers (Figure 27). In addition, the actin control locus shows amplification across all samples (Figure 27). There appears to be lower expression of actin in MeJA treated cultures (Figure 27). This could be due to a difference is the phase of the cell cycle or alternatively chance fluctuations. This experiment suggested that treatment with 50 μM MeJA was sufficient in this system for up-regulation of these JA response genes by 7 hours, with *VSP1* showing the most significant change.

4.3.1.2 Experiment B: Time-points 5 h and 25 h

To further investigate gene induction with MeJA treatment, additional time-points were selected for sample collection. This meant a broader view of this gene induction in *Arabidopsis* cell suspension culture could be established from earlier and later time-points. This would be beneficial in the selection of an optimal sampling point for the experiment. A time-point at which multiple marker genes showed consistent induction would be sufficient in this context to indicate that a genome wide transcriptional response had been induced. This would determine a likely stage at which chromatin conformation would give a general and stable representation of its state during response to hormone stimulus.

Additional genes tested at these time-points were *OPR3* and *JAZ1* as well as the salicylic acid (SA) marker gene *PR1* (see section 2.2.3.1 for primers; Wildermuth *et al*., 2001). This SA marker was used here as a negative control as SA pathways act antagonistically to JA (Gimenez-Ibanez and Solano, 2013). In additional, *ACT2* was examined for constitutive expression as previously described.

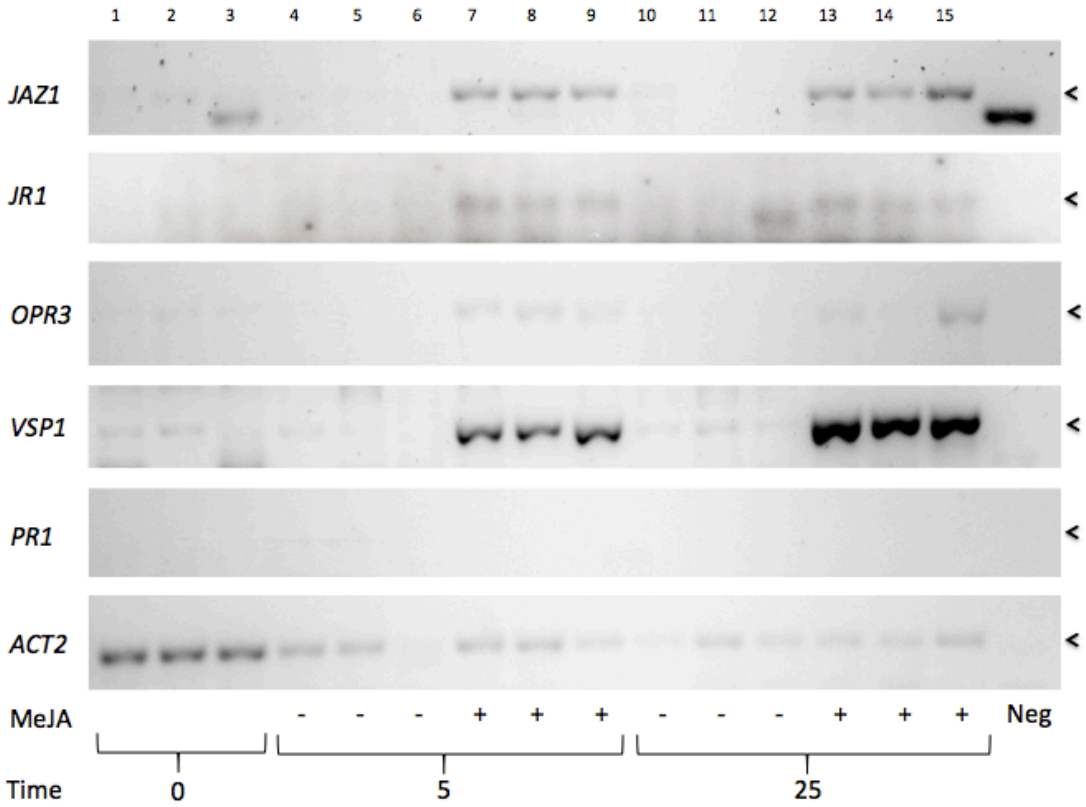

Figure 28. Relative gene expression analysed by PCR for MeJA induction experiment with *Arabidopsis* cell suspension culture (experiment B). The template cDNA was synthesised from 1 µg of RNA extracted from three biological replicates of *Arabidopsis* cell suspension cultures at time points 0 hours (0 h), 5 h and 25 h following treatment with 50 µM MeJA (+) or mock induction (-). The products of PCR reactions with primers designed for *JR1*, *VSP1* and *ACT2* were separated by agarose gel electrophoresis. The arrows indicate the position of the target amplification products for each primer pair. A negative control PCR without template is also shown for each gene transcript specific primer pair. Each lane labelled 1 to 15 represents an individual culture flask.

The results of this experiment showed that two JA marker genes were significantly up-regulated in comparison to mock treatment at both 5 and 25 hours. *VSP1* (AT5G24780) showed the highest induction at both the 5 and 25 hour time-points and this appeared to be highly consistent across all three biological replicates. Expression of *OPR3* was very low at each time-point and by 25 hours is undetectable in one out of three replicates. Actin showed amplification across most time-points, although this was consistently highest at 0 hours. Overall, it may be favourable to use an earlier time point of 5 to 7 hours to minimise variability in gene induction.

4.4 Selection of bacterial artificial chromosomes (BACs)

As part of the SCRIBL experiment, BACs are used as a template to generate RNA probes for specific regions. From the results of the MeJA induction experiments, BACs were selected for these genes of interest. These BACs were identified from the Institut für Genbiologische Forschung (IGF; roughly 10,000 clones, 100 kb average size) and Texas A&M University (TAMU; 100 kb average size) libraries for Col-0 from which individual clones are distributed (TAIR; ABRC, Ohio State University). As part of the selection process, the position of BACs on each chromosome was viewed using the Clone DB browser (Clone DB). The criteria used to determine which BAC was selected are illustrated in Figure 29. Briefly, a central position of the gene on the BAC was the main condition, as this would allow collection of high-resolution interaction data in both directions from the gene. This is an internal control for the technique to ensure distance decay is apparent in the interaction frequency of the gene of interest with the surrounding regions. This pattern of distance decay has been observed with other 3C related techniques including Hi-C (Grob *et al*., 2013; van Berkum *et al*., 2010). Where multiple BACs fitted this criterion, the longest of these would be selected. This would enable the capture of additional data from a larger region.

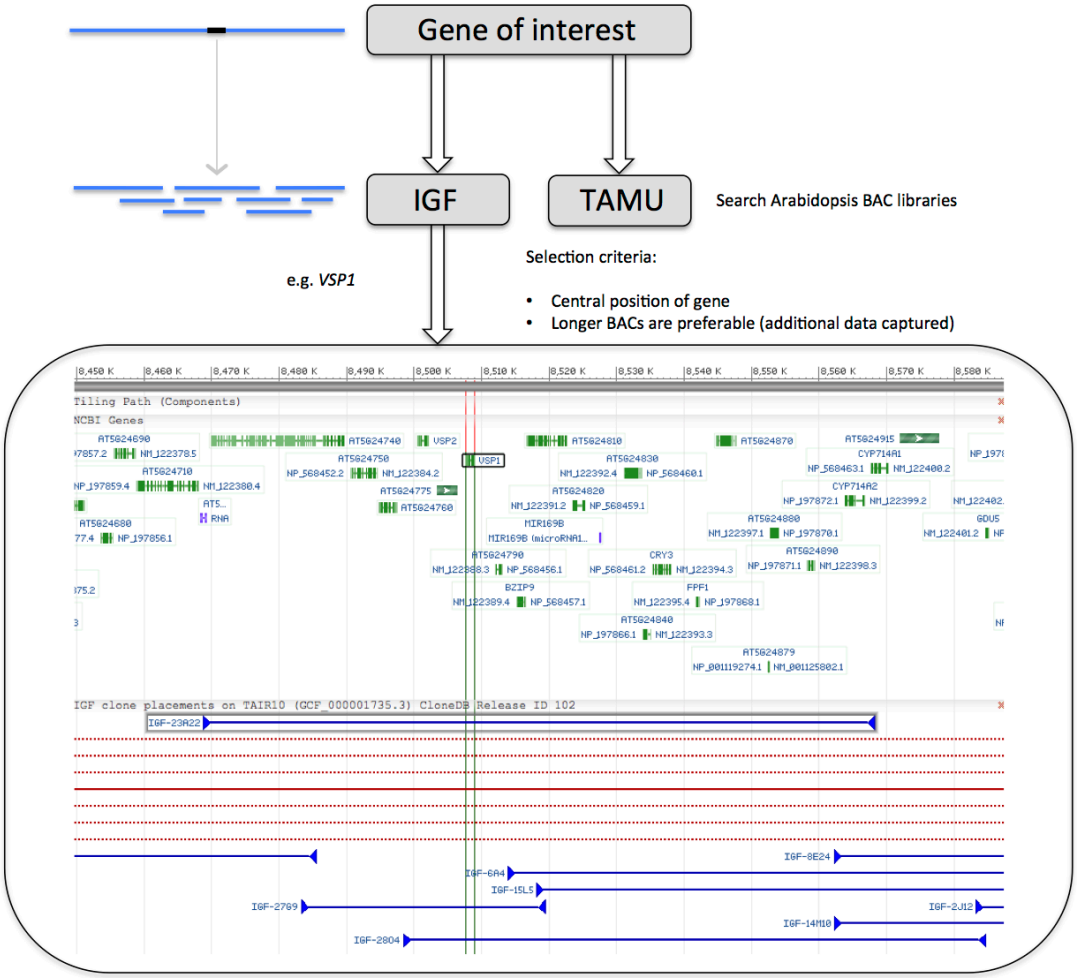

Figure 29. Schematic to show the selection process for BACs to be used as a template for biotinylated RNA probe generation. These BACs were chosen from two libraries: IGF and TAMU (distributed by ABRC resource centre). The genes were aligned against BACs from both libraries and the most appropriate was selected based on the central position of the gene. If two or more BACs met this criterion, the longest of these was selected facilitating greater data capture. The example shows a BAC selected for gene *VSP1* (AT5G24780).

4.4.1 Alignment of Landsberg erecta (Ler) to Col-0 BAC sequences

BAC clones used for the generation of RNA probes were selected from Columbia ecotype libraries. Since the cell culture used in the experiment derived from Landsberg erecta (Ler) an alignment was performed between the genes of interest and the Ler genome (Monsanto). This would ensure efficacy of the probes for the cell culture based experiment. The percentage alignment is shown in Table 14.

Table 14. Results of BAC selection for each of the genes chosen for the MeJA experiment. The names and IDs of each gene are given along with details of the corresponding BAC selected. The top identity, score and E values are given from alignments performed for TAIR *Arabidopsis* sequences of each gene to the Ler genomic sequence.

Name	**Gene ID**	**BAC Library**	**BAC ID**	**Top identity (%) / Score / E value**
ACT2	AT3G18780	TAMU	T17J17	85 / 513 / e-144
JAZ1	AT1G19180	IGF	F1B10	99 / 1181 / 0.0
JR1	AT3G16470	IGF	F22K24	99 / 880 / 0.0
OPR3	AT2G06050	TAMU	T7M23	97 / 1493 / 0.0
PR1	AT2G14610	TAMU	T15A5	98 / 531 / e-150
VSP1	AT5G24780	IGF	F23A22	96 / 632 / e-180

Overall, the gene sequences show very high similarity alignment (particularly *JAZ1*, *JR1* and *OPR3*) with the Ler genome sequence (Table 14). A high percentage identity and score indicate this similarity. An E value score close to zero is associated with an alignment that is unlikely to have occurred by chance. The PCR primers designed from the Col-0 sequence showed amplification with Ler template (Figure 28). However, the lower amplification of *ACT2* in Figure 27 and Figure 28 could be a result of the lower sequence similarity shown in Table 14. Overall, the difference in ecotype is unlikely to be problematic when hybridising the probes during the generation of the SCRIBL library. However, the results from the alignment are in agreement with the time-course gene expression experiment, suggesting that the primers may require redesigning for this gene or another to be selected.

4.5 Generation of biotinylated RNA probes

A key feature of SCRIBL Hi-C is the use of biotinylated RNA probes to enrich specific regions of interest from a pool of interacting regions (Figure 25). Briefly, this process involves the purification and digestion of BAC DNA with the restriction enzyme that is also used for the generation of the Hi-C interaction library. T7 promoter adapters are ligated to the sticky ends generated by this restriction enzyme. These fragments are then sonicated to a target size of 200 bp and size selected with DNA binding beads. Finally the T7 adapters and biotinylated RNA bases are used for the synthesis of the probes. These are purified to remove the template BAC DNA. The biotinylation is important as it allows the probes to be pulled down with streptavidin beads when hybridised to the Hi-C library.

The conditions described for the generation of the probes were tested before the completion of the MeJA induction experiment. Therefore an alternative group of BACs were used to optimise the condition for this process, which were immediately accessible. These BACs are from the JAtY library (Genome Enterprise Limited) and would not be hybridised to the final Hi-C library (Table 15). The examples shown in later quality control steps for biotinylated RNA probe generation are based on this set of BACs (Table 15).

Table 15. Five BACs were selected from the JAtY library (Genome Enterprise Limited) to verify the conditions for the generation of biotinylated RNA probes. The IDs for each of these BACs are given.

	BAC Library	**BAC ID**
1	JAtY	JAtY50F23
2	JAtY	JAtY59H10
3	JAtY	JAtY50F23
4	JAtY	JAtY61D23
5	JAtY	JAtY78J04

4.5.1 Identification and preparation of BAC DNA

Following extraction of BAC DNA, the identity of the extracted BAC DNA was verified by PCR. Primers were designed for a 200 bp region and the BAC DNA was used as a template for PCR reactions to verify their identity. As a negative control, these primers were tested with an alternative BAC as template.

The BACs were mixed in equimolar amounts in the region of 5 μg per BAC. The equimolar mixing ensured that a bias was not introduced due to a discrepancy in the length of the BACs in relation to one another, which influences their molecular weight. These equimolar BAC DNA mixtures were the input templates for probe generation.

4.5.2 Digestion of BAC DNA mixtures

Trial restriction digests of BAC DNA were performed to test the conditions for the overnight digestion reaction. This ensured that the length of the incubation was sufficient for complete digestion of the BAC DNA and could identify potential over digestion. The restriction digests for this test group of BACs were carried out with *Eco*RI, while the final library optimisation used *Hin*dIII. This was due to the *Eco*RI restriction sites generally having a greater frequency compared to *Hin*dIII in the region within and surrounding the genes of interest on the selected BACs. Therefore this would improve the resolution of the data to determine interactions of these specific regions. Both of these are six-base cutter restriction enzymes and produce similar fragment sizes with *Arabidopsis* genomic DNA (Biolabs).

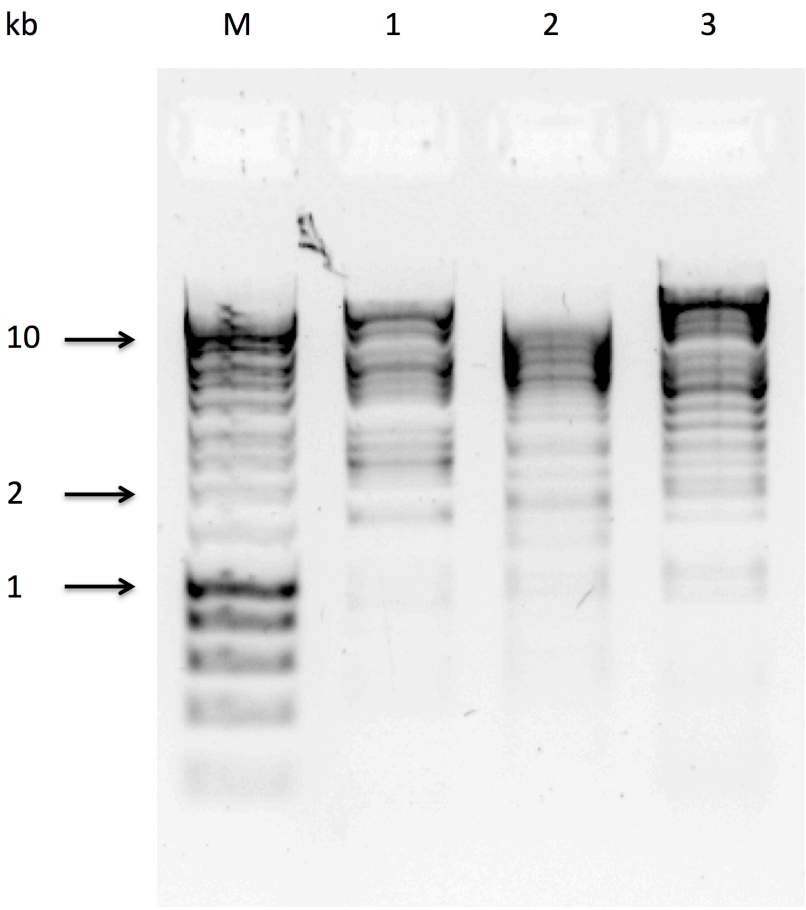

Figure 30. Restriction digest test for three individual BACs. The restriction digest was performed with *Eco*RI overnight and the products were purified by phenol-chloroform extraction and ethanol precipitation. The purified BAC DNA was run on an agarose gel with a marker (M) with band sizes indicated (kb). The products of these individual BAC restriction digests are labelled 1, 2 and 3.

Figure 30 shows an absence of a very high molecular weight band in any of the digests, which would indicate presence of undigested BAC DNA that is present in Figure 31. In addition, a lower proportion of fragments are below 1 kb compared to 1 to 10 kb, which would indicate over-digestion. The products of these restriction digest reactions have a regular banding pattern, which indicates that the BAC DNA is good quality and without clear signs of degradation. Overall, this confirms that the conditions for the restriction digest reaction were optimal and did not result in over or under digestion. Therefore the BAC DNA is a good quality template to proceed with further steps.

4.5.3 Sonication conditions efficiency test

A trial reaction was set up to test the manufacturer's recommended conditions for sonication of DNA to a target size of 200 bp (BioRuptor, Diagenode). According to the manufacturer's protocol, DNA should be sonicated in six 10-minute bursts of alternating 30 seconds on and 30 seconds off with low intensity and ice replenishment between these bursts. During this process it was noted that the sample splashed into the lid of the microfuge tube. Therefore, the samples were collected to the base of the microfuge tube by centrifugation between sonication bursts to ensure consistency and evenness of exposure within the reaction to the energy conducted via the water bath.

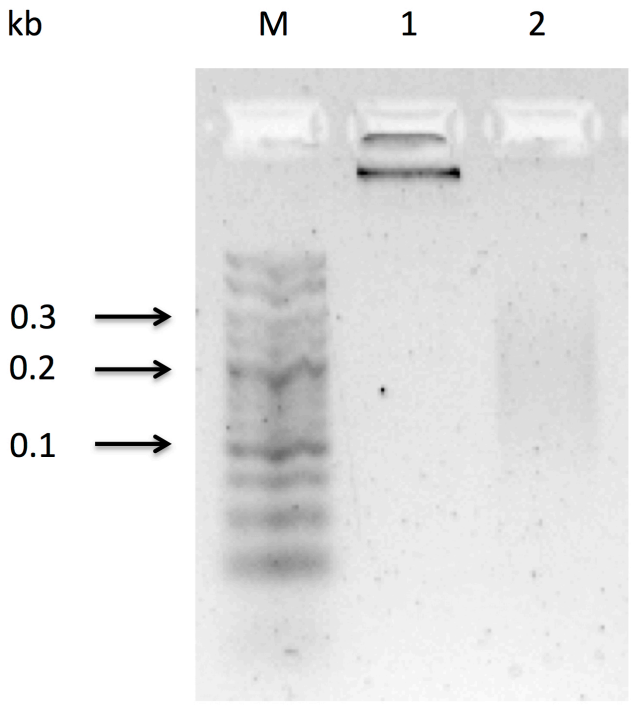

Figure 31. Trial sonication of BAC DNA. The target fragment size post sonication was 200 bp. Sonication was performed for 1 hour with alternating 30 seconds on and 30 seconds off with ice replenishment every 10 minutes. The pre- and post-sonicated BAC DNA (labelled 1 and 2 respectively) was run on an agarose gel with a marker (M) and band sizes indicated (kb).

It is clear from Figure 31 that the post-sonicated BAC DNA (as indicated by lane 2) has a complete absence of the high molecular weight input. Sonication generates a range of fragment sizes, with the degree of precision determined by the type of sonicator. The post-sonicated BAC DNA has an average length of 200 bp, which suggests that the recommended conditions are sufficient for generation of the desired fragment size.

4.5.4 BAC DNA fragments post T7 promoter ligation and sonication

The efficiency of the general conditions described in the SCRIBL protocol for T7 promoter adapter annealing followed by ligation to digested BAC DNA template were verified (Stefan Schoenfelder and Peter Fraser, unpublished). These promoters are required for RNA synthesis by T7 RNA polymerase during a later step.

The T7 promoter adapters (synthesised as single stranded oligos) were annealed with a step down thermocycler programme starting at 95 ^{o}C and dropping a degree each minute down to 14 ^{o}C. The promoters were specifically designed with sticky-ends complementary to *Eco*RI cut sites. These annealed double-stranded promoters were ligated to the overhangs in the BAC DNA generated by overnight restriction digestion with *Eco*RI. This would enable synthesis of biotinylated RNA probes for regions complementary to the sequences directly upstream and downstream of these restriction sites.

Chromosome conformation capture related methodologies are dependent on restriction digest sites as focal points for analysis. Chromatin conformation is fixed with formaldehyde and these cross-links are held intact during the restriction digest. These cut sites form the junctions at which physically interacting chromatin is then ligated under dilute conditions. This generates the hybrid chromatin fragments, which form the basis of a 3C library. Therefore it is important that the probes are complementary to regions adjacent to the cut site to analyse the identity of chromatin in close proximity.

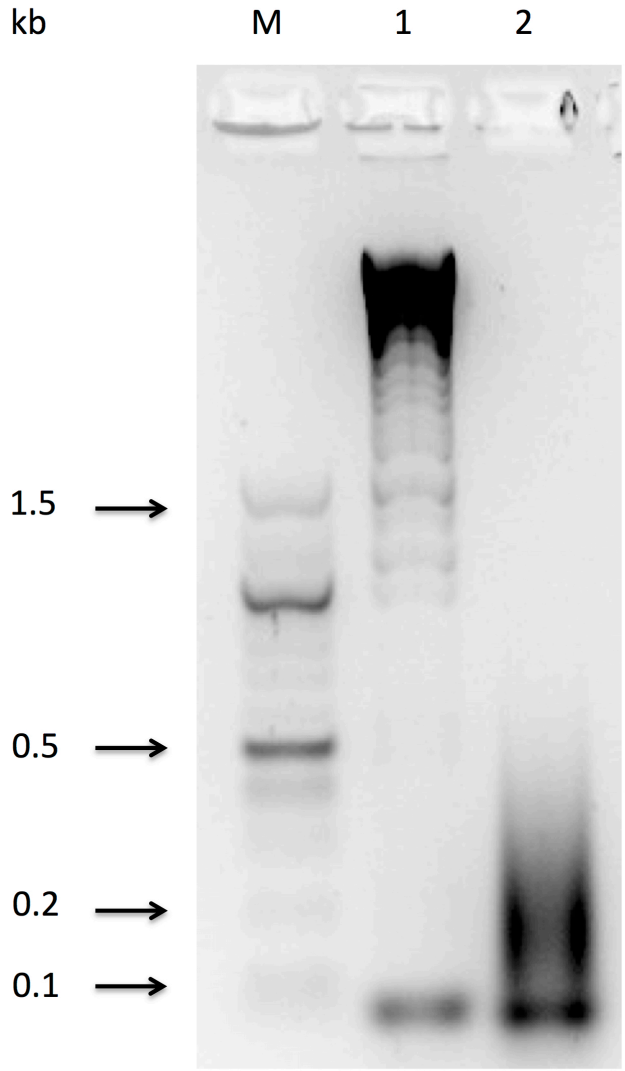

Figure 32. BAC DNA following restriction digestion and T7 adapter ligation, pre (1) and post (2) sonication. T7 adapters were ligated in excess to BAC DNA digested with *Eco*RI. The products of this reaction were sonicated for 1 hour with alternating 30 seconds on and 30 seconds off at high intensity (BioRupter, Diagenode). The pre and post sonicated BAC DNA (labelled 1 and 2 respectively) was run on an agarose gel with a marker (M) and band sizes indicated (kb). A band below 200 bp represents unligated adapters.

The BAC DNA following T7 promoter adapter ligation showed the regular banding pattern as previously described in section 4.5.2 and generally separated at large fragment sizes (Figure 32). The band below 100 bp represents the excess unligated T7 promoter adapters (Figure 32). The products of this reaction following adapter ligation were then sonicated for a peak fragment size of 200 bp with the conditions described previously from the test BAC DNA sonication. This step is important in generating template for RNA probe synthesis that is uniform in length. Longer probes would bind to streptavidin with greater efficiency, meaning these and their complementary Hi-C library interactors would be represented at a higher frequency in the final library. Therefore, consistency in the length of the template will not introduce bias during pull-down of the Hi-C library to generate the SCRIBL library. However, it is also crucial that the length of the RNA probe sequence should allow sufficient specificity to limit non-specific probe binding. From Figure 32 it is clear that the post-sonication products were generally below 500 bp with an average of 200 bp, meaning this sonication process was efficient in shearing the template to the optimal probe length.

4.5.5 Double-sided SPRI size selection of BAC DNA template with T7 promoter adapters

The T7 promoter adapter ligated and sonicated BAC DNA was size selected with double-sided Solid Phase Immobilization (SPRI) beads. These magnetic SPRI beads bind to DNA in a concentration dependent manner. This allows a specific target range of DNA fragments to be isolated from the reaction through altering the concentration of the solution during multiple binding steps. Therefore fragment sizes above and below a specific range may be excluded from the final product. This facilitated the removal of the unligated adapters from the reaction prior to RNA synthesis, as well as excluding DNA fragments not sonicated to a length within the desired range.

4.5.6 RNA synthesis and probe quality check

Following size selection of the BAC DNA template with ligated T7 promoter adapters, RNA probes were synthesized with biotinylated dNTPs. The biotinylated RNA probes were purified from the reaction pool with the template BAC DNA with a column based kit (Ambion MEGAclear kit).

The quality of the RNA was assessed with spectrophotometric analysis by Nanodrop, with 260/230 and 260/280 ratios both over 2 indicating good purity and integrity of the probes. The RNA quality can also be verified on a denaturing formaldehyde RNA agarose gel or with a Bioanalyser RNA chip (Agilent Technologies).

4.6 Hi-C library generation from *Arabidopsis* cell suspension culture

At the time of starting this investigation, 3C technology had recently been adapted for use with plants (Louwers *et al*., 2009). From a protocol developed for Maize, it was demonstrated that additional nuclear enrichment steps are necessary when working with plant material (Louwers *et al*., 2009). This is due to the additional compounds present in plants, which hinder the enzyme reactions and lead to the degradation of chromatin. During the course of this project, research was published detailing a Hi-C protocol for use with *Arabidopsis* leaf material (Grob *et al*., 2014). This also involved nuclear enrichment, with additional blunt-ending with biotin prior to ligation.

The investigation required development of appropriate conditions for generation of 3C and Hi-C libraries specifically for an *Arabidopsis* cell suspension culture. The current protocols for plant-based 3C and related techniques required integration and optimisation to suit the conditions of a plant cell suspension culture. Changes were necessary for steps including the fixation and collection of cells from the culture media, as well as ligation of the fixed chromatin.

4.6.1 Hi-C library generation with nuclear enrichment

As a starting point, the process of formaldehyde fixation was based on general conditions described for the fixation of chromatin in chromatin immunoprecipitation (ChIP; Abcam website). This involved fixation with 0.75% (v/v) formaldehyde (final concentration) for 10 minutes with gentle mixing. Variations introduced included that the fixed cells were filtered and washed with PBS on Miracloth (Merck Millipore) and stored in foil packages at -80 ^{o}C, rather than collection by centrifugation. It was found that collection by this method allowed a good recovery of cells prior to homogenisation by grinding.

As previously discussed, current protocols describing 3C and Hi-C with *Arabidopsis* leaf material use nuclear enrichment steps following fixation of the chromatin and before digestion. This should reduce interference of contaminants from the cell debris with these enzyme reactions. There is variation in the number of washes with nuclei isolation buffer in currently published protocols. Initially this was carried out with the five washes described in a recently published Hi-C paper and the following results were generated based on these steps (Grob *et al*., 2014).

Following the nuclear enrichment, the nuclei were permeabilized with SDS, which was then sequestered with Triton X-100. This ensured that the interference of SDS with the restriction enzyme was minimised. Following restriction digest, the sticky-ends generated by the restriction enzyme were blunted using a equimolar mix of dNTPs (with unbiotinylated dATP as a trial) with DNA polymerase I, large (Klenow) fragment at 37 ^{o}C for 1 hour. The Klenow was similarly inactivated prior to the addition the T4 DNA ligase with SDS. The SDS was sequestered during incubation in ligation buffer supplemented with Triton X-100 prior to the ligation step. Initially, triplicate ligation reactions were set up alongside an unligated control. To each of these ligation reactions, 50 units of T4 DNA ligase were added as is described in the SCRIBL protocol for blunt-end ligations (as described in section 2.7.2.5).

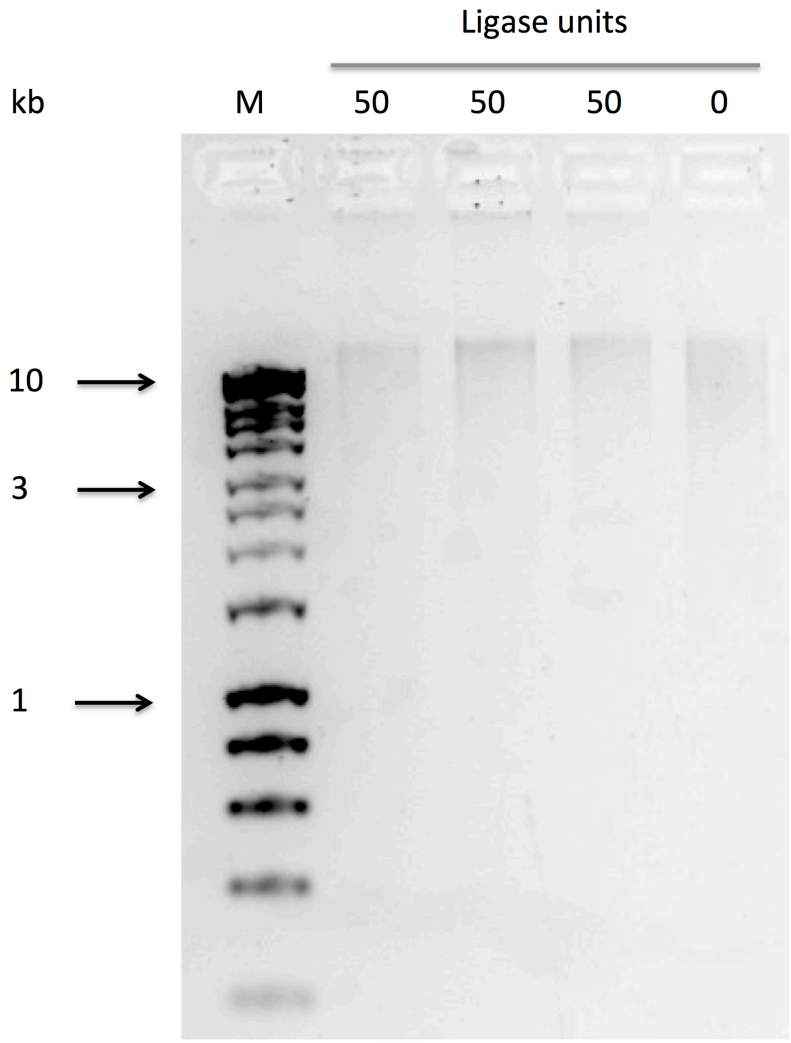

Figure 33. Conditions test for SCRIBL Hi-C blunt-end ligations. *Arabidopsis* cell suspension culture was fixed with a final concentration of 0.75% (v/v) formaldehyde for 10 minutes, followed by nuclear enrichment and permeabilisation. The chromatin was digested with 200 U of *Eco*RI overnight. Three reactions were set up with blunt-ending by Klenow and dNTPs followed by ligation with T4 DNA ligase units as indicated. An additional reaction was not ligated as a negative control. The chromatin cross-links were reversed by overnight incubation with proteinase K at 65 ^{o}C followed by RNase treatment and purified by phenol-chloroform extractions and ethanol precipitation. The reactions were separated by agarose gel electrophoresis with a marker (M) and band sizes indicated (kb).

The uncross-linked and purified DNA showed a limited degree of ligation in comparison to the unligated control (Figure 33). There appears to be a marginal increase in the highest molecular weight fragments in Figure 33, although a relatively tight band above 10 kb is not apparent as has been described for Hi-C libraries (van Berkum *et al*., 2010).

Further optimisation focussed on a comparison between 3C and Hi-C library generation efficiency in this system. In contrast to 3C, a Hi-C library has lower ligation efficiency of high molecular weight fragments due to the additional blunt-ending step. Therefore, it will be important to note whether the low ligation efficiency seen in this experiment is due specifically to the blunt ending reaction or if the ligation conditions were sub-optimal. If the ligation conditions are generally not efficient then this will be detectable in sticky-end 3C library generation.

4.6.2 Comparison of 3C and Hi-C library ligation efficiency

To determine the proportion of Hi-C blunt-end to 3C sticky-end ligations, test reactions were set up to generate each type of library in parallel. Both reactions were formaldehyde fixed, nuclear extracted and permeabilised before overnight digestion. The Hi-C library was blunt ended with Klenow and dNTPs as previously described, while the 3C library retained the sticky *Eco*RI overhangs. The enzymes were inactivated with SDS and sequestered with Triton X-100 before the libraries were incubated with 50 U of T4 DNA ligase under the same conditions.

A smaller and larger volume of each library was visualised on an agarose gel, in a similar way to that presented in literature describing the Hi-C methodology (van Berkum *et al*., 2010). As the amount of DNA increases, this should reveal any discrepancy between the two types of ligation in the reformation of the largest fragments. Blunt-end ligations are predicted to have a lower efficiency than sticky end ligations.

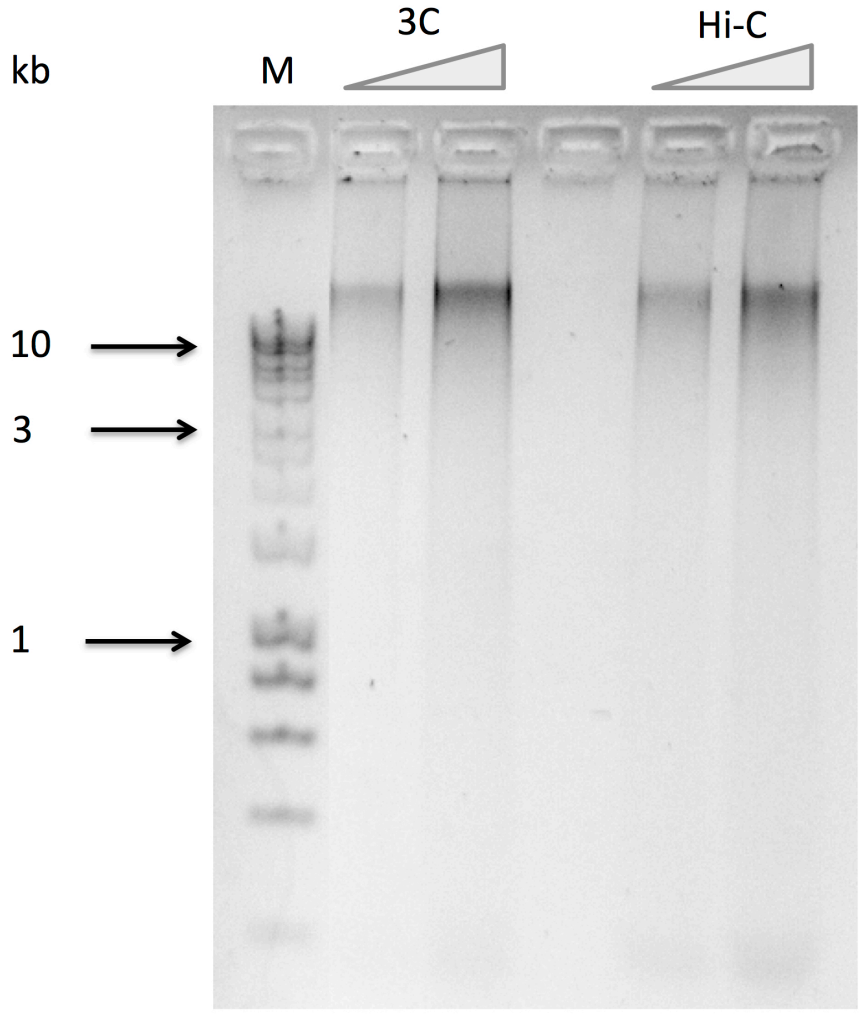

Figure 34. Increasing amount of 3C and Hi-C library to show relative DNA fragments sizes. The triangle indicates the relative amount of the ligated fragments loaded onto an agarose gel, with a marker (M) and fragment sizes indicated (kb). The 3C library was generated with sticky-end ligations, whereas Hi-C involved blunt-end ligations and therefore has a lower expected ligation efficiency.

Both of these libraries appear to have a relatively adequate efficiency, which is judged by the proportion of fragments above 10 kb and it appears that the 3C library has a tighter band over 10 kb as predicted (Figure 34). From Figure 34 it is not possible to determine whether these bands represents a relatively good level of ligation or incomplete digestion.

A group of restriction sites were selected to examine the relative completeness of digestion in comparison to an undigested site. For these PCR reactions the Hi-C library was used as template. The low amplification across these two restriction sites in comparison to that in an undigested region indicated that the restriction digest had relatively good efficiency (Figure 35). This suggests that the high molecular weight fragments in Figure 34 are likely to be products of ligation reactions.

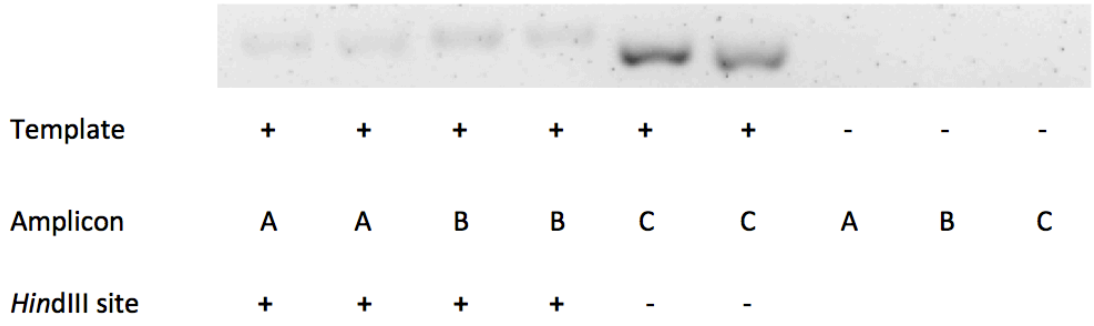

Figure 35. Completeness of restriction digestion during the generation of the Hi-C library as determined by PCR. Two sets of primers designed to amplify a region approximately 200 bp across restriction sites were tested (A (LHCh4) and B (LHCh5)) in comparison to an undigested region (C (LHCno)). PCR reactions were carried out in duplicate for each site, along with a negative control without template for each primer pair (template + or -). The presence of a *Hin*dIII site is indicated for each of the amplicons (*Hin*dIII site + or -). The products of each of the reactions were visualised on an agarose gel. The primer sequences are given in section 2.7.2.8.

Primers were also designed to amplify short-range ligation products. These PCR reactions will only amplify sequence resulting from a change in orientation of the regions in relation to each other. This occurs when chromatin is digested and ligated resulting in creation of products that would not otherwise be present in untreated cells. When the chromatin is cross-linked with formaldehyde prior to digestion and ligation this facilitates the generation of a snapshot of close proximity and physically interacting regions. The ligation products therefore represent either random collisions between regions (background noise) or those that have a higher likelihood than chance, which are classifiable in two main categories. These groups represent a bias due to their close proximity or a functional interaction. The functional interactions are what chromosome conformation capture technology aims to identify. Although, the category of ligation products representing interactions which occur due to their close proximity are critical as a quality control for the technique.

PCR reactions attempting to amplify these short-range ligation products were unsuccessful with this Hi-C library as template. This is problematic given that these short-range products should be formed at the highest frequency. These are most likely to be formed even without a functional interaction given the distance decay that has been previously described (van Berkum *et al*., 2010). This would mean lower frequency interactions could be barely detectable. Therefore, while digestion and ligation were successful during the Hi-C library generation to an extent, this may not be sufficient to produce an adequate picture of chromosome conformation.

As there are numerous variables in the generation of the Hi-C library, not simply the ligation efficiency, each of these required investigation and further optimisation. For instance, if the cross-linking is not held intact during the ligations then this could have contributed to undetectable short-range ligation products. In addition, during the course of these experiments in which the nuclei were washed five times, it was found in some cases that the nuclear pellet was almost entirely absent by the end of the enrichment process. This resulted in a low recovery of DNA by the end of the purification steps. It is possible that these additional washes may have resulted in a lower yield and perhaps less intact nuclei as is suggested by Louwers *et al*. (2009). Furthermore, it was observed that the nuclear pellet was considerable lighter in colour during extraction from *Arabidopsis* cell suspension culture than with other

plant species such as *N. benthamiana*. By the second wash little debris was visibly removed in the supernatant with *Arabidopsis* cell suspension culture. It is likely that the dependence of the *Arabidopsis* cell suspension culture on sucrose containing media means that these plant cells cultured in suspension have fewer chloroplasts and less cellular debris to be removed during nuclear isolation. Therefore, in further optimisation steps the number of nuclear washes was reduced to test whether this would improve consistency in the efficiency of the nuclear enrichment.

4.6.3 Optimisation of formaldehyde fixation conditions

The conditions for each of the key stages in the method were tested to ensure that these were optimal. As a starting point, a range of formaldehyde concentrations were tested for the efficient fixation of chromatin in *Arabidopsis* cell suspension culture. In previous experiments, conditions were based on a ChIP protocol for chromatin fixation using 0.75% (v/v) formaldehyde (final concentration) for 10 minutes with gentle mixing (Abcam website).

It is important that the fixation steps are optimal in order to maximise the efficiency of the ligation steps, which occur under very dilute conditions. The cross-linking favours generation of hybrid chromatin fragments, which represent physically interacting chromatin. If these cross-links are not held intact during ligation then this will result in a low ligation efficiency that is also not representative of interacting regions. Over cross-linking also presents a potential problem. While it is important that the cross-links are held intact, a high concentration of formaldehyde can result in cross-links that are difficult to reverse following the ligation steps. This could pose a problem for the subsequent purification of the chromatin, as heavy cross-linking hampers recovery of purified DNA during phenol-chloroform extractions.

A test was set up in a similar way to that described for formaldehyde fixation optimisation for ChIP in *Arabidopsis* plants (Haring *et al.*, 2007). In this experiment, two samples of *Arabidopsis* cell suspension culture were fixed over a range of formaldehyde concentrations. The cells were treated for 10 minutes with gentle mixing and the formaldehyde was quenched with glycine. Prior to purification of the

chromatin, one sample per formaldehyde concentration was uncross-linked by incubation overnight at 65 ^{o}C with proteinase K. All samples were treated with RNase A before purification of the chromatin by phenol-chloroform extractions and ethanol precipitation.

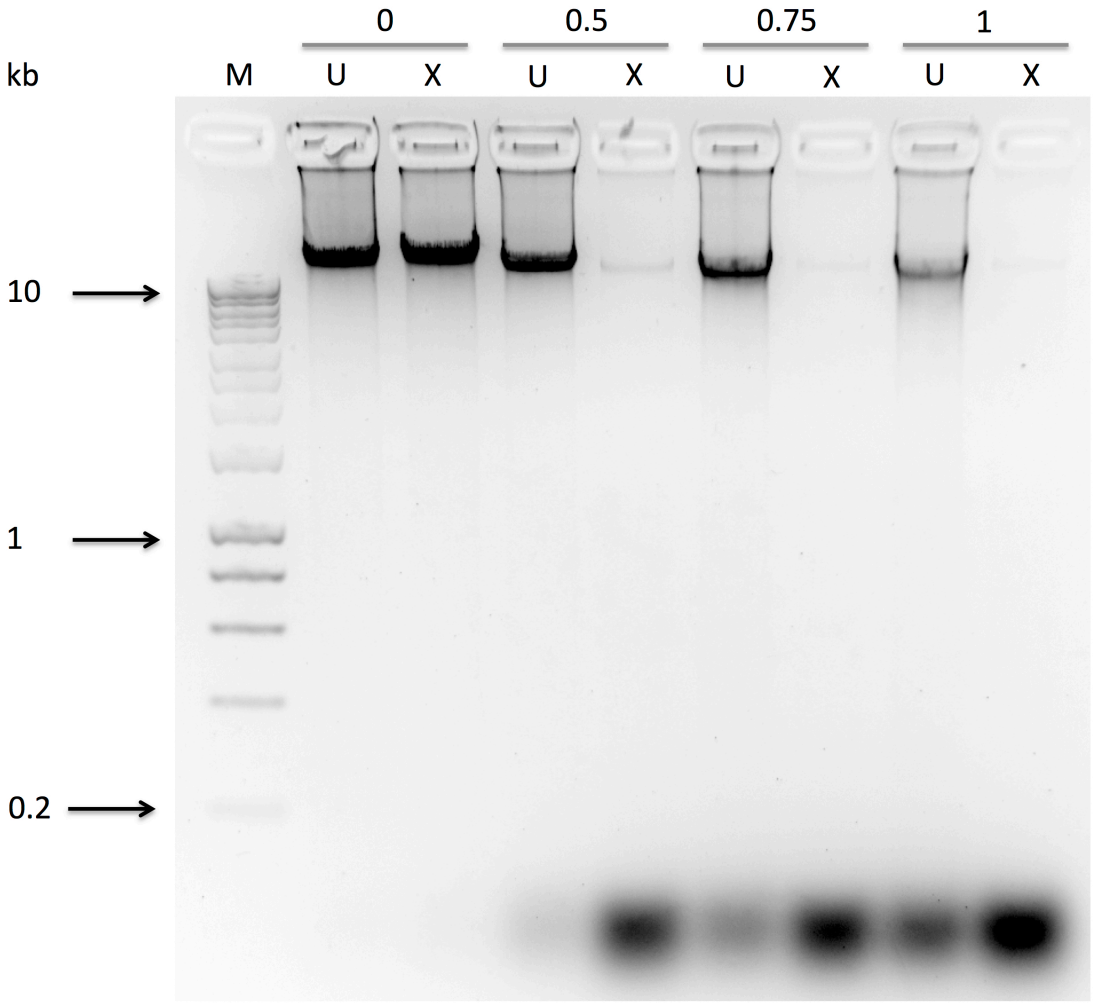

Figure 36. Optimisation of conditions for formaldehyde fixation of chromatin. *Arabidopsis* cell suspension culture was fixed with a range of formaldehyde concentrations for 10 minutes. The concentration of formaldehyde is indicated (as percentage formaldehyde (v/v) of the final volume). Following fixation, the nuclei were enriched and permeabilised. The chromatin cross-links were reversed for one sample at each formaldehyde concentration by overnight incubation at 65 ^{o}C with proteinase K. All samples were RNase treated and purified by phenol-chloroform extractions and ethanol precipitation. The cross-linked (X) and cross-link reversed (U) purified DNA was run on an agarose gel with a marker (M) and band sizes indicated (kb).

This experiment showed that formaldehyde treatment clearly generated efficient cross-linking at all of the concentrations tested. This is apparent from comparing the reactions without cross-linking reversal between concentrations (Figure 36). At 0% (v/v) formaldehyde the lack of the overnight cross-linking reversal step does not have any noticeable impact on the quality or quantity of the purified DNA. However, all other concentrations show a low yield of purified DNA recovered without de-cross-linking indicating that cross-links have been efficiently generated during this process (Figure 36).

In addition, the experiment showed that the quality of purified DNA from cross-link-reversed samples decreases and shows degradation as the formaldehyde concentration increases (Figure 36). There is also an apparent deterioration in the yield of DNA from cross-link-reversed samples with increasing formaldehyde concentration meaning that a higher concentration results in tighter and/or additional cross-linking (Figure 36). It is clear that 0.5% (v/v) formaldehyde shows comparable quality of purified DNA to the negative control. However, at a concentration of 0.75% (v/v) formaldehyde the DNA starts to show signs of degradation, which may impact on the efficiency of the Hi-C library. Therefore, 0.5% (v/v) formaldehyde appears to be the most efficient concentration for fixation of chromatin in *Arabidopsis* cell suspension culture.

4.6.4 Optimization of digestion conditions

Following on from testing the fixation conditions, the optimum amount of restriction enzyme for complete fragmentation of the chromatin was established. A complete digest is essential in order to maximise the resolution of the Hi-C library. An incomplete digest reduces the potential for fragments to ligate with cross-linked regions. This could make lower frequency interactions undetectable by this method.

A method which adapted 3C for Maize uses 400 U of restriction enzyme for DNA fragmentation (Louwers *et al*., 2009). This was used as a starting point for the experiments previously described. To test the efficiency of the restriction digest,

three amounts of restriction enzyme were tested (200, 400 and 600 U) to establish whether this affected the efficiency of the fragmentation (Figure 37).

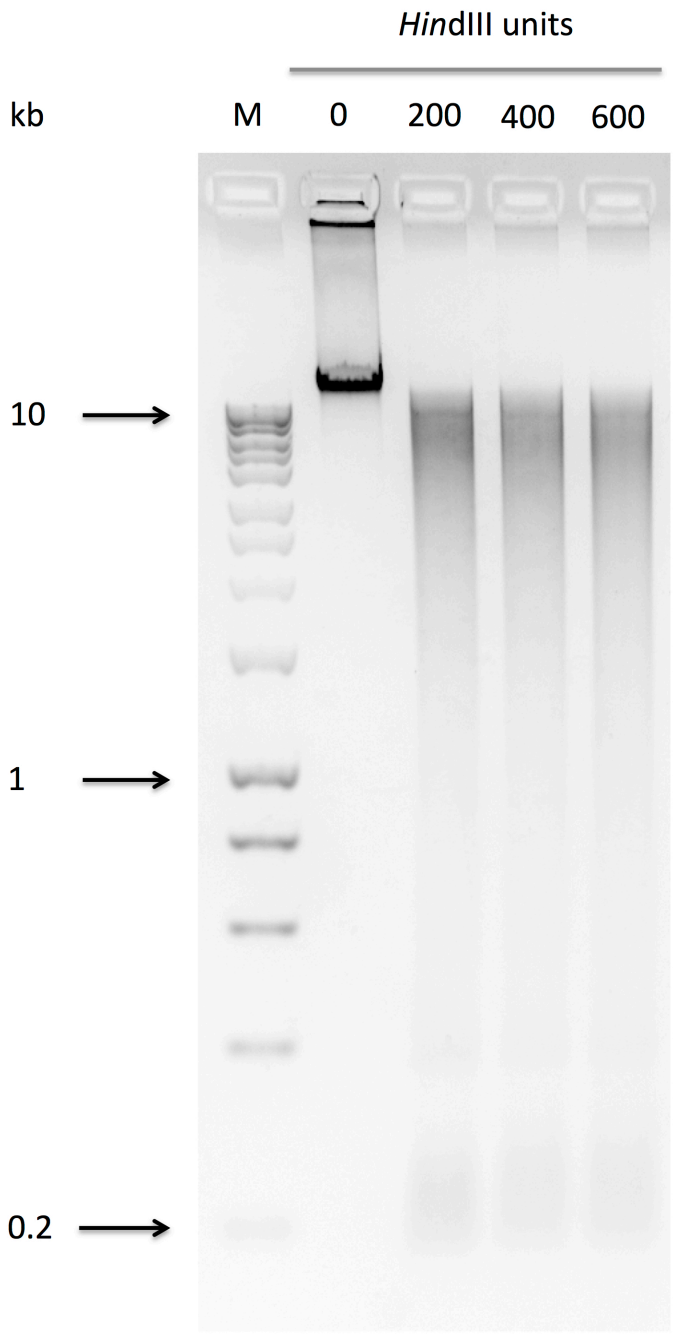

Figure 37. Optimisation of conditions for restriction digest of chromatin. *Arabidopsis* cell suspension culture was fixed with 0.5% (v/v) formaldehyde for 10 minutes, followed by nuclear enrichment and permeabilisation. The chromatin was digested with a range of units of *Hin*dIII overnight as indicated. The chromatin cross-links were reversed by incubation overnight at 65 ^{o}C with proteinase K followed by RNase treatment before DNA purification by phenol-chloroform extractions and ethanol precipitation. The purified DNA was run on an agarose gel with a marker (M) and band sizes indicated (kb).

Figure 37 shows that there is not a visible difference in digestion efficiency between the various amounts of restriction enzyme. All of the reactions appear to have a good level of digestion with a lower intensity of fragments below 1 kb. Therefore, further experiments used 400 U of restriction enzyme although from these results it appears that 200 U would also produce fairly comparable digestion efficiency.

4.6.5 Optimization of ligation conditions for 3C library generation

The conditions were tested for preparation of a 3C library in which ligations are carried out with sticky end fragments. It is important that this is optimal before introducing the additional blunting steps, which are necessary for Hi-C. An additional control was included to determine the efficiency of ligations in comparison to undigested DNA. This control was treated as a mock reaction meaning that the DNA integrity and quality was more representative of the further treatments and incubation steps.

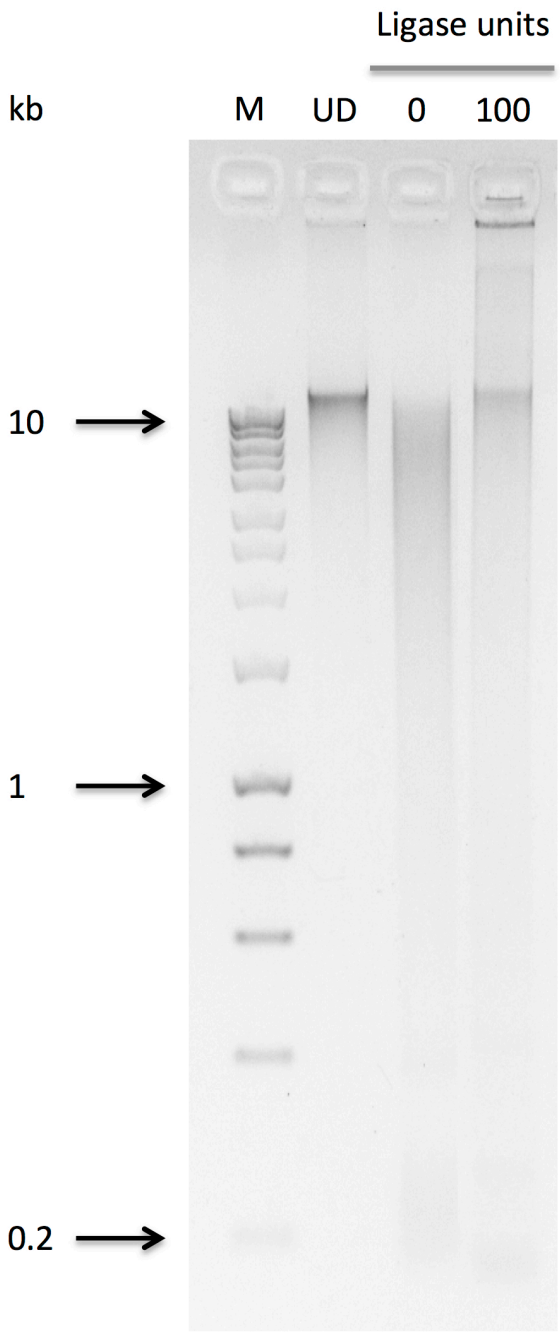

Figure 38. Efficiency test for sticky-end (3C type) ligations. *Arabidopsis* cell suspension culture was fixed with 0.5% (v/v) formaldehyde for 10 minutes, followed by nuclear permeabilisation. The chromatin was digested with 400 U of *Hind*III overnight with a mock undigested control (UD). Following the overnight restriction digest, the reactions were inactivated with 1.5% (v/v) SDS and ligated under dilute conditions with T4 DNA ligase (Invitrogen) units as indicated. The chromatin cross-links were reversed by incubation overnight at 65 ^{o}C with proteinase K, followed by RNase treatment and the DNA was purified by phenol-chloroform extractions and ethanol precipitation. Purified DNA was run on an agarose gel with a marker (M) and band sizes indicated (kb).

The 3C library here showed larger fragment sizes reforming following incubation with 100 U of T4 DNA ligase in comparison to the unligated control (Figure 38). This indicates that these conditions are adequate for sticky-end ligations to occur. However, it is unclear as to the proportion of successful ligations that occurred in comparison to the potential ligations. Therefore a further test was carried out using different brands and amounts of ligase in order to test whether this made a difference to the size of the band over 10 kb, representing successful ligation reactions. In addition, Louwers *et al*. (2009) suggested that the presence of SDS, which is used for inactivation of the restriction enzyme and Klenow, could hamper the ligation efficiency of T4 DNA ligase. Here it is recommended that the final concentration of SDS should be reduced if a low ligation efficiency is observed (Louwers *et al*., 2009). The concentration of SDS was also lowered to investigate whether a final concentration of 1.5% (v/v) SDS had an impact on the ligation efficiency. Therefore, in the subsequent experiment the restriction enzyme was not inactivated by an incubation with 1.5% (v/v) SDS at 65 ^{o}C.

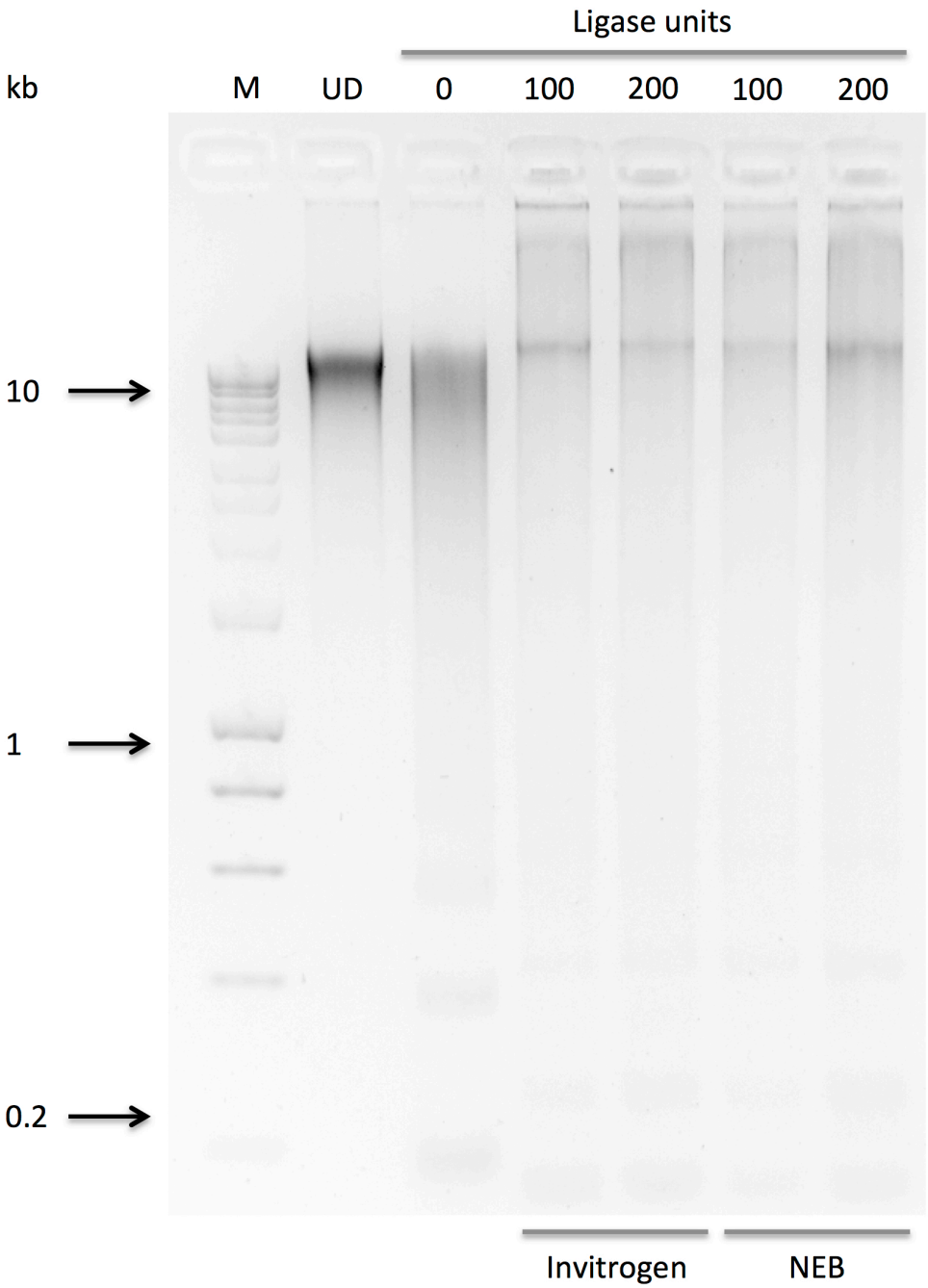

Figure 39. Efficiency test for 3C type sticky-end ligations with different brands and amounts of T4 DNA ligase, without SDS inactivation of the restriction enzyme. *Arabidopsis* cell suspension culture was fixed with 0.5% (v/v) formaldehyde for 10 minutes, followed by nuclear permeabilisation. The chromatin was digested with 400 U of *Hin*dIII overnight with an undigested control (UD). The 3C reactions were ligated under dilute conditions with Invitrogen or New England Biolabs (NEB) T4 DNA ligase units as indicated. Each brand of ligase was used for two separate ligation reactions with 100 or 200 U of ligase. The chromatin cross-links were reversed by incubation overnight at 65 ^{o}C with proteinase K for all of the reactions and the DNA was purified by phenol-chloroform extractions and ethanol precipitation. Purified DNA was run on an agarose gel with a marker (M) and band sizes indicated (kb).

The ligation reactions showed a clear formation of a high molecular weight band above 10 kb (Figure 40). The different brands and amounts of ligase did not appear to affect the efficiency of the reactions. However, it appears that between the previous efficiency test in Figure 38 and Figure 39 that there is an improvement in the tightness of the band above 10 kb. It is possible that the SDS could have been inhibiting the T4 DNA ligase and therefore it will be used at a lower concentration for the inactivation of the restriction enzyme and Klenow during the following Hi-C library generation. While it is possible that further variation to the conditions for the ligation reaction could improve the efficiency the 3C library generation, it seems that an appropriate level had been achieved. These ligation conditions were then used in optimising the generation of a Hi-C library.

4.6.6 Optimization of ligation conditions for Hi-C library generation

The ligation conditions, which had been optimised for 3C, were used for the generation of Hi-C libraries with the addition of the blunt-ending reactions. These reactions were carried out with and without biotinylated bases to determine whether this made a difference to the fill-in efficiency. As a control, a 3C library was also generated alongside these reactions. In this test, 100 U of T4 DNA ligase were used for these 3C and Hi-C ligation reactions.

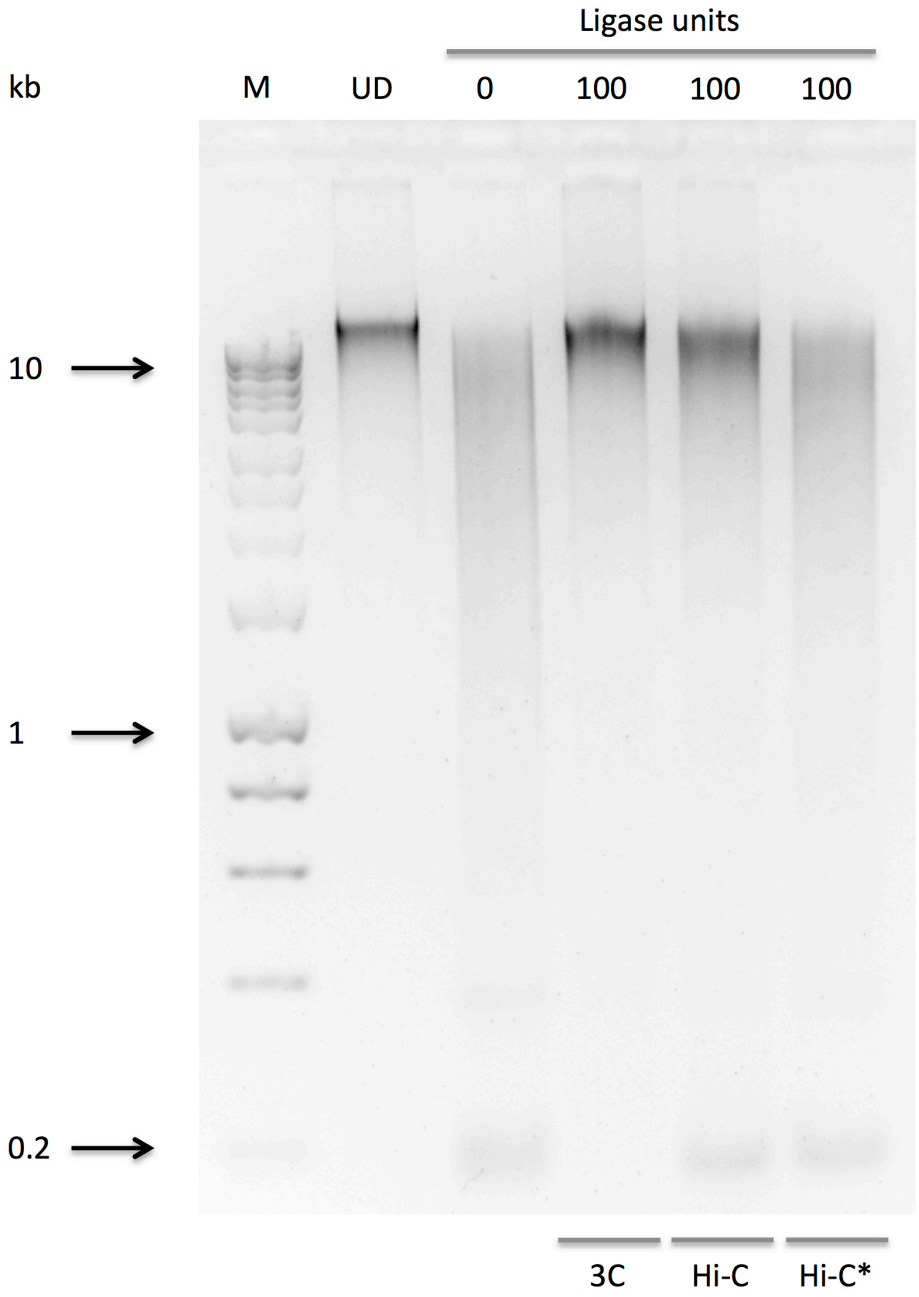

Figure 40. Efficiency test for Hi-C with and without biotin incorporation. *Arabidopsis* cell suspension culture was fixed with 0.5% (v/v) formaldehyde for 10 minutes, followed by nuclear permeabilisation. The chromatin was digested with 400 U of *Hind*III overnight with a mock undigested control (UD). The Hi-C reactions underwent fill-in with dNTPs in equal proportions (Hi-C) or with biotinylated dATP (Hi-C*) at 4X the concentration of other dNTPs with Klenow. Another reaction was a 3C control and therefore did not undergo the fill-in steps. The restriction enzyme and Klenow were inactivated with heating at 65 ^{o}C then 37 ^{o}C with 0.5% (v/v) SDS. The ligations were performed under dilute conditions with the amount of T4 DNA ligase units indicated. The chromatin cross-links were reversed for all of the reactions by incubation overnight at 65 ^{o}C with proteinase K and the DNA was purified by phenol-chloroform extractions and ethanol precipitation. Purified DNA was run on an agarose gel with a marker (M) and band sizes indicated (kb).

The Hi-C and 3C libraries showed relatively comparable ligation efficiency although partly lower for Hi-C. However, the addition of biotinylated dATP reduces the efficiency considerably and ligation is barely detectable (Figure 40). Therefore, it appears that while the blunt-ending reaction appears optimal, the incorporation of biotinylated dATP greatly reduces the ligation efficiency. It has previously been described that biotin incorporation has a low efficiency which generally accounts for 20 to 30% of fill-in reactions (Belton *et al*., 2012). This may be resolved by a longer incubation time for the fill-in and/or extending the ligation step to overnight (Belton *et al*., 2012).

A further experiment was set up to test additional conditions for biotin incorporation during blunt-ending and ligation of these fragments. In this test, 3C and Hi-C libraries were generated in parallel to directly compare efficiencies. During the blunt-ending reactions for the preparation of the Hi-C library, the incubation time was extended from 30 minutes to 4 hours. In addition, two incubation times were tested for the ligation step. These were 5 hours and overnight (ON). It is possible that the biotinylated bases could interfere with the T4 DNA ligase and therefore this reaction may be less efficient and required extension to maximise efficiency. Therefore, it was hypothesised that a longer biotin incorporation step alongside the extended ligation step could improve the overall efficiency of Hi-C library generation.

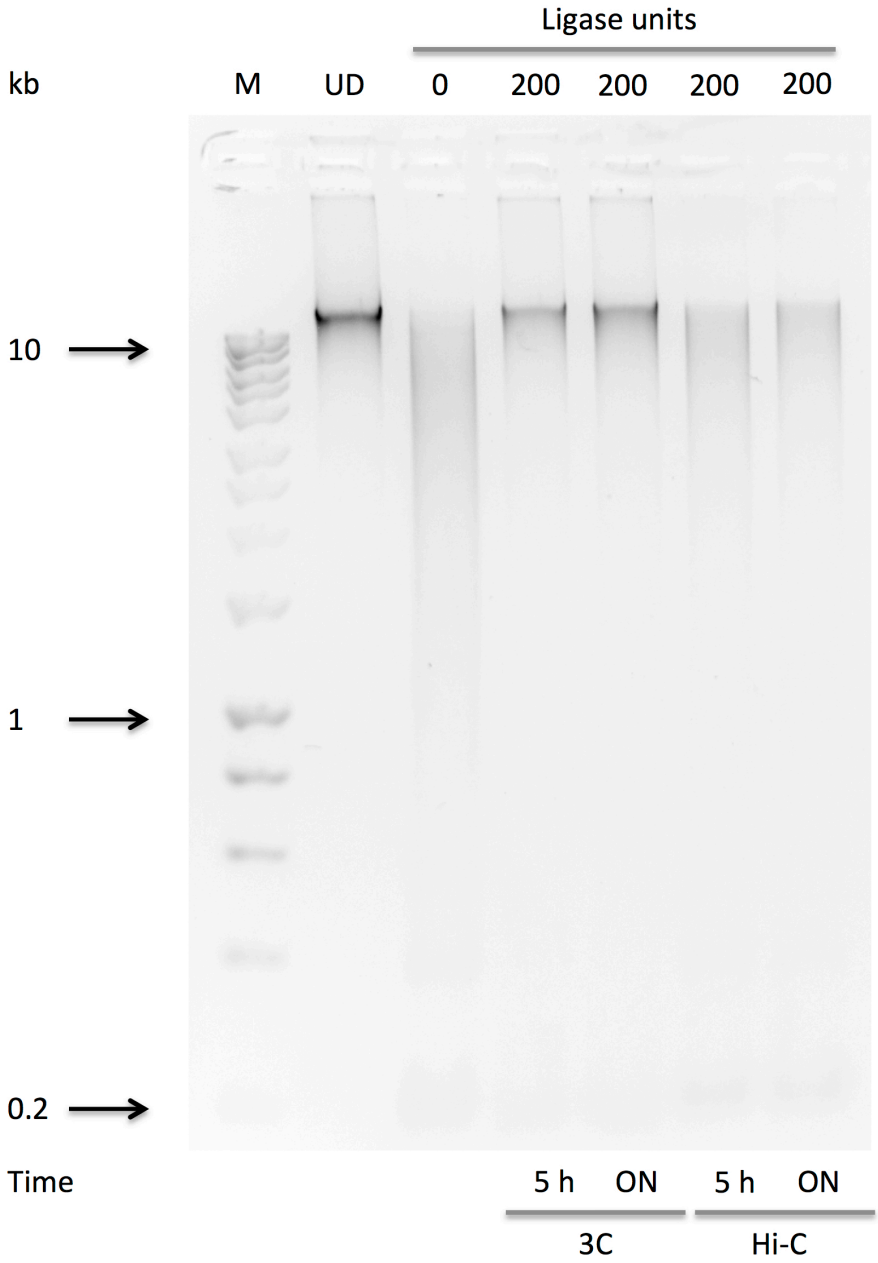

Figure 41. Efficiency test for 3C and Hi-C with biotin incorporation. *Arabidopsis* cell suspension culture was fixed with 0.5% (v/v) formaldehyde for 10 minutes, followed by nuclear permeabilisation. The chromatin was digested with 400 units of *Hin*dIII overnight with an undigested control (UD). The Hi-C reactions underwent fill-in with dNTPs in equal proportions with biotinylated dATP (Hi-C) at four times the concentration of other dNTPs with Klenow for 4 hours. Two 3C reactions did not undergo the fill-in steps. The restriction enzyme and Klenow were inactivated with heating at 65 ^{o}C then 37 ^{o}C with 0.5% (v/v) SDS. The ligations were performed at 16 ^{o}C under dilute conditions with the amount of T4 DNA ligase units indicated. The time for which the ligation reactions were incubated are indicated (5 h or overnight (ON)). The chromatin cross-links were reversed by incubation overnight at 65 ^{o}C with proteinase K for all of the reactions and the DNA was purified by phenol-chloroform extractions and ethanol precipitation. Purified DNA was run on an agarose gel with a marker (M) and band sizes indicated (kb).

The results in Figure 41 when compared to Figure 40 indicate that there could be a minor improvement in the regeneration of the larger fragment sizes in the Hi-C libraries with a longer step for blunt-ending. This is judged by comparing the 5-hour Hi-C reaction in Figure 41 with the reaction labelled Hi-C* in Figure 40, relative to the digested controls. It is possible that there is a shift towards larger molecular weight fragments in the case of the latter experiment. In addition, it is also possible that there could be a minor improvement in the efficiency of the Hi-C library generation with biotin, when comparing the 5-hour and overnight (ON) incubations with T4 DNA ligase (Figure 41). However, the Hi-C libraries without biotin are characterised by a relatively tight band above 10 kb, as is also the case with the 3C libraries (Figure 41). Therefore, at this stage the generation of the Hi-C library requires further optimisation, which was outside the timeframe of this project. Further work to optimise SCRIBL Hi-C would therefore need to make additional changes in order to address the poor efficiency of biotin incorporation, possibly through further adjustments to incubation times. A relatively high efficiency for this incorporation is essential in this technique as it marks the ligation junctions for enrichment and allows all of the regions that were not digested or ligated to be removed.

4.7 Discussion

These experiments aimed to optimise a recently developed enhanced Hi-C method (SCRIBL) for *Arabidopsis* cell suspension culture, to produce a more targeted analysis of chromosome conformation (Stefan Schoenfelder and Peter Fraser, unpublished). This approach could be a valuable tool to investigate whether specialised transcription factories are a mechanism utilised by plant cells for the transcriptional coordination of genes involved in the same or related processes. While various studies suggests that these transcription factories exist in other organisms, there remains uncertainty as to the significance of these in transcriptional coordination in plants (see section 1.5).

Initial investigations aimed to establish the conditions for hormone induction in *Arabidopsis* cell suspension culture. These conditions were based on the MeJA

treatment of *Arabidopsis* cell suspension culture in a microarray analysis of gene expression changes (Pauwels *et al*., 2008). From gene induction for several JA marker genes at 5, 7 and 25 hours after treatment, it was established that an earlier time point (5 h) would be most appropriate for the investigation, given that these genes showed generally more consistent expression.

RNA probes were generated from BAC DNA as described in the SCRIBL protocol for a group of trial BACs (Schoenfelder and Fraser, unpublished). The shearing conditions required optimisation for a different type of sonicator to that described in the SCRIBL protocol, although the conditions were otherwise found to be reproducible, generating good quality RNA probes (Schoenfelder and Fraser, unpublished). These probes are a key feature of SCRIBL Hi-C, allowing the enrichment of regions of interest. Therefore, it is important that the biotinylated RNA probes are of high quality in order to ensure that these hybridise to the target sequences efficiently. This will ensure that it is possible to enrich even low frequency ligation products representing interacting chromatin.

Further work aimed to optimise Hi-C library generation for *Arabidopsis* cell suspension culture. This involved several key variables for which modification of conditions was required. Initial conditions were based on a combination of protocols, which included ChIP-seq for *Arabidopsis* cell suspension culture and 3C and Hi-C with Maize and *Arabidopsis* seedlings (Haring *et al*., 2007; Louwers *et al*., 2009; Grob *et al*., 2013). From here, adjustments were made to optimise these to maximise the efficiency of the SCRIBL Hi-C protocol given the differences in the type and growth conditions of the cells. It was found that 0.5% (v/v) formaldehyde for 10 minutes resulted in the best fixation of chromatin without the noticeable deterioration in quality at higher concentrations. Furthermore, 400 U of restriction enzyme produced a good efficiency digest, although from the range tested here the amount of enzyme per reaction was demonstrated to have only a minor impact on the visible banding pattern formed. However, it is important that the chromatin is not over digested as this could produce a data set in which sequences have ligation junctions at non-restriction sites. This could make the data difficult to analyse when the interaction sequences are compared to a reference set of restriction sites.

The difficulties with improving ligation efficiency during the preparation of the Hi-C library meant that this became a sticking point in the protocol. Further work to adapt the method for use with *Arabidopsis* cell suspension culture would need to focus on optimising this key step. During optimisation of the conditions, it was found that decreasing the final concentration of SDS for the inactivation of the restriction enzyme improved efficiency of forming a 3C and blunt-ended non-biotinylated libraries. This is likely to be due to the inhibitory effect of residual SDS has on T4 DNA ligase. However, the introduction of biotinylated bases into the Hi-C blunt-ending reactions significantly reduced the efficiency of the ligation reaction. The biotinylated Hi-C library appeared to have a comparable range of fragment sizes to the digested control. Following extension of the fill-in reaction with biotinylated bases and Klenow to 4 hours and an overnight ligation, there appeared to be a slight improvement in the efficiency of the Hi-C library. However, this does not appear adequate particularly for detection of lower frequency interactions. It is important that the ligation efficiency is therefore improved in order to be able to give as broad and accurate a picture of chromosome interactions as possible.

The next steps of this investigation would have been to complete optimisation of the Hi-C library generation for *Arabidopsis* cell suspension culture. This would require the collection of *Arabidopsis* cell suspension culture samples at 0 hours and 5 hours treated with 50 μM MeJA and mock treated, from which to generate these Hi-C libraries. Following ligation of the biotinylated fragments these would be sheared by sonication and biotin pulled down with streptavidin beads, followed by PCR amplification to produce the final Hi-C library. The Hi-C library would then be hybridised to the biotinylated RNA probes to generate the final SCRIBL Hi-C library. The library is then paired-end sequenced on the Illumina Hi-seq platform (Illlumina, San Diego, California) and can be analysed using the HiCUP pipeline (Babraham Institute, University of Cambridge). This pipeline has been developed for the quality control of the sequences, preparation of a reference genome digested with the restriction enzyme used during the Hi-C library preparation and to make paired alignments of the sequences. From here the interactions can be visualised using software such as Seq Monk (Babraham Institute, University of Cambridge). This enables the user to look at genome wide interactions from any locus within the

region covered by the BAC sequences with which the biotinylated RNA probes were generated.

With this data it would have been possible to make an assessment as to whether there are any apparently functional spatial interactions of chromatin in *Arabidopsis* cell suspension culture. It may also be possible to determine whether there is a change in these spatial interactions that could be triggered by stimulus such as treatment with MeJA. However, despite a potentially good foundation of this hypothesis, it is possible that a specialisation of transcription factories would not be observable from these marker genes. In this case, the large number of genes in adjacent regions captured alongside these marker genes, could show unanticipated trends in spatial localisation that would also be identified in this analysis. Alternatively, no significant associations or changes in spatial localisation of genes may be identified aside from random and non-significant collisions (background noise) or the predicted higher frequency interactions with neighbouring regions (Belton *et al*., 2012).

Regardless of the nature of the results from the experiment, it is important to validate these with a contrasting technique. Therefore, a method such as fluorescent *in situ* hybridisation (FISH) could be used as further verification of the SCRIBL Hi-C results as described in Schoenfelder *et al.* (2010) to study the beta-globin gene associations in mice (see section 1.3.2). These types of technique were the forerunner of 3C and gave early insight into spatial interactions of chromatin (see section 1.3.1). More recent adaptations of microscopy based techniques including structured illumination microscopy (SIM) and photoactivated localization microscopy (PALM) have allowed an improved resolution of individual molecules beyond the diffraction limit of light (Schubert and Weisshart, 2015). This has allowed the numbers and patterns of activated and inactivated RNAPII to be determined using specific antibodies with aligned images from both SIM and PALM using *Arabidopsis* nuclei (Schubert and Weisshart, 2015). This revealed a relatively even distribution of both active and inactive forms of RNAPII within the nucleus (excluding the nucleolus with clustering also observable (Schubert and Weisshart, 2015). Overall, evidence from microscopy and DNA based methods could provide enhanced support for potential observations of transcription factory specialisation in *Arabidopsis*.

5 General Discussion

5.1 Overall aims

These experiments focussed on investigating plant-pathogen interactions and the mechanisms by which hormones induce transcriptional responses. Chapter 3 presented an investigation examining the interaction between a predicted oomycete effector from *Hpa* HaRxL14 and *Arabidopsis* protein PP2CA, which was previously identified in a yeast two-hybrid screen (Steinbrenner, Braun and Beynon, 2013, unpublished). PP2CA has a well-established role in coordinating ABA and metabolic signalling in plants. The experiments presented in Chapter 4 aimed to optimise an enhanced Hi-C method (SCRIBL) to examine changes in spatial gene association, as a result of hormone induction in *Arabidopsis*. This hypothesis arose from the concept of specialisation of transcription factories particularly from mammalian models, which suggests that transcription of related genes is coordinated at focal points of transcriptional machinery within the nucleus. Therefore, the aim of the work was to unravel the mechanism and role of this specific effector interaction, which could give additional insights into the role of ABA signalling in plant defence against oomycete pathogens. Furthermore, this project aimed to establish whether a coordinated transcriptional response to phytohormones could involve specialised transcription factories. These transcription factories could potentially be effector targets in a pathological context.

5.2 ABA in pathogen defence

The phytohormones SA, ET and JA have well established links to plant defence signalling (Cao *et al*., 2011; Glazebrook, 2005; Ma and Ma, 2016). Within the last decade, the role of ABA in plant immunity has been more extensively examined, although many intricacies that link the hormone to defence response are currently unknown. The role of the hormone is variable among pathogens with similar lifestyles and even between stages of infection (Asselbergh *et al*., 2008). For instance, ABA deficient tomato plants have a higher resistance to root infection by *P.*

capsici compared to wild-type, which can be reversed by exogenous application of the hormone (Dileo *et al*., 2010). These experiments also suggest that ABA signalling induced by abiotic stress predisposes the plant to infection with *P. capsici* as a result of its role in modulating SA defence gene induction (Audenaert *et al*., 2002; Dileo *et al*., 2010). This ABA deficient tomato mutant also exhibits enhanced resistance to *B. cinerea* despite the contrasting necrotrophic lifestyle of the fungus (Vidhyasekaran, 2014). In the latter case, the ABA deficient plants were found to more rapidly form hydrogen-peroxide associated cell wall strengthening in epidermal cells (Curvers *et al*., 2010). Therefore, it is clear that ABA has close links to the defence response, although at present these appear to be more case specific rather than general patterns as observed with SA and JA.

5.3 Cross-kingdom function of the PP2Cs

PP2CA is part of one of four families of protein serine/threonine phosphatases (type 2C), which have been shown to play broad roles in response to perturbations in environmental conditions (Shiozaki and Russell, 1995). These proteins are found across eukaryotic kingdoms including in animals, yeast and plants and generally have roles in coordinating cellular events and stress related pathways (Gaits *et al*., 1997; Shiozaki and Russell, 1993; Zhang *et al*., 2013). The mechanism involved in these functions include modulating regulators of MAPK signalling cascades, as well in interacting with specific kinases within these pathways (Lu and Wang, 2008). In *Saccharomyces cerevisiae* PP2Cs Ptc1 and Ptc3 regulate the High Osmolarity Glycerol (HOG) MAPK cascade which are crucial in coordinating the stress response to high osmolality conditions (Saito and Tatebayashi, 2004). Ptc1 is thought to dephosphorylate Hog1 (part of the MAPK cascade) via an adapter protein and has a key role in returning the conditions to a stable state following osmotic stress (Hohmann, 2015; Saito and Tatebayashi, 2004; Warmka *et al*., 2001).

There are thought to be at least 18 PP2C members in humans, which have variable expression patterns across tissue and have roles in stress signalling, cellular metabolism and cell death/survival (Lu and Wang, 2008). These varied roles have highlighted the PP2Cs as possible targets for drugs for human diseases including

anticancer therapy (Lu and Wang, 2008). Interestingly, PP2Cs may even act as pathogenicity factors since TgPP2C from *Toxoplasma gondii* has been shown to interact with structure-specific recognition protein 1 (SSRP1) in human cells, which regulates apoptosis (Gao *et al*., 2014a). During the stage of infection inside host cells, the pathogen protects the cell from various sources of apoptosis (Gao *et al*., 2014a; Nash *et al*., 1998; Robert-Gangneux and Dardé, 2012). Over-expression of TgPP2C was shown to dramatically reduce cell death in HeLa cells, although the mechanism of this interaction in the overall pathway is unclear (Gao *et al*., 2014a).

Similarly PP2Cs have key roles in coordinating various signalling pathways in plants, including the ABA response. During ABA response, the PYR/PYL/RCARs receptors bind to ABA and form a complex with specific PP2Cs preventing them from inhibiting the ABA associated SnRK2s (Fujii *et al*., 2009; Park *et al*., 2009). Three of the ten *Arabidopsis* SnRK2s (SnrK2.2, 2.3 and 2.6 (OST1)) have been identified as having a key role in ABA response (Kulik *et al*., 2011). The fourteen members of the PYR/PYL/RCAR receptors (with the exception of PYR13) show ABA induced binding to PP2Cs (Gonzalez-Guzman *et al*., 2012; Kline *et al*., 2010; Santiago *et al*., 2009). The downstream pathways of the SnrK2 include activation of the ABA-responsive element binding factors (ABFs) including ABF3, which are master regulators of the ABA transcriptional response (Yoshida *et al*., 2015). The diversity of receptors and signal transducers in the ABA pathway creates complexity. This complexity allows fine-tuning of the response of these pathways to environmental conditions across tissues, as previously noted with PP2Cs in other eukaryotes. There are thought to be sixty-nine PP2Cs in *Arabidopsis*, of which the nine clade A PP2Cs involved in binding to the ABA receptors are subcategorised into two main groups (Schweighofer *et al*., 2004; Sun *et al*., 2011; Zhang *et al*., 2013). The first group includes abscisic acid insensitive (ABI) 1 and 2 and homology to AB1 (HAB) 1 and 2, and a second group includes PP2CA among others (Schweighofer *et al*., 2004; Sun *et al*., 2011; Zhang *et al*., 2013). Interestingly, the observed interaction between HaRxL14 and PP2CA in yeast two-hybrid showed that the effector interacts specifically with PP2CA and did not interact with other PP2Cs (Steinbrenner, Braun and Beynon, 2013, unpublished).

5.4 Verification of the HaRxL14 and PP2CA interaction

The interaction between HaRxL14 and PP2CA was verified by bimolecular fluorescence complementation (BiFC) and was shown to occur in the nucleus. This pattern is consistent with the individual localisation of the effector and target and also with a previous study which demonstrated the presence of PP2CA predominantly in the nucleus (Pizzio *et al*., 2013). A BiFC analysis also showed a nuclear interaction between PYR4 and PP2CA, which did not require exogenous ABA, suggesting that endogenous ABA levels in *N. benthamiana* are sufficient to mediate the interaction (Pizzio *et al*., 2013). However, Co-IP experiments were unable to confirm an interaction between HaRxL14 and PP2CA under various conditions. It is possible that this is a low frequency interaction, although analysis of the pulled-down products by MS was also unable to verify the presence of both HaRxL14 and PP2CA. Further Co-IP experiments could investigate whether the interaction is observable with a whole cell extract rather than restricting the input to nuclear proteins.

5.5 The role of PP2CA in susceptibility of *Arabidopsis* to *Hpa*

It has been shown that PP2CA modulates the closure of stomata, which is a key response to water deprivation (Lee *et al*., 2009). PP2CA negatively regulates the SnRK2-type kinase Open Stomata 1 (OST1), which in turn controls the Slow Anion Channel 1 (SLAC1) in guard cells (Lee *et al*., 2009). ABA induced stomatal closure is dependent on the production of ROS, which is modulated in *ost1 Arabidopsis* lines (Mustilli *et al*., 2002). As previously described, ROS production has close links to pathogen response which may also induce stomatal closure (Sawinski *et al*., 2013; Torres, 2010). Therefore, a possible role for the effector in manipulating ROS production via PP2CA was explored. The knock-out *pp2ca-1* and *pp2ca-2 Arabidopsis* lines did not show altered ROS production when compared to wild-type upon flg22 induction. This result confirms recent findings that PP2CA acts upstream of the convergence between PTI induced and ABA associated ROS, which is thought to integrate at SLAC1 (Guzel Deger *et al*., 2015). Therefore, the targeting of PP2CA

by the effector is unlikely to suppress the induction of PTI-induced ROS production through its links with these convergent ABA pathways.

In order to further examine the implications of this interaction on host immunity, *Hpa* screens were carried out looking at changes in susceptibility caused by over-expression of the effector and manipulation of PP2CA. It was shown that *Arabidopsis* plants over-expressing the effector are more susceptible to *Hpa*. Interestingly, this pattern has higher variability when the effector is tagged with HA although the same enhanced susceptibility was observed. It was hypothesised that this enhanced susceptibility may also be a phenotype of knock-out *pp2ca-1* and *pp2ca-2 Arabidopsis* lines. This hypothesis arose from evidence suggesting that PP2CA is a key negative regulator of the ABA pathways via the SnRK2s, displaying a hypersensitive phenotype to ABA (Kuhn *et al*., 2006). It is possible that perturbation of the protein by the effector is equivalent to knocking-out PP2CA in terms of its role in suppressing these pathways. However, the knock-out and over-expressing PP2CA lines showed inconsistent susceptibility to *Hpa*. This ambiguity could be due to redundancy within the PP2C family meaning a single mutation of PP2CA does not induce an ABA response and therefore is insufficient to significantly enhance susceptibility. Furthermore, the knock-out *pp2ca-1* and *pp2ca-2* lines did not show significant gene expression changes from microarray analysis, demonstrating that these lines are not constitutively ABA responsive. Therefore, the presence of both HaRxL14 and PP2CA together may be required for the enhanced susceptibility to *Hpa*. In order to further examine the role of ABA in this host-pathogen interaction, a triple PP2C knock-out with constitutive ABA signalling could be screened for *Hp*a susceptibility (Rubio *et al*., 2009).

5.6 The role of ABA in susceptibility of *Arabidopsis* to *Hpa*

Microarray analysis highlighted the up-regulation of a large number of genes in the HA::HaRxL14 lines compared to wild-type. These included hormone related genes, many of which are ABA associated, such as biosynthesis enzyme NCED3 (AT3G14440) induced by salt stress and exogenous ABA (Barrero *et al*., 2006). Cold stress associated transcription factor DREB1A (AT4G25480) is also highly

induced by over-expression of HaRxL14 (Palva *et al*., 2001). This enhanced expression could be linked to the role of PP2CA in cold acclimation, which was demonstrated by the increased rate of freezing tolerance following antisense inhibition of PP2C (Palva *et al*., 2001). A significant up-regulation of PP2CA was also shown in two out of three HA::HaRxL14 lines. The up-regulation of signalling components including the PP2Cs is a well-established profile of ABA induction (Chan, 2012; Tähtiharju and Palva, 2001). Therefore, these finding are consistent with a role of the effector in targeting PP2CA to enhance ABA signalling in the host.

A mechanism for the interaction is represented in Figure 42, which shows potential binding of the effector to the active site through which PP2CA interacts with PYR/PYL/RCAR receptors. In this model, the effector acts as a mimic of receptor binding during ABA perception. It was further hypothesised that the presence of ABA may be required for an observable interaction *in planta*. It is possible that if the effector acts as a mimic of a PYR/PYL/RCAR receptor then ABA may similarly be a prerequisite for an interaction with PP2CA. However, a preliminary Co-IP experiment in which leaves expressing the tagged effector and PP2CA constructs were treated with exogenous ABA showed no interaction between the proteins. Therefore, this suggest that a higher than endogenous level of ABA is not likely to be a requirement for this interaction. Furthermore, it has been shown that not all of the interactions with the PYR/PYL/RCAR receptors are ABA dependent. In particular PP2CA may bind to PYR13 in the absence of ABA and is the only PP2C to show an interaction with this receptor (Li *et al*., 2013a). This specificity could explain the exclusive interaction between HaRxL14 and PP2CA, given the structural differences between the PP2Cs (Li *et al*., 2013a). An assay to test the phosphorylation of PP2CA and its targets during presence of HaRxL14 could confirm a role of the effector in functionally manipulating this ABA pathway.

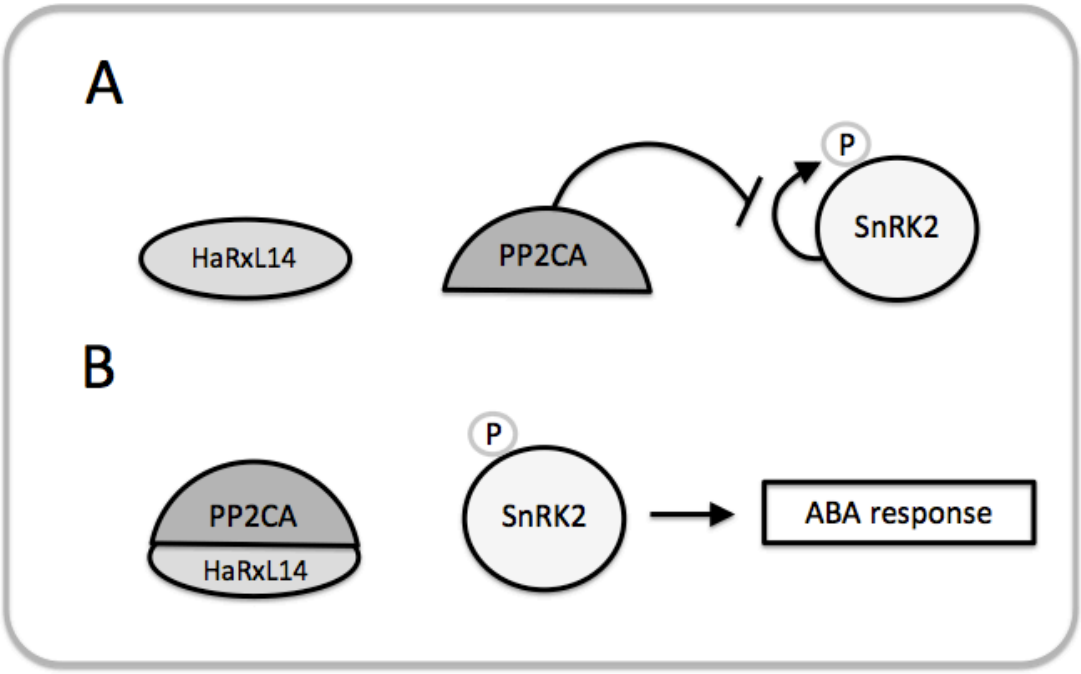

Figure 42. The role of the interaction of *Hpa* effector HaRxL14 with *Arabidopsis* protein PP2CA in manipulating ABA signalling. **A** In the absence of bound HaRxL14, PP2CA inhibits the phosphorylation of the SnRK2s, which suppresses ABA signalling. **B** When HaRxL14 binds to the active site of PP2CA, the SnRK2s are phosphorylated and this leads to an ABA response.

Studies examining the role of ABA in defence against biotrophic pathogens including *Hpa* generally show that enhanced ABA signalling is associated with host susceptibility. However, a recent study showed that *abi1-1* which is an ABA insensitive mutant that retains functioning in dephosphorylating SnRK2s, has enhanced susceptibility to *Hpa* (Hok *et al*., 2014). This result directly contrasts to a previous study which showed the *abi1-1* mutant did not change susceptibility to either *Hpa* or *P. syringae* pv. *tomato* DC3000 (Mohr and Cahill, 2003). Furthermore, an ABA biosynthetic mutant *aba3-1* was demonstrated to have three-fold less *Hpa* sporulation when compared to wild-type (Fan *et al*., 2009). As previously mentioned, it would be interesting to examine whether triple PP2C mutants (e.g. *hab1-1 abi1-2 abi2-3* and *hab1-1 abi1-2 pp2ca-1* (Rubio *et al*., 2009)) with partial constitutive ABA response, exhibit an enhanced susceptibility to *Hpa*. This enhanced susceptibility would be predicted in light of the gene expression changes associated with HA::HaRxL14 from these experiments. A study examining general changes in gene expression during *Hpa* infection, uncovered a set of compatibility specific

genes, which have over-representation of DREB1/CBF3 binding sites in their promoters (Huibers *et al*., 2009). This finding ties in with the strong up-regulation of DREB1A associated with over-expression of HA::HaRxL14 in *Arabidopsis*. Therefore expression of the effector *in planta* appears to mirror changes associated with a compatible interaction between *Hpa* and *Arabidopsis*. Therefore, the overall findings of these experiments suggest that ABA signalling is enhanced during *Hpa* infection. This finding is consistent with the cross talk between hormone pathways, which suggest that ABA acts synergistically with JA to antagonise SA, promoting susceptibility to biotrophic pathogens (Fan *et al*., 2009).

5.7 Phytohormones in coordinating transcriptional response to infection

Chapter 4 focussed on adapting an enhanced Hi-C method (SCRIBL) for the investigation of hormone-induced transcriptional response in *Arabidopsis*. The experiment aimed to determine whether hormone induction resulted in a change to the spatial environment of hormone-associated genes. This change in spatial environment could be due to co-localisation at specialised transcription factories, as has been hypothesised for mammalian systems (Schoenfelder *et al*., 2010). These specialised transcription factories may be targeted by effectors to manipulate host defence.

The optimisation process utilised a system of *Arabidopsis* cell suspension culture treated with MeJA, to elicit a broad and well characterised transcriptional response (Pauwels *et al*., 2008). This system has potential interest given the relevance of JA in host response to infection. The pathways through which hormones including JA regulate transcription are highlighted by the interactions of effectors. For instance, an investigation into the interaction of a predicted *Hpa* effector HaRxL44, showed that the effector targets the mediator subunit MED19a for degradation (Caillaud *et al*., 2013). The degradation of MED19a leads to attenuation of an SA transcriptional response through destabilising the specific group of genes that are coordinated by this subunit and results in the balance of transcribed genes being shifted towards an JA and ET response (Caillaud *et al*., 2013). Contrastingly, the *P. syringae* pv. *tabaci* effector HopXI promotes degradation of the JAZ repressor proteins through its

cysteine protease activity, in order to stimulate a JA transcriptional response (Gimenez-Ibanez *et al*., 2014). Overall, phytohormones are manipulated by pathogens on many levels from transcriptional perturbation of groups of specialised genes through to hijacking of pathways by pathogenic mimics such as coronatin (Bender *et al*., 1999; Caillaud *et al*., 2013).

5.8 Transcription factories in plants

Currently little is known regarding a potential role for transcription factories in plants. However studies within the last few years have begun to optimise approaches related to chromosome conformation capture for use in plants (Grob *et al*., 2014; Louwers *et al*., 2009). These approaches have produced initial insights into chromatin conformation, highlighting the structured arrangement of chromatin in the plant nuclei. This arrangement is shown to be much simpler than the highly structured chromosomal territories observed in mammalian nuclei, with islands of heterochromatin in which all five chromosomes interact, similar to those identified in *Drosophila* (Feng *et al*., 2014; Grob *et al*., 2014). Recent evidence has challenged whether conventionally described transcription factories exist in plants. Firstly, Hi-C analysis in *Arabidopsis* was unable to demonstrate strong associations of highly expressed genes which have been described in animal models (Feng *et al*., 2014). Secondly, RNAPII was detected with antibodies recognising specific phosphorylation sites reflecting the activation status of the enzyme (conjugated to fluorophores Alexa Fluor® 488 or Cyanine Dye Cy®5 (Thermo Fisher Scientific)) were examined by SIM and PALM (Schubert and Weisshart, 2015). These active and inactive RNAPII molecules were found to distribute fairly evenly within euchromatin, although clusters of each form were also observed in reticulate structures (Schubert and Weisshart, 2015). This evidence has not ruled out the possibility of spatial corporation of transcription at focal points within the nucleus, although the organisation may contrast to that of other eukaryotes.

Although the concept of specialised transcription factories is controversial in mammals, it remains to be established whether there is a possible basis for the theory in plants. A role of transcription factory specialisation in mice was suggested based

on the physical interaction of the mouse beta globin genes, which may be coordinated by transcription factor microenvironments (Schoenfelder *et al*., 2010). Hormone induction represents a promising system for the basis of initial steps towards addressing these key questions. The large-scale of these phytohormone-induced responses could be reflected in chromosome conformation rearrangements. These spatial chromatin changes may also have significance at a level of individual gene interactions. Given that techniques such as Hi-C and SCRIBL require input material equivalent to tens of millions of nuclei, the rapid growth of *Arabidopsis* cell suspension culture provides a good model system for these types of analysis. Furthermore, the cross talk between hormone pathways could present further opportunities for a more in depth analysis. It is possible that changes in composition of transcriptional machinery at transcription factories during hormonal antagonism may also be reflected in the observed physical interactions of genes. Overall, investigating the role of phytohormones in the spatial environment of genes is a means to further explore the fundamental basis of gene regulation in plants. This knowledge will undoubtedly have implications in understanding host-pathogen interactions.

6 References

Aarts, N., Metz, M., Holub, E., Staskawicz, B. J., Daniels, M. J. and Parker, J. E. (1998). Different requirements for EDS1 and NDR1 by disease resistance genes define at least two R gene-mediated signaling pathways in *Arabidopsis*. *Proc. Natl. Acad. Sci. U.S.A.* **95**, 10306–10311.

Abcam. Abcam: Beginner's guide to ChIP. http://docs.abcam.com/pdf/chromatin/A-beginners-guide-to-ChIP.pdf [accessed 28 September 2015].

Acosta, I. F. and Farmer, E. E. (2010). Jasmonates. The Arabidopsis Book. *American Society of Plant Biologists* **8**, e0129.

Adie, B. A. T., Pérez-Pérez, J., Pérez-Pérez, M. M., Godoy, M., Sánchez-Serrano, J.-J., Schmelz, E. A. and Solano, R. (2007). ABA is an essential signal for plant resistance to pathogens affecting JA biosynthesis and the activation of defenses in *Arabidopsis*. *Plant Cell* **19**, 1665–1681.

Akino, S., Takemoto, D. and Hosaka, K. (2013). Phytophthora infestans: a review of past and current studies on potato late blight. *J Gen Plant Pathol* **80**, 24–37.

Allen, R. L., Bittner-Eddy, P. D., Grenville-Briggs, L. J., Meitz, J. C., Rehmany, A. P., Rose, L. E. and Beynon, J. L. (2004). Host-parasite coevolutionary conflict between *Arabidopsis* and downy mildew. *Science* **306**, 1957–1960.

An, Y. Q., McDowell, J. M., Huang, S. and McKinney, E. C. (1996). Strong, constitutive expression of the *Arabidopsis* ACT2/ACT8 actin subclass in vegetative tissues. *The Plant Journal* **10**, 107-121.

Anderson, J. P., Gleason, C. A., Foley, R. C., Thrall, P. H., Burdon, J. B. and Singh, K. B. (2010). Plants versus pathogens: an evolutionary arms race. *Funct. Plant Biol.* **37**, 499–512.

Anderson, P. K., Cunningham, A. A., Patel, N. G., Morales, F. J., Epstein, P. R. and Daszak, P. (2004). Emerging infectious diseases of plants: pathogen pollution, climate change and agrotechnology drivers. *Trends Ecol. Evol. (Amst.)* **19**, 535–544.

Anderson, R. G., Casady, M. S., Fee, R. A., Vaughan, M. M., Deb, D., Fedkenheuer, K., Huffaker, A., Schmelz, E. A., Tyler, B. M. and McDowell, J. M. (2012). Homologous RXLR effectors from Hyaloperonospora arabidopsidis and Phytophthora sojae suppress immunity in distantly related plants. *The Plant Journal* **72**, 882–893.

Antoni, R., Gonzalez-Guzman, M., Rodriguez, L., Rodrigues, A., Pizzio, G.A. and Rodriguez, P.L. (2012). Selective inhibition of clade A phosphatases type 2C by PYR/PYL/RCAR abscisic acid receptors. *Plant physiol* **158**, 970-980.

***Arabidopsis* Genome Initiative** (2000). Analysis of the genome sequence of the flowering plant *Arabidopsis thaliana*. *Nature* **408**, 796–815.

Armstrong, M. R., Whisson, S. C., Pritchard, L., Bos, J. I. B., Venter, E., Avrova, A. O., Rehmany, A. P., Böhme, U., Brooks, K., Cherevach, I., *et al.* (2005). An ancestral oomycete locus contains late blight avirulence gene Avr3a, encoding a protein that is recognized in the host cytoplasm. *Proc. Natl. Acad. Sci. U.S.A.* **102**, 7766–7771.

Arvidsson, S., Kwasniewski, M., Riaño-Pachón, D. and Mueller-Roeber, B. (2008). QuantPrime–a flexible tool for reliable high-throughput primer design for quantitative PCR. *BMC bioinformatics*. **9**, 1.

Asai, S., Rallapalli, G., Piquerez, S. J. M., Caillaud, M.-C., Furzer, O. J., Ishaque, N., Wirthmueller, L., Fabro, G., Shirasu, K. and Jones, J. D. G. (2014). Expression profiling during *Arabidopsis*/downy mildew interaction reveals a highly-expressed effector that attenuates responses to salicylic acid. *PLoS Pathog.* **10**, e1004443.

Asselbergh, B., De Vleesschauwer, D. and Höfte, M. (2008). Global switches and fine-tuning-ABA modulates plant pathogen defense. *Mol. Plant Microbe Interact.* **21**, 709–719.

Audenaert, K., De Meyer, G. B. and Höfte, M. M. (2002). Abscisic acid determines basal susceptibility of tomato to Botrytis cinerea and suppresses salicylic acid-dependent signaling mechanisms. *Plant Physiol.* **128**, 491–501.

Axtell, M. J. and Staskawicz, B. J. (2002). Initiation of *RPS2*-Specified Disease Resistance in *Arabidopsis* Is Coupled to the AvrRpt2-Directed Elimination of RIN4. *Cell* **112**, 369 - 377.

Barrero, J. M., Rodriguez, P. L., Quesada, V., Piqueras, P., Ponce, M. R. and Micol, J. L. (2006). Both abscisic acid (ABA)-dependent and ABA-independent pathways govern the induction of NCED3, AAO3 and ABA1 in response to salt stress. *Plant Cell Environ.* **29**, 2000–2008.

Bartels, S. and Boller, T. (2015). Quo vadis, Pep? Plant elicitor peptides at the crossroads of immunity, stress, and development. *J. Exp. Bot.* **66**, 5183–5193.

Baxter, L., Tripathy, S., Ishaque, N., Boot, N., Cabral, A., Kemen, E., Thines, M., Ah-Fong, A., Anderson, R., Badejoko, W., *et al.* (2010). Signatures of adaptation to obligate biotrophy in the Hyaloperonospora arabidopsidis genome. *Science* **330**, 1549–1551.

Bebber, D. P., Holmes, T., Smith, D. and Gurr, S. J. (2014). Economic and physical determinants of the global distributions of crop pests and pathogens. *New Phytol.* **202**, 901–910.

Bebber, D. P., Ramotowski, M. A. T. and Gurr, S. J. (2013). Crop pests and pathogens move polewards in a warming world. *Nature Climate change* **3**, 985–988.

Belton, J.-M., McCord, R. P., Gibcus, J. H., Naumova, N., Zhan, Y. and Dekker, J. (2012). Hi-C: a comprehensive technique to capture the conformation of genomes. *Methods* **58**, 268–276.

Bender, C. L., Alarcón-Chaidez, F. and Gross, D. C. (1999). Pseudomonas syringae phytotoxins: mode of action, regulation, and biosynthesis by peptide and polyketide synthetases. *Microbiol. Mol. Biol. Rev.* **63**, 266–292.

Berardini, T. Z., Reiser, L., Li, D., Mezheritsky, Y., Muller, R., Strait, E. and Huala, E. (2015). The *Arabidopsis* information resource: Making and mining the "gold standard" annotated reference plant genome. *Genesis* **53**, 474–485.

Berger, S., Mitchell-Olds, T. and Stotz, H. U. (2002). Local and differential control of vegetative storage protein expression in response to herbivore damage in *Arabidopsis thaliana*. *Physiol. Plant* **114**, 85–91.

Bevan, M. and Walsh, S. (2005). The *Arabidopsis* genome: a foundation for plant research. *Genome Res.* **15**, 1632–1642.

Birch, P. R. J., Armstrong, M., Bos, J., Boevink, P., Gilroy, E. M., Taylor, R. M., Wawra, S., Pritchard, L., Conti, L., Ewan, R., *et al.* (2009). Towards understanding the virulence functions of RXLR effectors of the oomycete plant pathogen Phytophthora infestans. *J. Exp. Bot.* **60**, 1133–1140.

Birch, P. R. J., Boevink, P. C., Gilroy, E. M., Hein, I., Pritchard, L. and Whisson, S. C. (2008). Oomycete RXLR effectors: delivery, functional redundancy and durable disease resistance. *Curr. Opin. Plant Biol.* **11**, 373–379.

Blackwood, E. M. and Kadonaga, J. T. (1998). Going the distance: a current view of enhancer action. *Science* **281**, 60–63.

Boch, J., Bonas, U. and Lahaye, T. (2014). TAL effectors - pathogen strategies and plant resistance engineering. *New Phytol.* **204**, 823–832.

Bonas, U., Stall, R. E. and Staskawicz B. J. (1989). Genetic and structural characterization of the avirulence gene *avrBs3* from *Xanthomonas campestris* pv. *vesicatoria*. *Mol. Gen. Genet.* **218**, 127–36.

Bos, J. I. B., Armstrong, M. R., Gilroy, E. M., Boevink, P. C., Hein, I., Taylor, R. M., Zhendong, T., Engelhardt, S., Vetukuri, R. R., Harrower, B., *et al.* (2010). Phytophthora infestans effector AVR3a is essential for virulence and manipulates plant immunity by stabilizing host E3 ligase CMPG1. *Proc. Natl. Acad. Sci. U.S.A.* **107**, 9909–9914.

Boter, M., Ruíz-Rivero, O., Abdeen, A. and Prat, S. (2004). Conserved MYC transcription factors play a key role in jasmonate signaling both in tomato and *Arabidopsis*. *Genes Dev.* **18**, 1577–1591.

Boutemy, L. S., King, S. R. F., Win, J., Hughes, R. K., Clarke, T. A., Blumenschein, T. M. A., Kamoun, S. and Banfield, M. J. (2011). Structures of Phytophthora RXLR effector proteins: a conserved but adaptable fold underpins functional diversity. *J. Biol. Chem.* **286**, 35834–35842.

Bressan, R. A., Zhang, C., Zhang, H., Hasegawa, P. M., Bohnert, H. J. and Zhu, J. K. (2001). Learning from the *Arabidopsis* experience. The next gene search paradigm. *Plant Physiol.* **127**, 1354–1360.

Browse, J. (2009). Jasmonate Passes Muster: A Receptor and Targets for the Defense Hormone. *Annu. Rev. Plant Biol.* **60**, 183–205.

Bruce, T. J. A., Aradottir, G. I., Smart, L. E., Martin, J. L., Caulfield, J. C., Doherty, A., Sparks, C. A., Woodcock, C. M., Birkett, M. A., Napier, J. A., *et al.* (2015). The first crop plant genetically engineered to release an insect pheromone for defence. *Sci. Rep.* **5**, 11183.

Caillaud, M.-C., Asai, S., Rallapalli, G., Piquerez, S., Fabro, G. and Jones, J. D. G. (2013). A downy mildew effector attenuates salicylic acid-triggered immunity in *Arabidopsis* by interacting with the host mediator complex. *PLoS Biol.* **11**, e1001732.

Caillaud, M.-C., Piquerez, S. J. M., Fabro, G., Steinbrenner, J., Ishaque, N., Beynon, J. and Jones, J. D. G. (2012a). Subcellular localization of the Hpa RxLR effector repertoire identifies a tonoplast-associated protein HaRxL17 that confers enhanced plant susceptibility. *The Plant Journal* **69**, 252–265.

Caillaud, M.-C., Wirthmueller, L., Fabro, G., Piquerez, S. J. M., Asai, S., Ishaque, N. and Jones, J. D. G. (2012b). Mechanisms of nuclear suppression of host immunity by effectors from the *Arabidopsis* downy mildew pathogen Hyaloperonospora arabidopsidis (Hpa). *Cold Spring Harb. Symp. Quant. Biol.* **77**, 285–293.

Cairns, J. (1960). The initiation of vaccinia infection. *Virology* **11**, 603–623.

Canonne, J. and Rivas, S. (2012). Bacterial effectors target the plant cell nucleus to subvert host transcription. *Plant Signal Behav.* **7**, 217–221.

Cao, F. Y., Yoshioka, K. and Desveaux, D. (2011). The roles of ABA in plant-pathogen interactions. *J. Plant Res.* **124**, 489–499.

Carvalhais, L. C., Dennis, P. G., Badri, D. V., Tyson, G. W., Vivanco, J. M. and Schenk, P. M. (2013). Activation of the jasmonic acid plant defence pathway alters the composition of rhizosphere bacterial communities. *PLoS ONE* **8**, e56457.

Cesari, S., Bernoux, M., Moncuquet, P., Kroj, T. and Dodds, P. N. (2014). A novel conserved mechanism for plant NLR protein pairs: the "integrated decoy" hypothesis. *Front. Plant. Sci.* **5**, 606.

Chakalova, L. and Fraser, P. (2010). Organization of transcription. *Cold Spring Harb. Perspect. Biol.* **2**, a000729.

Chan, Z. (2012). Expression profiling of ABA pathway transcripts indicates crosstalk between abiotic and biotic stress responses in *Arabidopsis Genomics* **100**, 110–115.

Cheutin, T. and Cavalli, G. (2014). Polycomb silencing: from linear chromatin domains to 3D chromosome folding. *Curr. Opin. Genet. Dev.* **25**, 30–37.

Chisholm, S. T., Dahlbeck, D., Krishnamurthy, N., Day, B., Sjolander, K. and Staskawicz, B. J. (2004). Molecular characterization of proteolytic cleavage sites of the Pseudomonas syringae effector AvrRpt2. *PNAS* **102**, 2087–2092.

Chisholm, S. T., Coaker, G., Day, B. and Staskawicz, B. J. (2006). Host-microbe interactions: shaping the evolution of the plant immune response. *Cell* **124**, 803–814.

Chou, S., Krasileva, K. V., Holton, J. M., Steinbrenner, A. D., Alber, T. and Staskawicz, B. J. (2011). Hyaloperonospora arabidopsidis ATR1 effector is a repeat protein with distributed recognition surfaces. *Proc. Natl. Acad. Sci. U.S.A.* **108**, 13323–13328.

Christmann, A., Hoffmann, T., Teplova, I., Grill, E. and Müller, A. (2005). Generation of active pools of abscisic acid revealed by in vivo imaging of water-stressed *Arabidopsis*. *Plant Physiol.* **137**, 209–219.

Clone DB. NCBI. http://www.ncbi.nlm.nih.gov/clone/ [accessed 28 September 2015].

Coates, M. E. and Beynon, J. L. (2010). Hyaloperonospora Arabidopsidis as a pathogen model. *Annu. Rev. Phytopathol.* **48**, 329–345.

Coelho, P. S., Vicente, J. G., Monteiro, A. A. and Holub, E. B. (2012). Pathotypic diversity of Hyaloperonospora brassicae collected from Brassica oleracea. *Eur. J. Plant Pathol.* **134**, 763–771.

Cook, P. R. (1994). RNA polymerase: structural determinant of the chromatin loop and the chromosome. *Bioessays* **16**, 425–430.

Cook, P. R. (2010). A model for all genomes: the role of transcription factories. *J. Mol. Biol.* **395**, 1–10.

Cornforth, J. W., Milborrow, B. V. and Ryback, G. (1965). Chemistry and Physiology of `Dormins' In Sycamore: Identity of Sycamore `Dormin' with Abscisin II. *Nature* **205**, 1269-1270.

Cramer, P., Armache, K. J., Baumli, S., Benkert, S., Brueckner, F., Buchen, C., Damsma, G. E., Dengl, S., Geiger, S. R., Jasiak, A. J., *et al.* (2008). Structure of eukaryotic RNA polymerases. *Annu. Rev. Biophys.* **37**, 337–352.

Crevillén, P., Sonmez, C., Wu, Z. and Dean, C. (2013). A gene loop containing the floral repressor FLC is disrupted in the early phase of vernalization. *EMBO J.* **32**, 140–148.

Curvers, K., Seifi, H., Mouille, G., de Rycke, R., Asselbergh, B., Van Hecke, A., Vanderschaeghe, D., Höfte, H., Callewaert, N., Van Breusegem, F., *et al.* (2010). Abscisic acid deficiency causes changes in cuticle permeability and pectin composition that influence tomato resistance to Botrytis cinerea. *Plant Physiol.* **154**, 847–860.

Cutler, S. R., Rodriguez, P. L., Finkelstein, R. R. and Abrams, S. R. (2010). Abscisic acid: emergence of a core signaling network. *Annu. Rev. Plant Biol.* **61**, 651–679.

Dandanell, G., Valentin-Hansen, P., Larsen, J. E. and Hammer, K. (1987). Long-range cooperativity between gene regulatory sequences in a prokaryote. *Nature* **325**, 823–826.

Dangl, J. L. and Jones, J. D. (2001). Plant pathogens and integrated defence responses to infection. *Nature* **411**, 826–833.

de Torres-Zabala, M., Truman, W., Bennett, M. H., Lafforgue, G., Mansfield, J. W., Egea, P. R., Bögre, L. and Grant, M., (2007). Pseudomonas syringae pv. tomato hijacks the Arabidopsis abscisic acid signalling pathway to cause disease. *The EMBO journal* **26**, 1434-1443.

de Jonge, R. and Thomma, B. P. H. J. (2009). Fungal LysM effectors: extinguishers of host immunity? *Trends in Microbiology* **17**, 151–157.

de Wit, E. and de Laat, W. (2012). A decade of 3C technologies: insights into nuclear organization. *Genes Dev.* **26**, 11–24.

Dekker, J. (2006). The three "C" s of chromosome conformation capture: controls, controls, controls. *Nat. Methods* **3**, 17–21.

Dekker, J., Marti-Renom, M. A. and Mirny, L. A. (2013). Exploring the three-dimensional organization of genomes: interpreting chromatin interaction data. *Nat. Rev. Genet.* **14**, 390–403.

Dekker, J., Rippe, K., Dekker, M. and Kleckner, N. (2002). Capturing chromosome conformation. *Science* **295**, 1306–1311.

Delaney, T. P., Uknes, S., Vernooij, B., Friedrich, L., Weymann, K., Negrotto, D., Gaffney, T., Gut-Rella, M., Kessmann, H., Ward, E., *et al.* (1994). A central role of salicylic Acid in plant disease resistance. *Science* **266**, 1247–1250.

Denancé, N., Sánchez-Vallet, A., Goffner, D. and Molina, A. (2013). Disease resistance or growth: the role of plant hormones in balancing immune responses and fitness costs. *Front. Plant Sci.* **4**, 155.

Denby, K. J., Kumar, P. and Kliebenstein, D. J. (2004). Identification of Botrytis cinerea susceptibility loci in *Arabidopsis thaliana*. *Plant J.* **38**, 473–486.

Dileo, M. V., Pye, M. F., Roubtsova, T. V., Duniway, J. M., Macdonald, J. D., Rizzo, D. M. and Bostock, R. M. (2010). Abscisic acid in salt stress predisposition to phytophthora root and crown rot in tomato and chrysanthemum. *Phytopathology* **100**, 871–879.

Dixon, J. R., Selvaraj, S., Yue, F., Kim, A., Li, Y., Shen, Y., Hu, M., Liu, J. S. and Ren, B. (2012). Topological domains in mammalian genomes identified by analysis of chromatin interactions. *Nature* **485**, 376–380.

Dodds, P. N. and Rathjen, J. P. (2010). Plant immunity: towards an integrated view of plant-pathogen interactions. *Nat. Rev. Genet.* **11**, 539–548.

Dombrecht, B., Xue, G. P., Sprague, S. J., Kirkegaard, J. A., Ross, J. J., Reid, J. B., Fitt, G. P., Sewelam, N., Schenk, P. M., Manners, J. M., *et al.* (2007). MYC2 differentially modulates diverse jasmonate-dependent functions in *Arabidopsis*. *Plant Cell* **19**, 2225–2245.

Dou, D., Kale, S. D., Wang, X., Jiang, R. H. Y., Bruce, N. A., Arredondo, F. D., Zhang, X. and Tyler, B. M. (2008). RXLR-mediated entry of Phytophthora sojae effector Avr1b into soybean cells does not require pathogen-encoded machinery. *Plant Cell* **20**, 1930–1947.

Earley, K. W., Haag, J. R., Pontes, O., Opper, K., Juehne, T., Song, K. and Pikaard, C. S. (2006). Gateway-compatible vectors for plant functional genomics and proteomics. *Plant J.* **45**, 616–629.

Edelman, L. B. and Fraser, P. (2012). Transcription factories: genetic programming in three dimensions. *Curr. Opin. Genet. Dev.* **22**, 110–114.

Eltsov, M. and Zuber, B. (2006). Transmission electron microscopy of the bacterial nucleoid. *J. Struct. Biol.* **156**, 246–254.

Endo, A., Okamoto, M. and Koshiba, T. (2014). ABA Biosynthetic and Catabolic Pathways. In *Abscisic Acid: Metabolism, Transport and Signaling*, 21–45. Dordrecht: Springer Netherlands.

Fabro, G., Steinbrenner, J., Coates, M., Ishaque, N., Baxter, L., Studholme, D. J., Körner, E., Allen, R. L., Piquerez, S. J. M., Rougon-Cardoso, A., *et al.* (2011). Multiple candidate effectors from the oomycete pathogen Hyaloperonospora arabidopsidis suppress host plant immunity. *PLoS Pathog.* **7**, e1002348.

Fan, J., Hill, L., Crooks, C., Doerner, P. and Lamb, C. (2009). Abscisic acid has a key role in modulating diverse plant-pathogen interactions. *Plant Physiol.* **150**, 1750–1761.

Feng, F. and Zhou, J.-M. (2012). Plant-bacterial pathogen interactions mediated by type III effectors. *Curr. Opin. Plant Biol.* **15**, 469–476.

Feng, S., Cokus, S. J., Schubert, V., Zhai, J., Pellegrini, M. and Jacobsen, S. E. (2014). Genome-wide Hi-C Analyses in Wild-Type and Mutants Reveal High-Resolution Chromatin Interactions in *Arabidopsis*. *Mol. Cell* **55**, 694–707.

Ferrari, S., Savatin, D. V., Sicilia, F., Gramegna, G., Cervone, F. and Lorenzo, G. D. (2013). Oligogalacturonides: plant damage-associated molecular patterns and regulators of growth and development. *Front Plant Sci.* **4**, 49.

Finkelstein, R. (2013). Abscisic acid synthesis and response. *The Arabidopsis Book*, p.e0166.

Flors, V., Ton, J., Jakab, G. and Mauch Mani, B. (2005). Abscisic Acid and Callose: Team Players in Defence Against Pathogens? *J. Phytopathol* **153**, 377–383.

Fujii, H., Chinnusamy, V., Rodrigues, A., Rubio, S., Antoni, R., Park, S.-Y., Cutler, S. R., Sheen, J., Rodriguez, P. L. and Zhu, J.-K. (2009). In vitro reconstitution of an abscisic acid signalling pathway. *Nature* **462**, 660–664.

Gabriëls, S. H. E. J., Vossen, J. H., Ekengren, S. K., van Ooijen, G., Abd-El-Haliem, A. M., van den Berg, G. C. M., Rainey, D. Y., Martin, G. B., Takken, F. L. W., de Wit, P. J. G. M., *et al.* (2007). An NB-LRR protein required for HR signalling mediated by both extra- and intracellular resistance proteins. *Plant J.* **50**, 14–28.

Gaits, F., Shiozaki, K. and Russell, P. (1997). Protein phosphatase 2C acts independently of stress-activated kinase cascade to regulate the stress response in fission yeast. *J. Biol. Chem.* **272**, 17873–17879.

Gao, X. J., Feng, J. X., Zhu, S., Liu, X. H., Tardieux, I. and Liu, L. X. (2014a). Protein Phosphatase 2C of Toxoplasma Gondii Interacts with Human SSRP1 and Negatively Regulates Cell Apoptosis. *Biomed. Environ. Sci.* **27**, 883–893.

Gao, X., Cox, K., Jr and He, P. (2014b). Functions of Calcium-Dependent Protein Kinases in Plant Innate Immunity. *Plants* **3**, 160–176.

Gimenez-Ibanez, S. and Solano, R. (2013). Nuclear jasmonate and salicylate signaling and crosstalk in defense against pathogens. *Front. Plant Sci.* **4**, 72.

Gimenez-Ibanez, S., Boter, M., Fernández-Barbero, G., Chini, A., Rathjen, J. P. and Solano, R. (2014). The bacterial effector HopX1 targets JAZ transcriptional repressors to activate jasmonate signaling and promote infection in *Arabidopsis*. *PLoS Biol.* **12**, e1001792.

Glazebrook, J. (2005). Contrasting mechanisms of defense against biotrophic and necrotrophic pathogens. *Annu. Rev. Phytopathol.* **43**, 205–227.

Gonzalez-Guzman, M., Pizzio, G. A. and Antoni, R. (2012). *Arabidopsis* PYR/PYL/RCAR receptors play a major role in quantitative regulation of stomatal aperture and transcriptional response to abscisic acid. *Plant Cell* **24**, 2483-2496.

Govers, F. and Gijzen, M. (2006). Phytophthora genomics: the plant destroyers' genome decoded. *Mol. Plant Microbe Interact.* **19**, 1295–1301.

Grob, S., Schmid, M. W. and Grossniklaus, U. (2014). Hi-C analysis in *Arabidopsis* identifies the KNOT, a structure with similarities to the flamenco locus of Drosophila. *Mol. Cell* **55**, 678–693.

Grob, S., Schmid, M. W., Luedtke, N. W., Wicker, T. and Grossniklaus, U. (2013). Characterization of chromosomal architecture in *Arabidopsis* by chromosome conformation capture. *Genome Biol.* **14**, R129.

Guzel Deger, A., Scherzer, S., Nuhkat, M., Kedzierska, J., Kollist, H., Brosché, M., Unyayar, S., Boudsocq, M., Hedrich, R. and Roelfsema, M. R. G. (2015). Guard cell SLAC1-type anion channels mediate flagellin-induced stomatal closure. *New Phytol.* **208**, 162-173.

Haring, M., Offermann, S., Danker, T., Horst, I., Peterhansel, C. and Stam, M., (2007). Chromatin immunoprecipitation: optimization, quantitative analysis and data normalization. *Plant methods* **3**, 1.

Hemsley, P. A., Hurst, C. H., Kaliyadasa, E., Lamb, R., Knight, M. R., De Cothi, E. A., Steele, J. F. and Knight, H. (2014). The *Arabidopsis* mediator complex subunits MED16, MED14, and MED2 regulate mediator and RNA polymerase II recruitment to CBF-responsive cold-regulated genes. *Plant Cell* **26**, 465–484.

Hohmann, S. (2015). An integrated view on a eukaryotic osmoregulation system. *Curr. Genet.* **61**, 373–382.

Hok, S., Allasia, V., Andrio, E., Naessens, E., Ribes, E., Panabières, F., Attard, A., Ris, N., Clément, M., Barlet, X., *et al.* (2014). The receptor kinase IMPAIRED OOMYCETE SUSCEPTIBILITY1 attenuates abscisic acid responses in *Arabidopsis*. *Plant Physiol.* **166**, 1506–1518.

Holub, E. B. (2008). Natural history of *Arabidopsis thaliana* and oomycete symbioses. In *The Downy Mildews - Genetics, Molecular Biology and Control*, 91–109. Dordrecht: Springer Netherlands.

Hozák, P., Hassan, A. B., Jackson, D. A. and Cook, P. R. (1993). Visualization of replication factories attached to nucleoskeleton. *Cell* **73**, 361–373.

Hövel, I., Louwers, M. and Stam, M. (2012). 3C Technologies in plants. *Methods* **58**, 204–211.

Hu, Q., Kwon, Y.-S., Nunez, E., Cardamone, M. D., Hutt, K. R., Ohgi, K. A., Garcia-Bassets, I., Rose, D. W., Glass, C. K., Rosenfeld, M. G., *et al.* (2008). Enhancing nuclear receptor-induced transcription requires nuclear motor and LSD1-dependent gene networking in interchromatin granules. *Proc. Natl. Acad. Sci. U.S.A.* **105**, 19199–19204.

Huibers, R. P., de Jong, M., Dekter, R. W. and Van den Ackerveken, G. (2009). Disease-specific expression of host genes during downy mildew infection of *Arabidopsis*. *Mol. Plant Microbe Interact.* **22**, 1104–1115.

J**ackson, D.A. and Cook, P.R.** (1985). Transcription occurs at a nucleoskeleton. *The EMBO journal* **4**, 919.

Jackson, D. A., Iborra, F. J., Manders, E. M. and Cook, P. R. (1998). Numbers and organization of RNA polymerases, nascent transcripts, and transcription units in HeLa nuclei. *Mol. Biol. Cell* **9**, 1523–1536.

Janda, M. and Ruelland, E. (2015). Magical mystery tour: Salicylic acid signalling. *Envir. and Exp. Botany* **114**, 117–128.

Jiang, R. H. Y., Tripathy, S., Govers, F. and Tyler, B. M. (2008). RXLR effector reservoir in two Phytophthora species is dominated by a single rapidly evolving superfamily with more than 700 members. *Proc. Natl. Acad. Sci. U.S.A.* **105**, 4874–4879.

Jones, J. D. G. and Dangl, J. L. (2006). The plant immune system. *Nature* **444**, 323–329.

Jung, H. W., Tschaplinski, T. J., Wang, L., Glazebrook, J. and Greenberg, J. T. (2009). Priming in systemic plant immunity. *Science* **324**, 89–91.

Karimi, M., Inzé, D. and Depicker, A. (2002). GATEWAY vectors for Agrobacterium-mediated plant transformation. *Trends Plant Sci.* **7**, 193–195.

Katsir, L., Schilmiller, A.L., Staswick, P.E., He, S.Y. and Howe, G.A. (2008). COI1 is a critical component of a receptor for jasmonate and the bacterial virulence factor coronatine. *PNAS* **105**, 7100-7105.

Kay, S., Hahn, S., Marois, E., Hause, G. and Bonas, U. (2007). A bacterial effector acts as a plant transcription factor and induces a cell size regulator. *Science* **318**, 648-651.

Kazan, K. and Lyons, R. (2014). Intervention of Phytohormone Pathways by Pathogen Effectors. *Plant Cell* **26**, 2285–2309.

Kazan, K. and Manners, J. M. (2012). JAZ repressors and the orchestration of phytohormone crosstalk. *Trends Plant Sci.* **17**, 22–31.

Keen, N. T. (1990). Gene-for-gene complementarity in plant-pathogen interactions. *Annu. Rev. Genet.* **24**, 447–463.

Kerppola, T. K. (2006). Design and implementation of bimolecular fluorescence complementation (BiFC) assays for the visualization of protein interactions in living cells. *Nat. Protoc.* **1**, 1278–1286.

Kline, K. G., Sussman, M. R. and Jones, A. M. (2010). Abscisic acid receptors. *Plant Physiol.* **154**, 479-82.

Kocanova, S., Kerr, E. A., Rafique, S., Boyle, S., Katz, E., Caze-Subra, S., Bickmore, W. A. and Bystricky, K. (2010). Activation of estrogen-responsive genes does not require their nuclear co-localization. *PLoS Genet.* **6**, e1000922.

Koch, E. and Slusarenko, A. (1990). *Arabidopsis* is susceptible to infection by a downy mildew fungus. *Plant Cell* **2**, 437–445.

Koornneef, A. and Pieterse, C. M. J. (2008). Cross talk in defense signaling. *Plant Physiol.* **146**, 839–844.

Krivega, I. and Dean, A. (2012). Enhancer and promoter interactions-long distance calls. *Curr. Opin. Genet. Dev.* **22**, 79–85.

Kuhn, J. M., Boisson-Dernier, A., Dizon, M. B., Maktabi, M. H. and Schroeder, J. I. (2006). The protein phosphatase AtPP2CA negatively regulates abscisic acid signal transduction in *Arabidopsis*, and effects of abh1 on AtPP2CA mRNA. *Plant Physiol.* **140**, 127–139.

Kulik, A., Wawer, I., Krzywińska, E., Bucholc, M. and Dobrowolska, G. (2011). SnRK2 protein kinases--key regulators of plant response to abiotic stresses. *OMICS* **15**, 859–872.

Kuppusamy, K. T., Walcher, C. L. and Nemhauser, J. L. (2009). Cross-regulatory mechanisms in hormone signaling. *Plant Mol. Biol.* **69**, 375–381.

Lacerda, A. F., Vasconcelos, E. A. R., Pelegrini, P. B. and Grossi de Sa, M. F. (2014). Antifungal defensins and their role in plant defense. *Front. Microbiol.* **5**, 116.

Le Dily, F., Baù, D., Pohl, A., Vicent, G. P., Serra, F., Soronellas, D., Castellano, G., Wright, R. H. G., Ballare, C., Filion, G., *et al.* (2014). Distinct structural transitions of chromatin topological domains correlate with coordinated hormone-induced gene regulation. *Genes Dev.* **28**, 2151–2162.

Le Roux, C., Huet, G., Jauneau, A., Camborde, L., Trémousaygue, D., Kraut, A., Zhou, B., Levaillant, M., Adachi, H., Yoshioka, H. and Raffaele, S. (2015). A receptor pair with an integrated decoy converts pathogen disabling of transcription factors to immunity. *Cell* **161**, 1074-1088.

Lee, S. C., Lan, W., Buchanan, B. B. and Luan, S. (2009). A protein kinase-phosphatase pair interacts with an ion channel to regulate ABA signaling in plant guard cells. *Proc. Natl. Acad. Sci. U.S.A.* **106**, 21419–21424.

Lee, S. C., Lim, C. W., Lan, W., He, K. and Luan, S. (2013). ABA signaling in guard cells entails a dynamic protein-protein interaction relay from the PYL-RCAR family receptors to ion channels. *Mol. Plant* **6**, 528–538.

Leonard, K. J. and Szabo, L. J. (2005). Stem rust of small grains and grasses caused by Puccinia graminis. *Mol. Plant Pathol.* **6**, 99–111.

León, J., Rojo, E., Titarenko, E. and Sánchez-Serrano, J. J. (1998). Jasmonic acid-dependent and -independent wound signal transduction pathways are differentially regulated by Ca2+/calmodulin in *Arabidopsis thaliana*. *Mol. Gen. Genet.* **258**, 412–419.

Li, W., Wang, L., Sheng, X., Yan, C., Zhou, R., Hang, J., Yin, P. and Yan, N. (2013a). Molecular basis for the selective and ABA-independent inhibition of PP2CA by PYL13. *Cell Res.* **23**, 1369–1379.

Li, W., Yadeta, K. A., Elmore, J. M. and Coaker, G. (2013b). The Pseudomonas syringae effector HopQ1 promotes bacterial virulence and interacts with tomato 14-3-3 proteins in a phosphorylation-dependent manner. *Plant Physiol.* **161**, 2062–2074.

Lieberman-Aiden, E., van Berkum, N. L., Williams, L., Imakaev, M., Ragoczy, T., Telling, A., Amit, I., Lajoie, B. R., Sabo, P. J., Dorschner, M. O., *et al.* (2009). Comprehensive mapping of long-range interactions reveals folding principles of the human genome. *Science* **326**, 289–293.

Lim, C. W., Luan, S. and Lee, S. C. (2014). A prominent role for RCAR3-mediated ABA signaling in response to Pseudomonas syringae pv. tomato DC3000 infection in *Arabidopsis*. *Plant Cell Physiol.* **55**, 1691–1703.

Liu, Y., Bondarenko, V., Ninfa, A. and Studitsky, V. M. (2001). DNA supercoiling allows enhancer action over a large distance. *Proc. Natl. Acad. Sci. U.S.A.* **98**, 14883–14888.

Liu, J., Elmore, J. M., and Coaker, G. (2009). Investigating the functions of the RIN4 protein complex during plant innate immune responses. *Plant signaling & behavior*, **4**, 1107-1110.

Louwers, M., Splinter, E., van Driel, R., de Laat, W. and Stam, M. (2009). Studying physical chromatin interactions in plants using Chromosome Conformation Capture (3C). *Nat. Protoc.* **4**, 1216–1229.

Lu, G. and Wang, Y. (2008). Functional diversity of mammalian type 2C protein phosphatase isoforms: new tales from an old family. *Clin. Exp. Pharmacol. Physiol.* **35**, 107–112.

Ma, K.W. and Ma, W. (2016). Phytohormone pathways as targets of pathogens to facilitate infection. *Plant mol. biol.***1**, 1-13.

Ma, Y., Szostkiewicz, I., Korte, A., Moes, D., Yang, Y., Christmann, A. and Grill, E. (2009). Regulators of PP2C phosphatase activity function as abscisic acid sensors. *Science* **324**, 1064–1068.

Maere, S., Heymans, K. and Kuiper, M. (2005). BiNGO: a Cytoscape plugin to assess overrepresentation of gene ontology categories in biological networks. *Bioinformatics* **21**, 3448–3449.

Marín-de la Rosa, N., Pfeiffer, A., Hill, K., Locascio, A., Bhalerao, R. P., Miskolczi, P., Grønlund, A. L., Wanchoo-Kohli, A., Thomas, S. G., Bennett, M. J., *et al.* (2015). Genome Wide Binding Site Analysis Reveals Transcriptional Coactivation of Cytokinin-Responsive Genes by DELLA Proteins. *PLoS Genet.* **11**, e1005337.

Martienssen, R. A. (2000). Weeding out the genes: the *Arabidopsis* genome project. *Funct. Integr. Genomics* **1**, 2–11.

Mathur, S., Vyas, S., Kapoor, S. and Tyagi, A. K. (2011). The Mediator complex in plants: structure, phylogeny, and expression profiling of representative genes in a dicot (*Arabidopsis*) and a monocot (rice) during reproduction and abiotic stress. *Plant Physiol.* **157**, 1609–1627.

McDowell, J. M. (2014). Hyaloperonospora arabidopsidis: A Model Pathogen of *Arabidopsis*. In *Genomics of Plant-Associated Fungi and Oomycetes: Dicot Pathogens*, 209–234. Berlin, Heidelberg: Springer Berlin Heidelberg.

McDowell, J. M., Cuzick, A., Can, C., Beynon, J., Dangl, J. L. and Holub, E. B. (2000). Downy mildew (Peronospora parasitica) resistance genes in *Arabidopsis* vary in functional requirements for NDR1, EDS1, NPR1 and salicylic acid accumulation. *Plant J.* **22**, 523–529.

Meinke, D. W. (1998). *Arabidopsis thaliana*: A Model Plant for Genome Analysis. *Science* **282**, 662–682.

Melotto, M., Underwood, W., Koczan, J., Nomura, K. and He, S. Y. (2006). Plant Stomata Function in Innate Immunity against Bacterial Invasion. *Cell* **126**, 969–980.

Michelmore, R. W. and Meyers, B. C. (1998). Clusters of resistance genes in plants evolve by divergent selection and a birth-and-death process. *Genome Res.* **8**, 1113–1130.

Minsavage, G.V., Dahlbeck, D., Whalen, M.C., Kearney, B., Bonas, U., Staskawicz, B.J. and Stall, R.E. (1990). Gene-for-gene relationships specifying disease resistance in Xanthomonas campestris pv. vesicatoria—pepper interactions. *Mol. Plant-Microbe Inter.* **3**, 41-47.

Mitchell, J. A. and Fraser, P. (2008). Transcription factories are nuclear subcompartments that remain in the absence of transcription. *Genes Dev.* **22**, 20–25.

Mitchum, M. G., Hussey, R. S., Baum, T. J., Wang, X., Elling, A. A., Wubben, M. and Davis, E. L. (2013). Nematode effector proteins: an emerging paradigm of parasitism. *New Phytol.* **199**, 879–894.

Mohr, P. G. and Cahill, D. M. (2003). Abscisic acid influences the susceptibility of *Arabidopsis thaliana* to Pseudomonas syringae pv. tomato and Peronospora parasitica. *Functional Plant Biol*. **30**, 461-469.

Mukhtar, M. S., Carvunis, A.-R., Dreze, M., Epple, P., Steinbrenner, J., Moore, J., Tasan, M., Galli, M., Hao, T., Nishimura, M. T., *et al.* (2011). Independently evolved virulence effectors converge onto hubs in a plant immune system network. *Science* **333**, 596–601.

Mustilli, A.-C., Merlot, S., Vavasseur, A., Fenzi, F. and Giraudat, J. (2002). *Arabidopsis* OST1 protein kinase mediates the regulation of stomatal aperture by abscisic acid and acts upstream of reactive oxygen species production. *Plant Cell* **14**, 3089–3099.

Nash, P. B., Purner, M. B., Leon, R. P., Clarke, P., Duke, R. C. and Curiel, T. J. (1998). Toxoplasma gondii-infected cells are resistant to multiple inducers of apoptosis. *J. Immunol.* **160**, 1824–1830.

Nemri, A., Atwell, S., Tarone, A. M., Huang, Y. S., Zhao, K., Studholme, D. J., Nordborg, M. and Jones, J. D. G. (2010). Genome-wide survey of *Arabidopsis* natural variation in downy mildew resistance using combined association and linkage mapping. *Proc. Natl. Acad. Sci. U.S.A.* **107**, 10302–10307.

Nuez, B., Michalovich, D., Bygrave, A., Ploemacher, R. and Grosveld, F. (1995). Defective haematopoiesis in fetal liver resulting from inactivation of the EKLF gene. *Nature* **375**, 316–318.

Oerke, E. C. (2005). Crop losses to pests. *J. Agric. Sci.* **144**, 31–43.

Ohkuma, K., Lyon, J. L., Addicott, F. T. and Smith, O. E. (1963). Abscisin II, an abscission-accelerating substance from young cotton fruit. *Science* **142**, 1592-1593.

Ohm, R. A., Feau, N., Henrissat, B., Schoch, C. L., Horwitz, B. A., Barry, K. W., Condon, B. J., Copeland, A. C., Dhillon, B., Glaser, F., *et al.* (2012). Diverse lifestyles and strategies of plant pathogenesis encoded in the genomes of eighteen Dothideomycetes fungi. *PLoS Pathog.* **8**, e1003037.

Osborne, C. S. (2014). Molecular pathways: transcription factories and chromosomal translocations. *Clin. Cancer Res.* **20**, 296–300.

Palstra, R.-J. T. S. (2009). Close encounters of the 3C kind: long-range chromatin interactions and transcriptional regulation. *Brief Funct. Genomic Proteomic* **8**, 297–309.

Palva, E. T., Welling, A., Tähtiharju, S., Tamminen, I., Puhakainen, T., Mäkelä, P., Laitinen, R., Li, C., Helenius, E., Boije, M., *et al.* (2001). Cold acclimation and development of freezing and drought tolerance in plants. In *S. Sorvari, S. Karhu, E. Kanervo, and S. Pihakaski (Eds.) Proceedings of the 4th International Symposium on in Vitro Culture and Horticultural Breeding,* 277–284. Leuven, BEL: International Society for Horticultural Science.

Park, S.-W., Kaimoyo, E., Kumar, D., Mosher, S. and Klessig, D. F. (2007). Methyl salicylate is a critical mobile signal for plant systemic acquired resistance. *Science* **318**, 113–116.

Park, S.-Y., Fung, P., Nishimura, N., Jensen, D. R., Fujii, H., Zhao, Y., Lumba, S., Santiago, J., Rodrigues, A., Chow, T.-F. F., *et al.* (2009). Abscisic acid inhibits type 2C protein phosphatases via the PYR/PYL family of START proteins. *Science* **324**, 1068–1071.

Paterson, A. H., Lan, T., Amasino, R. and Osborn, T. C. (2001). Brassica genomics: a complement to, and early beneficiary of, the *Arabidopsis* sequence. *Genome Biol.* **2**, 1011.1–1011.4.

Pauwels, L. and Goossens, A. (2011). The JAZ proteins: a crucial interface in the jasmonate signaling cascade. *Plant Cell* **23**, 3089–3100.

Pauwels, L., Morreel, K., De Witte, E., Lammertyn, F., Van Montagu, M., Boerjan, W., Inzé, D. and Goossens, A. (2008). Mapping methyl jasmonate-mediated transcriptional reprogramming of metabolism and cell cycle progression in cultured *Arabidopsis* cells. *Proc. Natl. Acad. Sci. U.S.A.* **105**, 1380–1385.

Piekarski, G. (1937). Cytologische Untersuchungen an Paratyphus-und Colibakterien. *Archiv. Mikrobiol.* **8**, 428–439.

Pizzio, G. A., Rodriguez, L., Antoni, R., González-Guzmán, M., Yunta, C., Merilo, E., Kollist, H., Albert, A. and Rodriguez, P. L. (2013). The PYL4 A194T mutant uncovers a key role of PYR1-LIKE4/PROTEIN PHOSPHATASE 2CA interaction for abscisic acid signaling and plant drought resistance. *Plant Physiol.* **163**, 441–455.

Pritzkow, S., Morales, R., Moda, F., Khan, U., Telling, G. C., Hoover, E. and Soto, C. (2015). Grass plants bind, retain, uptake, and transport infectious prions. *Cell Rep.* **11**, 1168–1175.

Rehmany, A. P., Gordon, A., Rose, L. E., Allen, R. L., Armstrong, M. R., Whisson, S. C., Kamoun, S., Tyler, B. M., Birch, P. R. J. and Beynon, J. L. (2005). Differential recognition of highly divergent downy mildew avirulence gene alleles by RPP1 resistance genes from two *Arabidopsis* lines. *Plant Cell* **17**, 1839–1850.

Robert-Gangneux, F. and Dardé, M.-L. (2012). Epidemiology of and diagnostic strategies for toxoplasmosis. *Clin. Microbiol. Rev.* **25**, 264–296.

Robert-Seilaniantz, A., Grant, M. and Jones, J. D. G. (2011). Hormone crosstalk in plant disease and defense: more than just jasmonate-salicylate antagonism. *Annu. Rev. Phytopathol.* **49**, 317–343.

Rose, L. E., Bittner-Eddy, P. D., Langley, C. H., Holub, E. B., Michelmore, R. W. and Beynon, J. L. (2004). The maintenance of extreme amino acid diversity at the disease resistance gene, RPP13, in *Arabidopsis thaliana*. *Genetics* **166**, 1517–1527.

Rubio, S., Rodrigues, A., Saez, A., Dizon, M. B., Galle, A., Kim, T.-H., Santiago, J., Flexas, J., Schroeder, J. I. and Rodriguez, P. L. (2009). Triple loss of function of protein phosphatases type 2C leads to partial constitutive response to endogenous abscisic acid. *Plant Physiol.* **150**, 1345–1355.

Rustérucci, C., Aviv, D. H., Holt, B. F., Dangl, J. L. and Parker, J. E. (2001). The disease resistance signaling components EDS1 and PAD4 are essential regulators of the cell death pathway controlled by LSD1 in *Arabidopsis*. *Plant Cell* **13**, 2211–2224.

Saito, H. and Tatebayashi, K. (2004). Regulation of the osmoregulatory HOG MAPK cascade in yeast. *J. Biochem.* **136**, 267–272.

Samanta, S. and Thakur, J. K. (2015). Role of Plant Mediator Complex in Stress Response. In *Elucidation of Abiotic Stress Signaling in Plants*, 3–28. New York, NY: Springer New York.

Santiago, J., Dupeux, F., Betz, K., Antoni, R., González-Guzmán, M., Rodriguez, L., Márquez, J. A. and Rodriguez, P. L. (2012). Structural insights into PYR/PYL/RCAR ABA receptors and PP2Cs. *Plant Sci.* **182**, 3–11.

Santiago, J., Rodrigues, A., Saez, A., Rubio, S., Antoni, R., Dupeux, F., Park, S.-Y., Márquez, J. A., Cutler, S. R. and Rodriguez, P. L. (2009). Modulation of drought resistance by the abscisic acid receptor PYL5 through inhibition of clade A PP2Cs. *Plant J.* **60**, 575–588.

Sawinski, K., Mersmann, S., Robatzek, S. and Böhmer, M. (2013). Guarding the green: pathways to stomatal immunity. *Mol. Plant Microbe Interact.* **26**, 626–632.

Schaller, A. and Stintzi, A. (2009). Enzymes in jasmonate biosynthesis – Structure, function, regulation. *Phytochemistry* **70**, 1532–1538.

Schoenfelder, S., Sexton, T., Chakalova, L., Cope, N. F., Horton, A., Andrews, S., Kurukuti, S., Mitchell, J. A., Umlauf, D., Dimitrova, D. S., *et al*. (2010). Preferential associations between co-regulated genes reveal a transcriptional interactome in erythroid cells. *Nat. Genet.* **42**, 53–61.

Scholz, S. S., Reichelt, M., Boland, W. and Mithöfer, A. (2015). Additional evidence against jasmonate-induced jasmonate induction hypothesis. *Plant Sci.* **239**, 9–14.

Schubert, V. and Weisshart, K. (2015). Abundance and distribution of RNA polymerase II in *Arabidopsis* interphase nuclei. *J. Exp. Bot.* **66**, 1687–1698.

Schubert, V., Rudnik, R. and Schubert, I. (2014). Chromatin associations in *Arabidopsis* interphase nuclei. *Front. Genet.* **5**, 389.

Schweighofer, A., Hirt, H. and Meskiene, I. (2004). Plant PP2C phosphatases: emerging functions in stress signaling. *Trends Plant Sci.* **9**, 236–243.

Seo, M. and Koshiba, T. (2011). Transport of ABA from the site of biosynthesis to the site of action. *J. Plant Res.* **124**, 501–507.

Seyfferth, C. and Tsuda, K. (2014). Salicylic acid signal transduction: the initiation of biosynthesis, perception and transcriptional reprogramming. *Front. Plant Sci.* **5**, 697.

Shan, W., Cao, M., Leung, D. and Tyler, B. M. (2004). The Avr1b locus of Phytophthora sojae encodes an elicitor and a regulator required for avirulence on soybean plants carrying resistance gene Rps1b. *Mol. Plant Microbe Interact.* **17**, 394–403.

Sheard, L. B. and Zheng, N. (2009). Plant biology: Signal advance for abscisic acid. *Nature* **462**, 575–576.

Shiozaki, K. and Russell, P. (1993). Cellular function of protein phosphatase 2C in yeast. *Cell. mol. biol. res*. **40**, 241-3.

Shiozaki, K. and Russell, P. (1995). Counteractive roles of protein phosphatase 2C (PP2C) and a MAP kinase kinase homolog in the osmoregulation of fission yeast. *EMBO J.* **14**, 492–502.

Simon, A. and Biot, E. (2010). ANAIS: analysis of NimbleGen arrays interface. *Bioinformatics* **26**, 2468–2469.

Sinapidou, E., Williams, K., Nott, L., Bahkt, S., Tör, M., Crute, I., Bittner-Eddy, P. and Beynon, J. (2004). Two TIR:NB:LRR genes are required to specify resistance to Peronospora parasitica isolate Cala2 in *Arabidopsis*. *Plant J.* **38**, 898–909.

Singh, A., Pandey, A., Srivastava, A. K., Tran, L.-S. P. and Pandey, G. K. (2015). Plant protein phosphatases 2C: from genomic diversity to functional multiplicity and importance in stress management. *Crit. Rev. Biotechnol.* **1**, 1–13.

Sipos, L. and Gyurkovics, H. (2005). Long-distance interactions between enhancers and promoters. *FEBS J.* **272**, 3253–3259.

Slusarenko, A. J. and Schlaich, N. L. (2003). Downy mildew of *Arabidopsis thaliana* caused by Hyaloperonospora parasitica (formerly Peronospora parasitica). *Mol. Plant Pathol.* **4**, 159–170.

Smyth, G. K. (2005). limma: Linear Models for Microarray Data. Bioinformatics and comupational biology solutions using R and Bioconductor. In *Bioinformatics and Computational Biology Solutions Using R and Bioconductor*, 397–420. Springer New York.

Song, S., Qi, T., Wasternack, C. and Xie, D. (2014). Jasmonate signaling and crosstalk with gibberellin and ethylene. *Curr. Opin. Plant Biol.* **21**, 112–119.

Song, J., Zhu, C., Zhang, X., Wen, X., Liu, L., Peng, J., Guo, H. and Yi, C. (2015). Biochemical and Structural Insights into the Mechanism of DNA Recognition by Arabidopsis ETHYLENE INSENSITIVE3. *PloS one*, **10**, p.e0137439.

Spilianakis, C. G. and Flavell, R. A. (2004). Long-range intrachromosomal interactions in the T helper type 2 cytokine locus. *Nat. Immunol.* **5**, 1017–1027.

Spilianakis, C. G., Lalioti, M. D., Town, T., Lee, G. R. and Flavell, R. A. (2005). Interchromosomal associations between alternatively expressed loci. *Nature* **435**, 637–645.

Spoel, S. H. and Dong, X. (2012). How do plants achieve immunity? Defence without specialized immune cells. *Nat. Rev. Immunol.* **12**, 89–100.

Srivastava, L. M. (2002). Plant Growth and Development: Hormones and Environment, 217-231. Academic Press.

Staskawicz, B. J., Ausubel, F. M., Baker, B. J., Ellis, J. G. and Jones, J. D. (1995). Molecular genetics of plant disease resistance. *Science* **268**, 661–667.

Staskawicz, B. J., Dahlbeck, D. and Keen, N. T. (1984). Cloned avirulence gene of Pseudomonas syringae pv. glycinea determines race-specific incompatibility on Glycine max (L.) Merr. *Proc. Natl. Acad. Sci. U.S.A.* **81**, 6024–6028.

Steinbrenner, J., Eldridge, M., Tomé, D. F. A. and Beynon, J. L. (2014). A Simple and Fast Protocol for the Protein Complex Immunoprecipitation (Co-IP) of Effector: Host Protein Complexes. In *Plant-Pathogen Interactions: Methods and Protocols*, 195–211. Totowa, NJ: Humana Press.

Stergiopoulos, I. and de Wit, P. J. G. M. (2009). Fungal effector proteins. *Annu. Rev. Phytopathol.* **47**, 233–263.

Sun, H.-L., Wang, X.-J., Ding, W.-H., Zhu, S.-Y., Zhao, R., Zhang, Y.-X., Xin, Q., Wang, X.-F. and Zhang, D.-P. (2011). Identification of an important site for function of the type 2C protein phosphatase ABI2 in abscisic acid signalling in *Arabidopsis*. *J. Exp. Bot.* **62**, 5713–5725.

Sun, Y., Li, L., Macho, A. P., Han, Z., Hu, Z., Zipfel, C., Zhou, J.-M. and Chai, J. (2013). Structural basis for flg22-induced activation of the *Arabidopsis* FLS2-BAK1 immune complex. *Science* **342**, 624–628.

Sutherland, H. and Bickmore, W. A. (2009). Transcription factories: gene expression in unions? *Nat. Rev. Genet.* **10**, 457–466.

TAIR. About *Arabidopsis*. *Arabidopsis.org/portals/education/aboutArabidopsis.jsp*. [Accessed 05 March 2016].

Takken, F. L. W. and Goverse, A. (2012). How to build a pathogen detector: structural basis of NB-LRR function. *Curr. Opin. Plant Biol.* **15**, 375–384.

Tähtiharju, S. and Palva, T. (2001). Antisense inhibition of protein phosphatase 2C accelerates cold acclimation in *Arabidopsis thaliana*. *Plant J.* **26**, 461–470.

Tomé, D. F. A., Steinbrenner, J. and Beynon, J. L. (2014). A growth quantification assay for Hyaloperonospora arabidopsidis isolates in *Arabidopsis thaliana*. *Methods Mol. Biol.* **1127**, 145–158.

Torres, M. A. (2010). ROS in biotic interactions. *Physiol. Plant* **138**, 414–429.

Tyler, B. M. (2006). Phytophthora Genome Sequences Uncover Evolutionary Origins and Mechanisms of Pathogenesis. *Science* **313**, 1261–1266.

Valanne, S., Wang, J.-H. and Rämet, M. (2011). The Drosophila Toll signaling pathway. *J. Immunol.* **186**, 649–656.

van Berkum, N. L., Lieberman-Aiden, E., Williams, L., Imakaev, M., Gnirke, A., Mirny, L. A., Dekker, J. and Lander, E. S. (2010). Hi-C: a method to study the three-dimensional architecture of genomes. *J. Vis. Exp*.

van der Biezen, E. A. and Jones, J. D. (1998). The NB-ARC domain: a novel signalling motif shared by plant resistance gene products and regulators of cell death in animals. *Curr. Biol.* **8**, R226–R227.

van der Hoorn, R. A. L. and Kamoun, S. (2008). From Guard to Decoy: a new model for perception of plant pathogen effectors. *Plant Cell* **20**, 2009–2017.

Vidhyasekaran, P. (2014). *Plant Hormone Signaling Systems in Plant Innate Immunity*. Springer.

Vlot, A. C., Dempsey, D. A. and Klessig, D. F. (2009). Salicylic Acid, a multifaceted hormone to combat disease. *Annu. Rev. Phytopathol.* **47**, 177–206.

Voinnet, O., Rivas, S., Mestre, P. and Baulcombe, D. (2003). An enhanced transient expression system in plants based on suppression of gene silencing by the p19 protein of tomato bushy stunt virus. *Plant J.* **33**, 949–956.

Wansink, D. G., Schul, W., van der Kraan, I., van Steensel, B., van Driel, R. and de Jong, L. (1993). Fluorescent labeling of nascent RNA reveals transcription by RNA polymerase II in domains scattered throughout the nucleus. *J. Cell Biol.* **122**, 283–293.

Warmka, J., Hanneman, J., Lee, J., Amin, D. and Ota, I. (2001). Ptc1, a type 2C Ser/Thr phosphatase, inactivates the HOG pathway by dephosphorylating the mitogen-activated protein kinase Hog1. *Mol. Cell. Biol.* **21**, 51–60.

Weßling, R., Epple, P., Altmann, S., He, Y., Yang, L., Henz, S. R., McDonald, N., Wiley, K., Bader, K. C., Gläßer, C., *et al.* (2014). Convergent targeting of a common host protein-network by pathogen effectors from three kingdoms of life. *Cell Host Microbe* **16**, 364–375.

Whalen, M. C., Innes, R. W., Bent, A. F. and Staskawicz, B. J. (1991). Identification of Pseudomonas syringae pathogens of *Arabidopsis* and a bacterial locus determining avirulence on both *Arabidopsis* and soybean. *Plant Cell* **3**, 49–59.

Whisson, S. C., Boevink, P. C., Moleleki, L., Avrova, A. O., Morales, J. G., Gilroy, E. M., Armstrong, M. R., Grouffaud, S., van West, P., Chapman, S., *et al.* (2007). A translocation signal for delivery of oomycete effector proteins into host plant cells. *Nature* **450**, 115–118.

Wildermuth, M. C., Dewdney, J., Wu, G. and Ausubel, F. M. (2001). Isochorismate synthase is required to synthesize salicylic acid for plant defence. *Nature* **414**, 562–565.

Williams, S. J., Sohn, K. H., Wan, L., Bernoux, M., Sarris, P. F., Segonzac, C., Ve, T., Ma, Y., Saucet, S. B., Ericsson, D. J. and Casey, L. W. (2014). Structural basis for assembly and function of a heterodimeric plant immune receptor. *Science* **344**, 299-303.

Win, J., Chaparro-Garcia, A., Belhaj, K., Saunders, D. G. O., Yoshida, K., Dong, S., Schornack, S., Zipfel, C., Robatzek, S., Hogenhout, S. A., *et al.* (2012a). Effector Biology of Plant-Associated Organisms: Concepts and Perspectives. *Cold Spring Harb. Symp. Quant. Biol.* **77**, 235–247.

Win, J., Krasileva, K. V., Kamoun, S., Shirasu, K., Staskawicz, B. J. and Banfield, M. J. (2012b). Sequence divergent RXLR effectors share a structural fold conserved across plant pathogenic oomycete species. *PLoS Pathog.* **8**, e1002400.

Wu, C.-H., Krasileva, K. V., Banfield, M. J., Terauchi, R. and Kamoun, S. (2015). The "sensor domains" of plant NLR proteins: more than decoys? *Front Plant Sci* **6**, 134.

Xu, M. and Cook, P. R. (2008). Similar active genes cluster in specialized transcription factories. *J. Cell Biol.* **181**, 615–623.

Yoshida, T., Fujita, Y., Maruyama, K., Mogami, J., Todaka, D., Shinozaki, K. and Yamaguchi-Shinozaki, K. (2015). Four *Arabidopsis* AREB/ABF transcription factors function predominantly in gene expression downstream of SnRK2 kinases in abscisic acid signalling in response to osmotic stress. *Plant Cell Environ.* **38**, 35–49.

Yu, X., Tang, J., Wang, Q., Ye, W., Tao, K., Duan, S., Lu, C., Yang, X., Dong, S., Zheng, X., *et al.* (2012). The RxLR effector Avh241 from Phytophthora sojae requires plasma membrane localization to induce plant cell death. *New Phytol.* **196**, 247–260.

Zhang, J., Li, X., He, Z., Zhao, X., Wang, Q., Zhou, B., Yu, D., Huang, X., Tang, D., Guo, X., *et al.* (2013). Molecular character of a phosphatase 2C (PP2C) gene relation to stress tolerance in *Arabidopsis thaliana*. *Mol. Biol. Rep.* **40**, 2633–2644.

Zipfel, C., Robatzek, S., Navarro, L., Oakeley, E. J., Jones, J. D. G., Felix, G. and Boller, T. (2004). Bacterial disease resistance in *Arabidopsis* through flagellin perception. *Nature* **428**, 764–767.